# Rogue waves in the southern North Sea

Dissertation
zur Erlangung des Doktorgrades
an der Fakultät für Mathematik, Informatik und Naturwissenschaften
Fachbereich Erdsystemwissenschaften
der Universität Hamburg

vorgelegt von
Ina Teutsch

Hamburg, 2022

Fachbereich Erdsystemwissenschaften

| | |
|---|---|
| Datum der Disputation: | 07.07.2022 |
| Gutachter/innen der Dissertation: | Prof. Dr. Corinna Schrum<br>Dr. Ralf Weisse |
| Zusammensetzung der Prüfungskommission: | Prof. Dr. Corinna Schrum<br>Dr. Ralf Weisse<br>Dr.-Ing. Markus Brühl<br>Prof. Dr. Felix Ament<br>Prof. Dr. Johanna Baehr |
| Vorsitzender des Fach-Promotionsausschusses Erdsystemwissenschaften: | Prof. Dr. Hermann Held |
| Dekan der Fakultät MIN: | Prof. Dr. Heinrich Graener |

# Abstract

Rogue waves are exceptionally high waves, relative to the surrounding sea state. They occur rarely, which makes them difficult to predict. Due to their particular height and limited predictability, they pose a threat to offshore structures and operations. A first step towards the prediction of rogue waves in a region is the investigation of their occurrence frequency. Knowing whether rogue waves occur as often as expected at random, or more frequently, gives a hint on the mechanisms that may have contributed to their formation. It is likely that different processes can be responsible for rogue wave formation. In deep and intermediate water, rogue wave occurrence frequencies beyond the expectations of common wave height distributions have been explained mathematically and experimentally, for example, by nonlinear focusing. In shallow water, in which wave dynamics experience the influence of the sea floor, the presence of solitons has been suspected as a cause of increased rogue wave occurrence. An improved understanding of the mechanisms that form rogue waves is crucial for their prediction. The prediction of rogue waves can prevent accidents at sea.

This thesis concerns rogue waves in the southern North Sea, in both intermediate-water and shallow-water regimes. In an extensive set of surface elevation data from six buoy and five radar measurement stations, rogue waves with exceptional crest and crest-to-trough heights were identified. Their occurrence frequencies were compared to the expectations of common wave height distributions of a Weibull type. The statistical analysis in intermediate water depths revealed that wave buoys did not identify more rogue waves than expected. However, rogue wave frequencies recorded at radar stations exceeded the expectations of the common wave height distributions. The discrepancy between the results might be due to the different measurement techniques. Following the statistical analysis at intermediate-water sites, it was investigated whether nonlinear focusing, that has led to deep-water rogue wave formation in numerical and physical experiments, provides a conceivable explanation for rogue wave generation at the considered sites. An investigation of wave energy spec-

tra at the intermediate-water stations yielded broad-banded conditions in both frequency and angular direction. These are unlikely conditions for nonlinear focusing to occur. In shallow water, the statistics revealed an exceptionally high number of rogue waves at one buoy and one radar device. In the shallow-water time series at these sites, the recorded rogue waves could be associated with the presence of solitons.

The study leads to the conclusion that intermediate-water rogue waves in the southern North Sea are probably not the result of nonlinear focusing. At some sites in shallow water above a sloping sea floor, rogue wave occurrence frequencies exceeding the expectations of common wave height distributions, could be explained by the presence of solitons.

# Zusammenfassung

Extremwellen oder "Rogue Waves" sind außergewöhnlich hohe Wellen, bezogen auf den umgebenden Seegangszustand. Sie treten selten auf, was ihre Vorhersage erschwert. Auf Grund ihrer ungewöhnlichen Höhe und eingeschränkten Vorhersagbarkeit stellen sie eine Bedrohung für Bauwerke und Tätigkeiten auf See dar. Ein erster Schritt auf dem Weg zur Vorhersage von Extremwellen in einer Region ist die Ermittlung ihrer Häufigkeit. Das Wissen darüber, ob Extremwellen so oft auftreten wie zufällig erwartet, oder häufiger, gibt einen Hinweis darauf, welche Mechanismen zu ihrer Entstehung beigetragen haben könnten. Es ist anzunehmen, dass unterschiedliche Prozesse für das Entstehen von Extremwellen verantwortlich sein können. In großen und mittleren Wassertiefen wird eine Extremwellenhäufigkeit, die über die Erwartungen gebräuchlicher Verteilungen von Wellenhöhen hinausgeht, mathematisch und experimentell beispielsweise durch nichtlineare Fokussierung erklärt. In flachem Wasser, in welchem die Dynamik von Wellen den Einfluss des Meeresbodens erfährt, wird das Vorhandensein von Solitonen als Ursache für eine erhöhte Extremwellenhäufigkeit in Betracht gezogen. Ein verbessertes Verständnis der Mechanismen, die Extremwellen ausbilden, ist wesentlich für deren Vorhersage. Die Vorhersage von Extremwellen kann Unfällen auf See vorbeugen.

Diese Dissertation betrifft Extremwellen in der südlichen Nordsee, sowohl in mittleren, als auch in geringen Wassertiefen. In einem umfangreichen Satz von Wasserspiegelauslenkungsdaten von sechs Bojen- und fünf Radarmessstationen wurden Extremwellen mit außergewöhnlichen Wellenbergen und Wellenhöhen von Berg zu Tal identifiziert. Ihre Häufigkeiten wurden mit den Erwartungen üblicher Wellenhöhen-Verteilungen der Art einer Weibull-Verteilung verglichen. Die statistische Auswertung in mittleren Wassertiefen zeigte, dass Wellenbojen nicht mehr Extremwellen identifizierten als erwartet. Extremwellenhäufigkeiten, die an Radarstationen erfasst wurden, überschritten jedoch die Erwartungen der üblichen Wellenhöhen-Verteilungen. Die Unstimmigkeiten zwischen den Ergebnissen liegen möglicherweise in den unterschiedlichen Messmethoden begründet. Im Anschluss an die statistische Auswertung an Standorten in mittlerer Wassertiefe wurde überprüft, ob nichtlineare Fokussierung, die in numerischen und physikalischen Experimenten zur Entstehung von Extremwellen in tiefem Wasser geführt hat, eine denkbare Erklärung für die Erzeugung von Extremwellen an den betrachteten Standorten bietet. Die Untersuchung von Wellenenergiespektren an den Stationen in mittleren Wassertiefen ergab breitbandige Zustände, sowohl in der Frequenz-, als auch in der Richtungsverteilung. Diese Bedingungen machen die Entstehung nichtlinearer Fokussierung unwahrscheinlich. In flachem Wasser offenbarte die Statistik eine außergewöhnlich hohe Anzahl an Extremwellen an einer Boje, sowie an einem Radargerät. In den Flachwasser-Zeitreihen dieser Standorte konnten die aufgezeichneten Extremwellen mit dem Vorhandensein von Solitonen in Verbindung gebracht werden.

Die Studie kommt zu dem Schluss, dass Extremwellen in den mittleren Wassertiefen der südlichen Nordsee wahrscheinlich nicht das Ergebnis nichtlinearer Fokussierung sind. An einigen Standorten in flachem Wasser oberhalb eines abschüssigen Meeresbodens konnten Extremwellenhäufigkeiten, die die Erwartungen üblicher Wellenhöhen-Verteilungen überschritten, durch das Vorhandensein von Solitonen erklärt werden.

# Publications related to this dissertation

**Research article 1 in Appendix A:**

Teutsch, I., Weisse, R., Moeller, J. and Krueger, O., 2020:

A statistical analysis of rogue waves in the southern North Sea.

*Natural Hazards and Earth System Sciences*, **20 (10)**, 2665–2680,

https://doi.org/10.5194/nhess-20-2665-2020

**Research article 2 in Appendix B:**

Teutsch, I. and Weisse, R., 2022:

Intermediate-Water Rogue Waves in the Southern North Sea-

Generated by a Modulational Instability?

Submitted to *Journal of Physical Oceanography.*

**Research article 3 in Appendix C:**

Teutsch, I., Brühl, M., Weisse, R., and Wahls, S., 2022:

Contribution of solitons to enhanced rogue wave occurrence in shallow water:

a case study in the southern North Sea.

*Natural Hazards and Earth System Sciences Discussions* [preprint],

https://doi.org/10.5194/nhess-2022-28, in review.

# Abbreviations

**ADCP** Acoustic Doppler Current Profiler

**AWG** Ameland Westgat- gas platform off Ameland

**IACS** International Association of Classification Societies

**IST** Inverse Scattering Transform

**KdV** Korteweg–de Vries

**NLS** Nonlinear Schrödinger

**NS** North Sea

**NS1** Nordsee One- offshore wind farm off Juist

**RQ** research question

**SEE** buoy measurement site off Norderney

**US** United States

# Symbols

$\alpha$ shape parameter of the Weibull distribution

$\beta$ scale parameter of the Weibull distribution

$C$ crest height [m]

$h$ water depth [m]

$H$ crest-to-trough wave height [m]

$H_{1/3}$ time series definition of the significant wave height [m]

$H_{m0}$ spectral definition of the significant wave height [m]

$H_s$ significant wave height [m]

$k$ wave number [$\mathrm{m}^{-1}$]

$m_0$ zeroth moment of the wave energy spectrum [$\mathrm{m}^2$]

# Contents

# 1 Introduction

From the perspective of a traveller on a ship in an average rough sea, a rogue wave would be the one wave that is different from the ordinary waves the ship has passed. It would appear all of a sudden, quickly build up to great height and develop a high acceleration, while not breaking, as one could expect from a wave of this asymmetry and steepness (Magnusson et al., 2003; Adcock et al., 2011). Hopefully, the wave will leave the ship unscathed, just wash over its deck and disappear as quickly as it arrived. Hopefully, because more unfortunate incidents are known (Didenkulova, 2020). Janssen and Bidlot (2009) have estimated the probability of a rogue wave with a height of 16 m or higher to occur anywhere in the world at any time as 0.024 % [1].

Due to their rare occurrence and exceptional heights, rogue waves are relevant for any kind of offshore operation, especially when they occur during large significant wave heights. They may develop tremendous forces and as a consequence pose a risk to ships, platforms and coastal defense structures (Bitner-Gregersen and Gramstad, 2016). In the context of marine safety, it is important to assess rogue waves in the best possible manner and by finding possible causes, pave the way towards rogue wave prediction.

Rogue waves, as concerned in this dissertation, are described by a relative definition, thus, not all rogue waves are waves of great absolute height. They are rather exceptional compared to the sea state in which they occur. According to a definition by Haver and Andersen (2000), a rogue wave with the crest-to trough height $H$ follows the definition

$$\frac{H}{H_s} \geq 2.0, \tag{1}$$

in which $H_s$ is the significant wave height, defined as $H_s = H_{m0} = 4 \cdot \sqrt{m_0}$, with $m_0$ denoting the 0th moment of the wave energy spectrum, or variance. $\sqrt{m_0}$ is the standard deviation of the surface elevation. According to second-order theory, the relative wave height in Eq. 1 is expected to be exceeded

[1] This figure was calculated by multiplying an estimate of the rogue wave occurrence probability in buoy measurement data and nonlinear theory with the probability of observing significant wave heights larger than 8 m, estimated from satellite altimetry and wave models.

only once in 100 measurement samples of 20 minutes duration (Haver and Andersen, 2000). In second-order theory, the surface elevation is described by a linear superposition of wave components on the one hand, and a second-order correction, which accounts for an interaction between waves of different frequencies, on the other hand. The crest height $C$, which likewise is exceeded once in 100 records according to second-order theory, was identified by Haver and Andersen (2000) as

$$\frac{C}{H_s} \geq 1.25. \tag{2}$$

A rogue wave is defined either by Eq. 1 (in this thesis referred to as "height rogue waves"), by Eq. 2 (in the following called "crest rogue waves") or by both equations. Although Haver and Andersen (2000)'s definitions were based on 20 minute samples, they have been adopted to time series of different duration (Forristall, 2005; Baschek and Imai, 2011, e.g.).

In the past, reports on rogue waves by sailors were dismissed as nautical yarns (Lawton, 2001). It is documented that as early as 1826, the scientist and naval officer Jules Dumont d'Urville reported on waves higher than 30 m in the Indian Ocean and as a consequence was publicly ridiculed by fellow scientists (Jones and Jones, 2008). Since that time, the possibilities of measurements and communication have vastly improved and frequent observations of rogue waves have been documented Sand et al. (1990, e.g.). The term "freak wave", which is commonly used as an equivalent to "rogue wave", was introduced by Draper (1964). Rogue wave research was intensified when in 1995 the so-called New Year Wave with a crest-to-trough height of 25.6 m and a crest height of 18.5 m, with a reference significant wave height of approximately 12 m, hit the Draupner platform off the Norwegian coast, for which evidence was seen in laser measurements (Haver and Andersen, 2000). The platform owner made the measurement data publicly available (Trulsen, 2018), which offered the scientific community the possibility to study and model the sea state accompanying the New Year Wave (Soares et al., 2003; Adcock et al., 2011, e.g.). Furthermore, the famous wave could be reproduced in wave tanks (McAllister et al., 2018, e.g.) and numerical studies (Fedele et al., 2016, e.g.). Rogue waves have been discovered both in the open ocean, in shallow water and in coastal areas (Baschek and Imai, 2011, e.g.). They have been recorded in various field studies by radar devices (Karmpadakis et al., 2020, e.g.), laser altimeters (Stansell, 2004, e.g.), surface-following buoys (Häfner et al., 2021, e.g.) and ADCP measurements (Fedele et al., 2019).

Already Draper (1964) elaborated on the occurrence probability of rogue waves and came to the conclusion that it can be estimated by the statistics of a stationary random process. Haver and Andersen (2000) posed the question whether rogue waves according to the equations 1 and 2 are "Rare Realizations of a Typical Population or Typical Realizations of a Rare Population" (Haver and Andersen, 2000). In an area like the southern North Sea, which is highly frequented by ship traffic (Savvopoulos and Cerquenich, 2021) and characterised by a rapid expansion of the offshore energy sector (Freeman et al., 2019), it is crucial to know whether rogue waves are to be expected more often than predicted in a stationary random process. While this knowledge is of great interest for the safety of humans at sea, it might additionally bear a hint on possible rogue wave generation mechanisms.

Commonly used wave height and crest distributions were developed under the assumption of a stationary random and Gaussian-distributed sea state. Under the additional assumption that the surface elevation process is narrow-banded, which means that the frequencies of the wave components in this process are comparable, wave heights may be described by a Rayleigh distribution (Longuet-Higgins, 1952). The Rayleigh distribution is a special case of the Weibull distribution. A large number of studies have been conducted that compare measured rogue wave occurrence frequencies to the theoretically deduced Rayleigh distribution. Depending on the applied measurement instrument and the area of interest, their authors have come to different conclusions. While some studies found rogue wave occurrence frequencies close to the expectations of a Rayleigh or the more general Weibull distribution, others found them overestimated or under-predicted by common distributions (Table 1.1). Some authors stated that the unlikeliness of rogue wave events strongly depends on the length of the record (Forristall, 2005; Mendes et al., 2021, e.g.). Tayfun (2008) for instance came to the conclusion that the largest measured waves would not appear that unusual in a longer record.

While the scientific effort of the past decades has on the one hand been dedicated to the observation and documentation of the frequency of rogue wave occurrences, on the other hand attempts have been made to explain rogue wave occurrence beyond the expectations of common wave height and crest distributions. Different mechanism have been proposed to explain rogue wave dynamics in deep water. One common explanation assigns the formation of deep-water rogue waves to the dispersive focusing of wave energy (Kharif and Pelinovsky, 2003, e.g.). Dispersive focusing describes the interaction of waves traveling at different velocities and/or in different directions, which temporarily produces a high concentration of wave energy at a specific location (Donelan and Magnusson, 2005, e.g.). Dispersive focusing is based on the linear wave theory for a Gaussian sea, that is, rogue waves form as a result of the linear superposition of phase-coherent wave components. A number of measurement studies that found rogue wave occurrence frequencies in agreement with the common distributions, came to the conclusion that dispersive focusing is the most probable mechanism of rogue wave formation in the ocean (Christou and Ewans, 2014, e.g.). Some authors mentioned the slightly nonlinear nature of ocean waves and stated that rogue wave occurrence may be enhanced by second-order bound nonlinearities, in addition to the linear superposition of waves (Tayfun, 2008; Fedele et al., 2016, 2019, e.g.). Second-order bound nonlinearities are not directly generated by wind, but they are rather produced by longer waves, for instance as nonlinear distortions or in the form of turbulence due to wave breaking (Kinsman, 1965).

Another possible mechanism of rogue wave generation is spatial focusing. It describes the interaction of waves with currents or a varying bathymetry (Peregrine, 1976). This interaction induces a nonlinear instability to the waves (Janssen and Herbers, 2009): an opposing current forces the wave steepness to increase. The interaction of waves with opposing currents results in a higher rogue wave occurrence probability than that of a Gaussian sea state (Toffoli et al., 2015). The discussion on the effect of spatial focusing on rogue wave occurrence dates back to the early days of rogue wave research. In the Agulhas

Current off the coast of South Africa, a number of encounters of ships with large rogue waves have been documented (Mallory, 1974). Lavrenov (1998) explained the regionally increased rogue wave occurrence by the interaction of waves with the opposing current. This type of spatial focusing has been reproduced in numerical simulations (Janssen and Herbers, 2009) and tank experiments (Toffoli et al., 2015). It is conceivable that some areas of the North Sea, in which tidal elevations induce strong currents, have the potential to become such rogue wave hot spots as a result of spatial focusing.

A third effect besides dispersive and spatial focusing is referred to as the modulational instability. This process causes a regular wave train to disintegrate into groups, when subjected to small sideband perturbations (Benjamin and Feir, 1967). As a result of this behaviour, the statistics of weakly nonlinear gravity waves will deviate significantly from Gaussian statistics. In deep water (defined by $kh \geq 1.36$ with the wave number $k$ and the water depth $h$), the evolution of a unidirectional and uniform wave train may be described analytically by the Nonlinear Schrödinger (NLS) equation (Onorato et al., 2001; Slunyaev, 2005). The exact solutions of the NLS equation that explain the modulational instability, are called breathers and represent large wave occurrences "out of nowhere" (Slunyaev et al., 2011). They have been suggested as a model of rogue waves in a unidirectional case (Dysthe and Trulsen, 1999). While the previously described dispersive focusing generates rogue waves as frequently as expected at random, nonlinear focusing would further increase the rogue wave occurrence frequency. Therefore, the knowledge of the occurrence frequency of rogue waves in a data set gives a hint on the potential formation mechanism of these rogue waves. The modulational instability has been frequently demonstrated mathematically and experimentally (Lake et al., 1977; Onorato et al., 2001, 2004, e.g.). However, its validity in the real ocean is still under debate (Slunyaev and Shrira, 2013). It has been argued that the preconditions for a modulational instability are unlikely to occur in wind waves (Dysthe et al., 2008). It is difficult to retrace the dynamics that led to the formation of a rogue wave measured in the ocean. One possible method is to model the sea state conditions during which the rogue wave occurred, as to evaluate the probability that a modulational instability contributed to its formation. For a number of historical rogue waves measured in the North Sea, this was done by Fedele et al. (2016), who came to the conclusion that the modulational instability is unlikely to have generated the New Year Wave and others. In a recent study, a rogue wave measured in Canada in November 2021 by a wave buoy was investigated numerically (Gemmrich and Cicon, 2022). The study concluded that the modulational instability did not contribute significantly to the generation of this rogue wave. Research concerning the applicability of the modulational instability theory to real ocean waves is still ongoing in the scientific community.

The development of a modulational instability has been shown to be limited by the water depth: in shallow water, the instability stabilises and nonlinear focusing ceases to exist (Benjamin, 1967; Janssen and Onorato, 2007). Below the depth limit of $kh = 1.36$, the wave evolution is no longer governed by the NLS equation (Osborne, 2010). Waves in shallow water experience the influence of the bathymetry (Prevosto, 1998; Soomere, 2010). The water depth is therefore included in the evolution equation for shallow-water waves, the Korteweg–de Vries (KdV) equation (Korteweg and de Vries, 1895). The solutions of the KdV equation are stable, meaning that the wave amplitude does not alter significantly when the initial wave train is perturbed. The KdV equation may be solved by means of the inverse scattering transform (IST) (Gardner et al., 1967). This method yields a nonlinear spectrum, analogous to the Fourier spectrum in the linear case (Ablowitz et al., 1974). The nonlinear spectrum consists of a continuous part, representing oscillatory waves, and a discrete spectrum of solitons. These solitons have been suggested to play a crucial role for rogue wave generation in shallow water (Zakharov and Shabat, 1974; Pelinovsky et al., 2000; Peterson et al., 2003). Shallow-water measurement studies concerning the role of solitons are rare, although a study by Osborne et al. (1991) in the Adriatic Sea indicates that solitons play a significant role for surface elevation processes in shallow water.

Knowing about rogue wave dynamics is a first step towards the prediction of rogue wave occurrences, which in turn is essential for the prevention of accidents at sea or near the shore. This dissertation intends to add a puzzle piece to the scientific question on rogue wave formation. Prior to the investigation on formation mechanisms, it must be known how frequently rogue waves are observed in the southern North Sea. The comparison of rogue wave occurrence frequencies to common wave height distributions may give a hint on probable generation mechanisms. In a first step, I derived rogue wave statistics from surface elevation measurement data during the period 2011 to 2016 at 11 sites in the southern North Sea to evaluate how uncommon rogue waves actually are in this region. Subsequently, I evaluated possible formation mechanisms separately for intermediate- and for shallow-water stations. At the intermediate-water stations, I investigated the preconditions for modulational instabilities. At shallow-water stations displaying unexpectedly high rogue wave occurrence frequencies, I investigated to what extent these could be related to the presence of solitons. The statistical overview, the investigation at intermediate-water stations and finally the analysis of shallow-water data, were documented in three research papers, which are presented in the appendices A, B and C of this thesis, respectively. In Chapter 2, I derive the underlying research questions and provide the answers given by the three articles. In Chapter 3, I discuss these answers in connection with each other and in relation to the results of other authors. In Chapter 4, I suggest further investigations of issues highlighted in this dissertation. Chapter 5 provides a concluding remark.

**Table 1.1:** Comparison of wave and crest height distributions from measurements with common distributions from the literature.

| Authors | Region | Water depth | Instrument type | Wave height distribution | Wave crest distribution |
|---|---|---|---|---|---|
| Mori et al. (2002) | Japan | 43 m | Wave gauge | Rayleigh | underestimated |
| Magnusson et al. (2003) | NS | 10-70 m | Buoy, Laser, Radar | mostly Rayleigh/ Weibull | mostly Rayleigh/ Weibull |
| Stansell (2004) | North Alwyn | 130 m | Laser | underestimated | |
| de Pinho et al. (2004) | Brazil | $\approx$ 1000 m | Buoy | underestimated | |
| Forristall (2005) | Tern | 167 m | Radar, Laser | Forristall | 2nd order simulations |
| Casas-Prat et al. (2009) | Medit. Sea | 45-74 m | Buoy | Weibull | Rayleigh |
| Baschek and Imai (2011) | US Coast | 16-550 m | Buoy | overestimated | mostly overestimated |
| Waseda et al. (2011) | Northern NS | 190 m | Radar | Forristall | |
| Christou and Ewans (2014) | mostly NS | 7-1300 m | Radar | Gaussian/ 2nd order | Rayleigh/ Forristall |
| Fedele et al. (2019) | Ireland | 37 and 45 m | ADCP | Tayfun | Tayfun |
| Karmpadakis et al. (2020) | NS | 7.7-45 m | Radar | depth-dependent | |
| Orzech and Wang (2020) | US Coast | >75 m | Buoy | overestimated | |
| Teutsch et al. (2020) | southern NS | 6.3-30 m | Buoy, Radar | Forristall | underestimated |

# 2 Rogue wave occurrence frequency and possible formation mechanisms in the southern North Sea

## 2.1 Statistical analysis

Assume a linear sea state in which the wave elevation is randomly Gaussian distributed. If this sea state in addition is narrow-banded, thus, the individual wave components possess frequencies in a comparable range, wave heights may be described by a Rayleigh distribution, which is a special case of the Weibull distribution (Longuet-Higgins, 1952). The Weibull distribution has the probability density function

$$F(x) = exp[-(x/\beta)^{\alpha}] \tag{3}$$

with the shape parameter $\alpha$ and the scale parameter $\beta$. For the Rayleigh distribution that describes the probability density distribution of the relative wave height $x = H/H_s$, the shape and scale parameters are $\alpha = 2$ and $\beta = 1/\sqrt{2}$. According to the Rayleigh distribution, rogue waves with a relative height of $H/H_s \geq 2.0$ are expected to occur approximately once in 3000 waves. If this expectation proves true in a set of measurement data, this suggests that the wave height distribution is in agreement with the theory of linear wave interaction, while nonlinear interactions play a minor role. It is worth keeping in mind that rogue waves resulting from a linear superposition do not occur more often than expected at random. Forristall (1978) analysed wave measurement data during hurricanes and empirically fitted the wave height data to a Weibull distribution. A Weibull distribution with the parameters $\alpha = 2.126$ and $\beta = 0.7218$ is now commonly referred to as the Forristall distribution. According to the Forristall distribution, a rogue wave with $H/H_s \geq 2.0$ is expected to occur only once in approximately 6000 waves. The Forristall fit shows that large waves occur less frequently in real ocean storm data than predicted by the Rayleigh distribution, which is a theoretical model. Along with the empirical distribution that may be used as a more realistic fit for the prediction of large wave heights, Forristall (1978) provided some suggestions why the occurence frequency of large waves is underestimated by the Rayleigh distribution. Firstly, the assumption of narrow-bandedness is not given in the real ocean. Secondly, and much more evidently, Forristall (1978) found real wave profiles to be skewed: crests were usually higher than troughs were deep. The Rayleigh distribution, however, describes waves with normal profiles. The skewness of wave profiles is associated with nonlinearity. Thus, by fitting the wave height distribution to realistic wave profiles, Forristall (1978) included slight nonlinear contributions. Nonlinear interactions of higher order are not specifically included in the distribution. Rogue waves in the scope of the Forristall distribution may be assumed to be the result of dispersive focusing, at most enhanced by the nonlinearity of the wave profile. It is worth noting that the Forristall distribution was developed for relative wave heights based on the spectral definition of the significant wave height, $H_s = H_{m0}$ (Forristall, 1978). The significant wave height may also be determined directly from a time series as the mean of the highest third of waves, $H_s = H_{1/3}$. $H_s = H_{m0}$ is typically 5% higher than $H_s = H_{1/3}$ (Forristall, 1978). Forristall (1978) states that the occurrence frequency of rogue waves based on $H_{m0}$ is in any case overestimated by the Rayleigh distribution. In this work, I decided to use $H_s = H_{1/3}$ in the relative wave height definition, for comparability with previous statistical measurement studies (Stansell, 2004; Waseda et al., 2011; Baschek and Imai, 2011, e.g.).

For this thesis, I had access to an extensive measurement data set from the southern North Sea, which I investigated with regard to the research question

**RQ1- Are rogue wave occurrence frequencies adequately described by common wave height distributions?**

To answer this question, I derived wave height distributions at each available measurement station by comparing the crest-to-trough wave height $H$ of each individual wave with the significant wave height $H_s$ of the underlying half-hour record. A wave in this context was defined as the surface elevation between two subsequent zero-upcrossings of the still water level. I compared wave height distributions not only by location, but also by year and month. In doing so, I was able to answer RQ1 for each of the years 2011-2016, while additionally monitoring seasonal changes in rogue wave occurrence. At the majority of stations, rogue wave occurrence frequencies were in agreement with the predictions by the Forristall distribution (Teutsch et al., 2020). While the wave height data measured at buoy stations in intermediate water usually followed the Forristall distribution closely, an interesting development was observed in the wave height distributions calculated from radar data. At the radar stations, wave heights typically followed the Forristall distribution up until a threshold of approximately $H/H_s = 2.3$. The occurrence frequency of relative wave heights above this threshold was strongly underestimated by the Forristall distribution. Therefore, in the further process of this work, I treated rogue waves above the threshold $H/H_s = 2.3$ as a separate group and called them "extreme rogue waves". This finding gave rise to a comparison of the peculiarities of buoy and radar measurements. It is conceivable that the wave buoys were not able to capture the highest wave crests correctly (Allender et al., 1989). Surface-following wave buoys possess their own Lagrangian movement, which is known to lead to an underestimation of crest heights (Seymour and Castel, 1998). Forristall (2000) described how a wave buoy might in addition miss the maximum of a crest by getting dragged through or sliding away from it. Furthermore, wave buoys are restricted by their anchoring. Then again, the fixed Eulerian radar sensors have their own vagueness issues. They may for example overestimate wave crests by mistaking spray or fog for the water surface (Grønlie, 2006). Considering that rogue crests might have been underestimated by wave buoys and overestimated by radar sensors, it is impossible to definitely determine which of the measurements is correct (Forristall, 2005). The task was additionally hampered by the fact that the investigated wave buoys and radar devices were installed in different regions of the southern North Sea.

Within the buoy and within the radar data set, slight differences in rogue wave occurrence frequencies were found among the measurement stations, which could not simply be related to the water depth (Teutsch et al., 2020). A more suitable explanation for the differences could be geographic characteristics of the sites. While some of the measurement instruments were located in the German Bight, with the coastline to their south or east, others were placed further offshore. Waves would approach the measurement devices from different directions, having experienced different bathymetric impacts. The sea state close to Helgoland, for instance, might be sheltered by the island. It has been shown that the interaction of waves with currents- here induced by the tidal range- may lead to spatial focusing and enhance the rogue wave occurrence probability (Toffoli et al., 2015). Depending on the measurement location, the influence of the tides would vary in strength.

In a recent study, Orzech and Wang (2020) observed seasonal differences in rogue wave occurrence frequencies, which they attributed to seasonal variations in the directional spread of sea states or the surface current vorticity. In the present study, however, seasonal variations were marginal. Rogue wave frequencies nearly remained constant at one station throughout the year, when related to the total number of waves (Teutsch et al., 2020). This indicates that seasonal changes in wind, wave or tidal conditions did not alter the rogue wave probability at the considered stations.

Another interesting observation revealed by the statistical analysis was a conspicuously increased rogue wave occurrence frequency at the shallow-water stations AWG and SEE, which both are characterised by a sloping bathymetry (Karmpadakis et al., 2020; Teutsch et al., 2022).

Based on the statistical evaluation of rogue waves in intermediate water, I support a conclusion formulated by L. Draper as early as 1964: "Exceptionally high waves are not curious and unexplained quirks of Nature. Their occurrence can be calculated with an acceptable degree of precision." (Draper, 1964) His conclusion suggests that rogue waves are well explained by common distributions. The buoy data in the present study reinforce this statement at most sites, at which the occurrence frequency of rogue waves was well within the predictions of the Forristall distribution. However, some stations in shallow and in intermediate water showed deviations from the Forristall distribution. Rogue wave occurrence frequencies exeeding the predictions of the Forristall distribution suggest that rogue wave generation mechanisms other than dispersive focusing were active. These mechanisms were evaluated in the in the course of this work. The results will be discussed in the following.

## 2.2 Intermediate-water rogue waves: generated by a modulational instability?

In deep water, the modulational instability that triggers a regular wave train to dissolve into groups and may provoke single waves inside the group to grow as high as three times the initial wave train (Shrira and Geogjaev, 2009), is one possible mechanism that has been proposed to explain rogue wave occurrence frequencies beyond the predictions of common distributions (Dysthe et al., 2008; Slunyaev and Shrira, 2013). In this study, the majority of time series recorded in intermediate water depths classifies as deep-water samples in mathematical terms (Teutsch and Weisse, 2022). However, here, they will be referred to as "intermediate-water samples", as to differentiate them from waves in the deep sea. In the present study, the statistical investigation revealed rogue wave occurrence frequencies to be close to the Forristall distribution in wave buoy data, while under-predicted by the Forristall distribution in radar data. For reasons described in Section 2.1, none of the measurement devices can be identified as the correct one. Following the radar results, rogue waves occurred more frequently than predicted, which demands an explanation of rogue wave formation beyond the prediction of the Forristall distribution. On the other hand, even in the buoy data not all rogue wave occurrences are necessarily a result of pure coincidence. For intermediate-water samples, the second research question is therefore given as

**RQ2- Is the modulational instability a likely mechanism for rogue wave generation in the southern North Sea?**

In this part of the work, I investigated whether the preconditions favouring a modulational instability are given at the intermediate-water stations in the southern North Sea. The question is interesting because, even though the formation of the modulational instability is robust in its mathematical derivation and has frequently been demonstrated in physical experiments (Lake et al., 1977; Onorato et al., 2004), its relevance for rogue wave generation in the real ocean remains unclear (Slunyaev and Shrira, 2013). Thus, the present work has been an investigation of the transferability of insights from numerical and physical experiments to the conditions of a real ocean. In experiments, the modulational instability is typically the result of small side-band perturbations acting on a train of monochromatic waves (Onorato et al., 2001; Slunyaev and Shrira, 2013). These are nearly impossible conditions in the fully-developed spectrum of an ocean, in which a single train of monochromatic waves is unlikely to occur. Ocean waves are rather the result of an interplay of wave components with different frequencies. Furthermore, perturbations in the ocean are, as opposed to in a controlled experiment, not small. However, experiments have shown that the development of a modulational instability is possible even when the original wave train consists of different wave components, as long as the bandwidth is small (Alber, 1978). Meanwhile, the favorable depth range for a modulational instability to occur has been extended to intermediate water (Karmpadakis et al., 2019). Therefore, it is reasonable to investigate the preconditions of modulational instability evolution in the southern North Sea, even if real spectra are not comparable with the conditions in a one-dimensional laboratory wave tank. These preconditions would be a narrow spectrum in both frequency and angular direction during rogue wave occurrence. A narrow frequency distribution implies that the wave energy in the spectrum accumulates near the peak frequency. The frequency bandwidth may therefore be calculated based on the moments of the frequency spectrum (Teutsch and Weisse, 2022). Beyond the frequency bandwidth, there is consensus amongst the community that the effect of modulational instability is strongly dependent on the directional spreading of a wave field, in a sense that it appears stronger for unidirectional waves than for short-crested waves (Gramstad and Trulsen, 2007; Janssen and Bidlot, 2009). At the buoy measurement stations, which register not only vertical, but also horizontal movement in all compass directions, it is possible to reconstruct the directional spreading of the wave energy within recorded time series. I compared the spectral bandwidth in frequency direction and the directional spreading (for buoy samples only) in time series with and without rogue wave occurrence. It became clear that the preconditions of a narrow spectrum were not given in the data set, neither during rogue wave occurrence, nor in their absence, and neither in frequency, nor in direction. In generally broad spectra, the modulational instability is unlikely to have been the guiding mechanism in rogue wave formation at the considered stations (Fedele et al., 2016). Interesting to note, however, is a result observed at this stage of the study, that height rogue waves typically occurred in a more narrow frequency spectrum than usual. For crest rogue waves, this was not the case. This narrowing of the frequency spectrum does probably not point to the presence of a modulational instability because the spectra are still broad compared to the preconditions in tank experiments (Waseda, 2006; Onorato et al., 2009). However: could a narrow frequency spectrum give a hint on the presence of a height rogue wave in the underlying time series? Such a conclusion would imply that the background field of a height rogue wave contains some information on its presence. The conclusion can only be drawn if the narrowness of the spectrum is not induced by the rogue wave itself. I ensured, by removing the rogue wave from the time series and re-calculating the directional energy spectrum, that the narrowness, compared to time series without rogue waves, was actually caused by the waves accompanying the rogue wave. Thus, it is conceivable that the background field of a height rogue wave contains some information on its presence.

To summarise the results of the investigation on RQ2, the preconditions for a modulational instability to occur were not given in the time series measured in the years 2011 to 2016 in the southern North Sea. The modulational instability is therefore unlikely to have generated the rogue waves measured at these stations. However, height rogue wave samples occurred during narrower spectral conditions than normal.

While the modulational instability is a common explanation for intermediate-water rogue waves, shallow-water rogue waves should have different causes. This will be discussed in the following.

## 2.3 Shallow-water rogue waves and the role of solitons

In shallow water, the modulational instability has been shown to play a minor role (Benjamin, 1967; Janssen and Onorato, 2007; Fernandez et al., 2014). However, the statistical analysis conducted to answer RQ1 led to the recognition that at some shallow-water stations, more rogue waves were measured than expected according to the Forristall distribution. If the modulational instability cannot have caused this increased rogue wave occurrence, other mechanisms should be responsible for the formation of shallow-water rogue waves exceeding the expectations of a random process. Wave evolution in shallow water is guided by the KdV equation (Korteweg and de Vries, 1895), which may be applied to surface elevation series measured in the space or in the time domain. In the ocean, the recording in time domain is usually preferred, as it requires only one point measurement device. Solving the KdV equation by the IST partitions the contributions of (nonlinear) oscillatory waves and solitons (Gardner et al., 1967). Solitons are identified at the eigenvalues of the solution (Peregrine, 1983) and the discrete part of the nonlinear spectrum shows the amplitudes of all identified solitons. Solitons are not waves in a common sense, with one crest and one trough in between two zero-crossings. They are special in that they do not cross the still water level, but consist of a crest only, which propagates without changes in shape or velocity (Miles, 1980). Miles (1980) quotes John Scott Russell, who in 1845 encountered a soliton and thereupon noted: "I believe I shall best introduce this phaenomenon by describing the circumstances of my own first acquaintance with it. I was observing the motion of a boat which was rapidly drawn along a narrow channel by a pair of horses, when the boat suddenly stopped -not so the mass of water in the channel which it had put in motion; it accumulated round the prow of the vessel in a state of violent agitation, then suddenly leaving it behind, rolled forward with great velocity, assuming the form of a large solitary elevation, a rounded, smooth and well-defined heap of water, which continued its course along the channel apparently without change of form or diminution of speed. I followed it on horseback, and overtook it still rolling on at a rate of some eight or nine miles an hour, preserving its original figure some thirty feet long and a foot to a foot and a half in height. Its height gradually diminished, and after a chase of one or two miles I lost it in the windings of the channel. Such, in the month of August 1834, was my first chance interview with that singular and beautiful phaenomenon." The development of the solution to the KdV equation with time eventually leads to a decay of the oscillatory part and solitons asymptotically dominate the solution (Zabusky and Kruskal, 1965). In the context of coastal zones, it has been shown (within the framework of the KdV equation) that solitons frequently emerge when waves pass a slope and reach shallow-water areas (Sergeeva et al., 2011). The authors related this enhanced soliton occurrence to an increased rogue wave probability.

By answering

**RQ3- Are solitons involved in the increased occurrence of rogue waves in shallow water in the southern North Sea?**

I assessed whether these long-persisting wave-type elements might play a role in rogue wave generation at the shallow-water stations with exceptionally high rogue wave occurrence frequencies. Soliton spectra were calculated by applying an IST to the measured time series. A discrete spectrum consisting of several solitons was found for all considered time series, with and without rogue waves, supporting the statement by Sergeeva et al. (2011), that solitons are common in shallow-water areas behind slopes. In the case of buoy SEE at Norderney, the results in Teutsch et al. (2022) suggest that solitons play a role for rogue wave generation: each recorded rogue wave could directly be associated with at least one soliton in the discrete spectrum. This was demonstrated by scaling down all measured surface elevation values between the two zero-crossings of a rogue wave, re-calculating the discrete spectrum for the modified time series and observing changes in comparison with the initial soliton spectrum. Solitons whose amplitudes changed with the reduction in rogue wave height, were associated with the rogue wave. In most cases, the associated soliton was outstanding with respect to the remaining solitons in the spectrum. I declared a soliton outstanding if it was at least 1.25 times higher than the second-largest soliton in the spectrum. In fact, the probability of observing an outstanding soliton in the discrete spectrum was higher when the time series contained a rogue wave, as opposed to normal time series. This showed to be true for crest rogue waves, but even more pronounced for height rogue waves and in particular for rogue waves satisfying both criteria. In the category of "extreme rogue waves" ($H/H_s \geq 2.3$), the vast majority of samples showed an outstanding soliton in the discrete spectrum. The study further revealed that the presence of a *strongly* outstanding soliton more than three times larger than the second-largest soliton, was an indicator for the presence of a rogue wave in the corresponding time series. Time series without rogue waves typically yielded discrete spectra with clustered solitons of comparable amplitudes.

As a supplement to Teutsch et al. (2022), I repeated the analysis for the radar station AWG, which likewise stands out by an increased rogue wave occurrence frequency. Both, SEE and AWG, are known for a sloping bathymetry, which may give rise to an increased nonlinearity of waves (Trulsen et al., 2020). At AWG, outstanding solitons in the discrete spectrum were not as common as at SEE. However, the statistical trend identified at SEE, that outstanding solitons are more typical for rogue wave than for normal time series, could be confirmed.

The investigation on RQ3 yielded the following conclusions. First of all, solitons were also found in the discrete spectra calculated from time series without rogue waves, thus, the mere presence of a soliton did not indicate the presence of a rogue wave. Secondly, each rogue wave detected in a time series could be attributed to at least one soliton, thus, solitons played a role for the presence of rogue waves. Finally, the attributed solitons were smaller in height than the rogue crests and heights themselves, hence a rogue wave was not identical with a soliton and interaction of the soliton with the oscillatory part of the spectrum is required for the formation of a rogue wave.

# 3 Discussion

The scope of this thesis included a statistical analysis of rogue wave occurrences in the southern North Sea, based on a data set containing approximately 329 million waves, including approximately 55.000 rogue waves, measured in the time period from 2011 until 2016. The statistical analysis was followed by the assessment of common explanations of rogue wave formation in deep or intermediate, as well as in shallow water. A statistical analysis of rogue wave occurrences in this area has not been presented to this extent before. It revealed that in the intermediate water depths of the southern North Sea, rogue waves are a common phenomenon. The deep-water modulational instability that has been demonstrated in numerical and physical experiments, does not seem to play a role for the generation of rogue waves in this part of the ocean. The shallow-water theory that is based on the KdV equation, however, is transferable to some shallow-water sites in the southern North Sea. At these stations, solitons seem to play a role in the increased rogue wave occurrence frequency. While the work closed some of the knowledge gaps described in the introduction by describing the rogue wave occurrence frequency in the North Sea and discussing possible contributions from different generation mechanisms, other issues arose that will be discussed in the following. Some of the issues may not be solved by the available data and further research is needed. Suggestions for future studies are given in Chapter 4.

Like all kinds of data, wave elevation measurements are subject to interpretation. At the outset of the study, I chose to define a wave as the surface elevation between to successive zero-upcrossings (as opposed to zero-downcrossings) of the still water level. This decision offered the possibility to compare results to other field studies that used the same definition (Vandever et al., 2008; Christou and Ewans, 2014; Cattrell et al., 2018). Several authors elaborated on the influence of the decision between up- and downcrossing. Sergeeva and Slunyaev (2013) reported that in a common sea state, up- and downcrossing rogue waves occur equally often. In their numerical simulations, the choice on the zero-crossing method had an effect only in very steep sea states, in which the typical rogue wave case was a high crest followed by a deep trough (Sergeeva and Slunyaev, 2013; Slunyaev et al., 2016). A wave of this shape might be identified as rogue only when applying a zero-upcrossing method. de Pinho et al. (2004) confirmed that in their measurement data set, more rogue waves were identified by zero-upcrossing than by zero-downcrossing analysis. It should be the task of an experienced sailor to determine which rogue wave shape is the most challenging at sea. A rogue wave starting out with an exceptionally high crest, followed by a deep trough, is often described as a "white wall of water" (Rosenthal, 2005). Rogue waves starting out with an exceptionally deep trough, followed by a high crest, might be just as dangerous. These are identified by zero-downcrossing analysis.

Besides, how is the exact zero-crossing instance to be defined in measurement data with discrete sampling points? If no data point records the zero-crossing exactly- should the data point before or after the crossing be chosen instead? Will one wave end and the subsequent wave begin at the exact same data point or should data points rather not be used twice? Decisions on these details will yield small differences in the significant wave height, subsequently influencing the number of waves satisfying the rogue wave criteria. When having passed the stage of wave and rogue wave definition, the selection of rogue waves is still subjective. Most authors, after having performed a quality control of their measurement data, inspect the elevation of the rogue waves visually (Casas-Prat et al., 2009; Christou and Ewans, 2014; Cattrell et al., 2018; Teutsch et al., 2020). They decide upon this visual inspection whether the course of a rogue wave is reasonable or if they have identified a spike. This assessment is to some extent subjective, the resulting number of rogue waves is affected accordingly and thus are the statistics, which especially becomes relevant in small data sets.

The comparison with previous studies is then, as in all scientific undertakings, not trivial. Each study follows its own definitions and data filtering mechanisms. Some previous studies included waves of all heights (Cattrell et al., 2018; Karmpadakis et al., 2020), others excluded the fraction of lower wave heights in a sea state (Casas-Prat et al., 2009; Stansell, 2004; Christou and

Ewans, 2014; Häfner et al., 2021). Some authors considered a wide range of water depths (Baschek and Imai, 2011; Fedele et al., 2016; Häfner et al., 2021), while others presented data from only one station, which can clearly be assigned to, for instance, deep-water conditions (Forristall, 2005; Waseda et al., 2011). While some studies used data from one measurement instrument (Waseda et al., 2011), others included different types of measurement devices (Christou and Ewans, 2014). The influence of the type of measurement instrument on the results is not always easily identified. This issue will be discussed in the following.

Throughout this study, the comparison of different measurement instruments was in a direct focus and identified possible inaccuracies that did not reflect actual physical effects. In fact, it showed in all parts of the study that the type of measurement instrument and/or the sampling frequency played a significant role for the results. This has been suspected before (Forristall, 2000; Stansell et al., 2002) and could now be substantiated by a data set consisting of different measurement data recorded in the same region. Differences between buoy and radar data were found in rogue wave occurrence frequencies, as well as in spectral parameters calculated from the data. An exact comparison of the time series from buoys and radar devices was not possible even by this extensive data set. The individual instruments were positioned too far apart to measure the exact same time series, which made it impossible to identify differences resulting from the measurement technique. The distance would not have been such a problem in swell conditions, in which waves travel long distances without significant changes in shape and may still be recognized even kilometres further downstream. In the broad-banded wind sea conditions of the southern North Sea, however, waves change too much during the propagation from one measurement instrument to the next. The solution would be the comparison of waves measured by different instruments in exactly the same position. In addition to the results described in the three research papers, I have compared measurements of a wave buoy at NS1 to the record of a radar device that was mounted 150 m further east. Even this small distance between the instruments was enough to entirely change the arrangement of wave components, which made the two time series incomparable. In addition, I had access to data from two sensors that were installed inside an additional wave buoy near the location SEE for approximately three months. Although the additional buoy was installed in sight of the original buoy SEE, it was still too far apart to record the exact same waves. Interestingly, the two sensors in the additional buoy recorded at different frequencies, which made an assessment of the influence of measurement frequency on wave heights possible. It showed that the sensor with the lower measurement frequency registered surface elevations up to 10% lower than the high-frequency sensor, which had a strong influence on the rogue wave statistics. This result is in agreement with Stansell et al. (2002), who found the wave height distribution in measurements with low sampling rates to deviate significantly from the Rayleigh distribution: an insufficient sampling rate led to an underestimation of large wave heights. Another discussion point concerning the procedure in this study is the restriction to 30 minute time windows. Focusing on windows of constant length, in which the sea state is assumed to be unchanged, is a common procedure. For the comparison of spectral parameters (Section 2.2), I regard the approach as sufficient. However, for detailed information on the actual formation of a rogue wave, one could have a more precise look at the waves immediately preceding the rogue wave. For this purpose, time windows should be arranged in a way that the rogue wave is the last wave in the window (or the first wave in the subsequent window), rather than occurring at a random point in time within the 30 minute time window. An example for this detailed approach is provided in Teutsch et al. (2020), in which the steepness and asymmetry of ten waves preceding a large rogue wave were analysed. A recent study by Häfner et al. (2021) implements this approach on a much larger scale. The authors calculated sea state parameters prior to each individual wave, using a running window. I agree with Häfner et al. (2021) that this should yield a much more complete picture of the wave climate just before and during the emergence of a rogue wave. With increasing computing and storing capacities, it should be most useful to apply this technique to measurement data sets from different parts of the ocean.

As described in Chapter 1, Haver and Andersen (2000) proposed two different criteria to define a rogue wave, one of them based on the height and one based on the crest height of an individual wave. In the investigation of RQ1, I focused on the first criterion, for which more comparison studies were available. Meanwhile, a number of studies additionally compared wave crests with the common distributions. These studies came to diverse conclusions. While some found crest heights well described by a Rayleigh distribution or located in between Rayleigh and Forristall distributions, others observed significant deviations from the common distributions (Table 1.1). In addition to the statistical evaluation in Teutsch et al. (2020), I have repeated the comparison with the Rayleigh and Forristall distributions for crest heights. The results resemble the findings of Mori et al. (2002): at the considered stations in intermediate and in shallow water, high wave crests were significantly underestimated by these distributions. A description of wave heights and crests by the same type of distribution is possible if the wave profile is uniform, thus, wave crests and wave troughs are of comparable size. If wave crests deviate from the distribution being followed by wave heights, it indicates that the wave profiles are skewed and wave crests are larger than wave troughs– an indication of nonlinearity (Forristall, 1978). The comparison with the common distributions revealed that crest rogue waves occurred more often than to be expected at random. Thus, there should be more mechanisms responsible for the formation of these rogue waves than dispersive focusing. When working on RQ2 and RQ3, I performed separate analyses of rogue waves of different categories and found that crest rogue waves behaved differently than height rogue waves. In intermediate water, the latter emerged from much narrower sea states. The preconditions for the development of a modulational instability were even more unfavourable during the occurrence of crest rogue waves. In shallow water, height rogue waves could be connected to solitons more often than crest rogue waves, indicating that solitons played a lesser role in the formation of crest rogue waves. These results are particularly interesting because breather solutions to the NLS in deep water, as well as the interaction of solitons as a possible explanation of rogue wave formation in shallow water, should lead to the formation of exceptional wave crests, not necessarily wave heights (Peterson et al., 2003; Slunyaev et al., 2011). For future works, I suggest to continue investigating crest and height rogue waves separately.

The rogue wave definition used in this work, allows some room for discussion. Many studies, including the present one, have come to the conclusion that rogue waves according to Haver and Andersen (2000)'s definition are not uncommon in the real ocean. It seems, however, that the common wave distributions discussed in this thesis do not account for the the most extreme wave events possible in the ocean. The New Year Wave at the Draupner platform, for example, possessed an exceptionally high crest, followed by a shallow trough (Haver, 2000). Both, its exceptional crest height and its unusual shape, were highly unlikely to occur according to second-order statistics (Haver, 2000). Häfner et al. (2021) suggested to apply the term "rogue wave" only to those that clearly belong to a different population, such as strongly nonlinear high waves. In this context, the New Year Wave would clearly deserve to be called "rogue".

# 4 Outlook

The present thesis has been a preparation for the task of rogue wave prediction, in that it evaluated rogue wave occurrence frequencies and discussed the possibility of proposed rogue wave mechanisms to work in the southern North Sea. The detection of rogue waves in the measurement data, and especially the manual check of their surface elevation, has been a laborious task. It is conceivable that a machine learning algorithm trained to distinguish between physical rogue waves and erroneously detected spikes could carry out this task more efficiently. Not only for the detection, but also for the prediction of rogue waves, machine learning algorithms can possibly play a crucial role. It is conceivable that some sea state characteristics are more favourable for the formation of rogue waves than others. Machine learning is possibly able to identify sea state parameters or combinations of them, that might enhance the rogue wave probability. And- probably even more relevant for the planning of offshore activities- could machine learning help to forecast rogue waves on a short-time scale? For a supply vessel approaching an offshore wind farm, it should be most useful to know the rogue wave probability within the upcoming time window, even if it is short.

The question on the involvement of nonlinear interactions in the formation of rogue waves was a major concern of this study. Indications were found that solitons played a role in the formation of the identified shallow-water rogue waves, in an interplay with oscillatory waves (Teutsch et al., 2022). The latter was presumed, but could not be validated. Evidence for the hypothesis could be provided by reversing the IST, thus, reproducing a time series from a given nonlinear spectrum. This was not possible at this stage, because the suitable code has not been developed yet, but it could be a task for the future. Evidence for the role of solitons in rogue wave formation could also be provided by additional measurements along the propagation direction of the waves. The KdV equation is an evolution equation and its predictions could be verified at a subsequent measurement buoy. Additional measurements could give an idea on how long rogue waves persist, once they have formed. This task has been initiated already: a buoy measurement field was installed off Norderney, with the original buoy SEE in the centre. Surface elevation data from the time period between May 2019 and December 2021 was recorded and is available for investigation. The setup will potentially give an indication on the influence of bathymetry changes on rogue wave formation and occurrence frequency, as suggested in Trulsen et al. (2020, e.g.). The investigation of the new measurement data will be the next step following the present work.

The influence of meteorological conditions on rogue wave occurrence has not been investigated satisfactorily. Pleskachevsky et al. (2012) suggested the presence of atmospheric open cells in cold air outbreaks, which produce a local increase in wind speed on the sea surface, to be informative on an enhanced rogue wave occurrence frequency. This theory may be substantiated by wind and temperature measurements that could be compared to the identified rogue wave frequencies.

So far, spatial focusing as a possible mechanism for rogue wave formation in the southern North Sea has not been discussed, although strong currents due to tidal elevations are present in the area (Teutsch et al., 2022). By now, current measurements are available at least at one of the stations considered in this thesis (FINO1, 2022). Together with new surface elevation measurements, these should give an indication on the influence of current velocity and direction on rogue wave occurrence.

# 5 Concluding remark

The overarching question behind this thesis was: are rogue waves really that special? It seems that in intermediate water and for broad-banded spectra, they are not. In shallow water, however, and under specific bathymetry conditions, rogue waves may occur more often than expected. These are valuable insights from an engineering point of view. For the design of offshore structures, a design wave must be defined, that the structure is required to withstand (Goda, 2000). Due to the impossibility of determining the definite maximum wave to occur in the respective region during the lifetime of the structure, the design wave is usually chosen as one with an acceptably low exceedance probability (Jahns and Wheeler, 1973). For vessels, the International Association of Classification Societies (IACS) recommends to calculate e.g. design wave bending moments or the pressure on horizontal deck plates based on a wave with a return period of 20 years (IACS, 2001). For jacket structures, the air gap between the deck and the still water level is even designed such that the wave crest with a return period of 10.000 years does not reach the deck (Haver, 2000). According to this thesis, in intermediate water, these design practices sufficiently account for the occurrence of rogue waves. For coastal defense structures in shallow water, like dikes and seawalls, wave run-up and overtopping are relevant. At present, it is recommended to estimate these factors based on a linear assumption of the sea surface elevation process (Peters and Pohl, 2020). It is common to use standard spectra based on linear theory (Holthuijsen, 2007). According to this thesis, this practice may not account for the heights and occurrence frequencies of rogue waves possible in shallow water. Engineering constructions in shallow water might therefore require stronger design criteria.

# Appendix

## A Statistical analysis

This appendix contains a paper, which has been published in the journal "Natural Hazards and Earth System Sciences" as

**Teutsch, I., Weisse, R., Moeller, J. and Krueger, O., 2020:**
**A statistical analysis of rogue waves in the southern North Sea.**
***Natural Hazards and Earth System Sciences*, 20 (10), 2665–2680,**
**https://doi.org/10.5194/nhess-20-2665-2020**


The contribution of Ina Teutsch and the other authors to this paper is as follows.
All authors contributed to the idea and scope of the paper. Ina Teutsch took conceptual decisions upon the basic definitions used in this work, like the choice of zero-crossing method and the definition of the significant wave height to be used, furthermore upon the inclusion of the full range of sea states for a comprehensive statistical analysis of rogue waves. Ralf Weisse suggested the use of the applied quality control flags. Ina Teutsch performed the quality control and the visual check of all rogue waves, as to decide whether these were actual physical waves and not spikes. Ina Teutsch initiated the analysis of the data by comparing rogue wave occurrence frequencies spatially and in time. Ralf Weisse, Jens Moeller and Oliver Krueger suggested statistical techniques. These were carried out by Ina Teutsch, this was supervised by Oliver Krueger. All authors discussed the results and suggested further evaluations. Ralf Weisse guided the work towards the investigation of seasonality and the waves in the background field. Ina Teutsch examined, based on practices used in the investigation of wave breaking, characteristics of waves directly preceding large rogue waves. Ina Teutsch wrote the draft of the paper, all authors contributed to its improvement. Ina Teutsch was supervised by Ralf Weisse.

Nat. Hazards Earth Syst. Sci., 20, 2665–2680, 2020
https://doi.org/10.5194/nhess-20-2665-2020


Natural Hazards and Earth System Sciences
Open Access

# A statistical analysis of rogue waves in the southern North Sea

**Ina Teutsch**[1], **Ralf Weisse**[1], **Jens Moeller**[2], **and Oliver Krueger**[1]

[1]Helmholtz-Zentrum Geesthacht, Max-Planck-Str. 1, 21502 Geesthacht, Germany
[2]Federal Maritime and Hydrographic Agency, Bernhard-Nocht-Str. 78, 20359 Hamburg, Germany

**Correspondence:** Ina Teutsch (ina.teutsch@hzg.de)

Received: 27 February 2020 – Discussion started: 16 March 2020
Revised: 16 July 2020 – Accepted: 24 August 2020 – Published: 9 October 2020

**Abstract.** A new wave data set from the southern North Sea covering the period 2011–2016 and composed of wave buoy and radar measurements sampling the sea surface height at frequencies between 1.28 and 4 Hz was quality controlled and scanned for the presence of rogue waves. Here, rogue waves refer to waves whose height exceeds twice the significant wave height. Rogue wave frequencies were analyzed and compared to Rayleigh and Forristall distributions, and spatial, seasonal, and long-term variability was assessed. Rogue wave frequency appeared to be relatively constant over the course of the year and uncorrelated among the different measurement sites. While data from buoys basically correspond with expectations from the Forristall distribution, radar measurement showed some deviations in the upper tail pointing towards higher rogue wave frequencies. The amount of data available in the upper tail is, however, still too limited to allow a robust assessment. Some indications were found that the distribution of waves in samples with and without rogue waves was different in a statistical sense. However, differences were small and deemed not to be relevant as attempts to use them as a criterion for rogue wave detection were not successful in Monte Carlo experiments based on the available data.

## 1 Introduction

Waves that are exceptionally higher than expected for a given sea state are commonly referred to as rogue waves (Bitner-Gregersen and Gramstad, 2016). What exactly "expected" and "exceptionally" mean is a matter of definition which is not addressed consistently throughout the literature (e.g., Dysthe et al., 2008). A common approach is to define a rogue wave as a wave whose height exceeds twice the significant wave height of the surrounding seas. Here, significant wave height refers to the average height of the highest third of the waves in a record and is intended to correspond to the height estimated by a "trained observer".

The above definition of a rogue wave is based on a criterion developed by Haver and Andersen (2000). As rogue waves are often associated with incidents and damages to ships and offshore platforms (Haver and Andersen, 2000), these authors were primarily interested in whether or not such waves represent rare realizations of typical distributions of waves in a sea state. Based on 20 min wave samples, Haver (2000) called a wave a rogue wave when it represented an outlier in reference to the second-order model commonly used in engineering design processes. He concluded that "... the ratio of wave height to significant wave height that is likely to be exceeded in 1 out of 100 cases [in a second-order process] is about 2.0" (Haver, 2000).

Since the late 1990s, there has been an increasing number of studies analyzing observed rogue waves or studying potential mechanisms for rogue wave generation. Such studies comprise the description and analysis of measurements of individual rogue wave events (e.g., Skourup et al., 1997; Haver, 2004; Magnusson and Donelan, 2013) or the description of rogue wave statistics from longer records (e.g., Chien et al., 2002; Mori et al., 2002; Stansell, 2004; Baschek and Imai, 2011; Christou and Ewans, 2014). Several studies contain attempts to identify potential physical mechanisms of rogue wave formation, such as second-order nonlinearities (Fedele et al., 2016), modulational instability (Benjamin, 1967) caused by nonlinear wave focusing (Janssen, 2003), or the directionality of the wave spectrum (Onorato et al., 2002). Soares et al. (2003) analyzed laser records from the Draupner and North Alwyn platforms in the North Sea and found that rogue waves in stormy conditions here

Published by Copernicus Publications on behalf of the European Geosciences Union.

showed higher skewness coefficients and a lower steepness than waves simulated from second-order theory. They concluded that rogue waves must result from higher than second-order models. Based on an analysis of waves from two locations in the North Sea and the North Atlantic, Olagnon and van Iseghem (2000) reported that in high sea states, extreme waves occurred more frequently in seas steeper than on average. From the analysis of a large data set, mostly from radars and lasers in the North Sea complemented with some data from other regions, Christou and Ewans (2014), on the other hand, concluded that rogue wave frequencies were not governed by steepness and other parameters describing the overall sea state. Based on analyses of laser altimeter data, Stansell (2004) described rogue wave frequencies to be only weakly dependent on significant wave height, significant wave steepness, and spectral bandwidth. Cattrell et al. (2018) emphasized that predictors for rogue wave probability can probably not be derived for an entire data set but argued that location-specific forecasts might be possible. In general, Kharif et al. (2009) concluded that the complexity of processes in the ocean makes it difficult to link the probability of rogue wave occurrences to typical sea state characteristics.

So far, there is still no generally accepted picture, and the overarching question raised by Haver and Andersen (2000) on whether rogue waves can be considered "rare realizations of a typical population" or "typical realizations of a rare population" is still being debated. To address this question, a definition of what is "typical" for a given sea state and/or location is needed. In deep water and under the assumption that the sea surface represents a stationary Gaussian process, wave heights of waves with a narrow spectrum can be shown to be Rayleigh distributed (Holthuijsen, 2007). The Rayleigh distribution represents a special form of a Weibull distribution,

$$P\left(H > cH_{\mathrm{s}}\right) = \exp\left(-\frac{c^{\alpha}}{\beta}\right), \tag{1}$$

with parameters $\alpha = 2$ and $\beta = 0.5$. Here, $P$ denotes the probability that the height $H$ of an individual wave exceeds the significant wave height $H_{\mathrm{s}}$ by a factor $c$. Forristall (1978) analyzed the frequency of large waves from 116 h with hurricane wind speeds in the Gulf of Mexico. He found that for these cases the Rayleigh distribution substantially overestimated the frequency of large wave heights. From his data and analyses, he estimated that a Weibull distribution with parameters $\alpha = 2.126$ and $\beta = 0.5263$ provided a better fit to the observed data. Note that in this fit, the significant wave height used for normalization was estimated as being 4 times the standard deviation of the sea surface elevation, which, especially in very shallow water, leads to lower estimates compared to the traditional definition of $H_{\mathrm{s}}$ as the average of the highest third of waves in a record. In the ocean wave literature, a Weibull distribution with these parameters is commonly referred to as the Forristall distribution. Compared to the Rayleigh distribution, it is characterized by smaller probabilities for large wave heights, the differences increasing with wave height. More complex models and distributions accounting for the effects of spectral bandwidth were developed by, e.g., Tayfun (1990) or Naess (1985).

To address the question of whether or not rogue waves represent typical realizations of such distributions, several studies compared them with data from observations. For stormy seas, Waseda et al. (2011) found that radar measurements were in agreement with expectations from a Weibull distribution with parameters close to those found by Forristall. Including both stormy and fair weather conditions, de Pinho et al. (2004) found rogue waves in the Campos Basin, Brazil, to occur more often than expected, while for coastal rogue waves, the occurrence probability was found to remain below the expectations of a Rayleigh distribution (Chien et al., 2002). Mori et al. (2002) considered the distribution of wave heights, crests, and troughs independently in the same sample. They found that wave heights closely followed the Rayleigh distribution, while the distributions of crests and troughs substantially deviated. Data from different types of instruments and different kinds of sea states were found to be located in-between Gaussian and second-order statistics (Christou and Ewans, 2014). Magnusson et al. (2003) found an agreement in the majority of their laser and buoy measurement data with Rayleigh and Weibull distributions but reported deviations from the known distributions in the upper tail. They were, however, undetermined about the significance of those deviations. Similar deviations from the Forristall distribution were reported by Forristall (2005) in which individual 30 min wave records were analyzed. When the records were combined, the data were again found to fit the Forristall distribution. These results suggest that larger samples including rogue waves might be needed to derive robust results.

In the present study, we analyze new data that have not been available for analysis before. Compared to previous studies, the data set is large, comprising 6 common years of nearly uninterrupted measurements from 11 radar stations and wave buoys located in the southern North Sea. From these data, observed wave heights were compared with Rayleigh and Forristall distributions, and seasonality, trends, and spatial correlation were assessed. Whether or not information from the background field may be derived that points towards increased rogue wave probability for given sea states was further tested.

## 2 Data and methods

### 2.1 Data

The 6 common consecutive years of sea surface elevation data from 2011 to 2016 were available from 11 measurement stations in the southern North Sea (Fig. 1). At the five stations represented by red circles, radar devices are installed

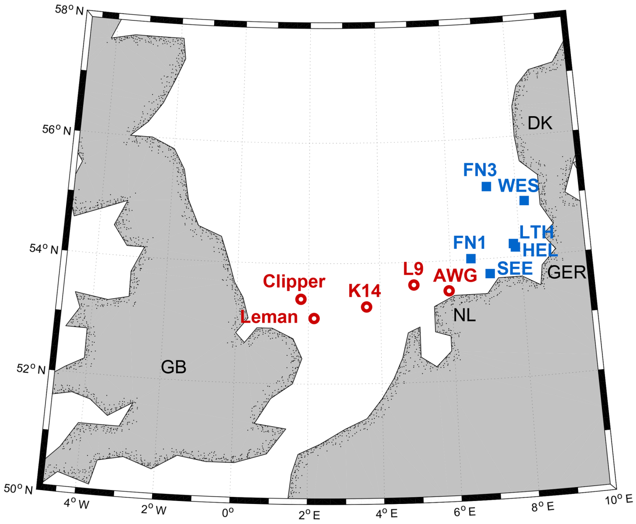


**Figure 1.** Wave measurement sites in the southern North Sea considered in this study. Blue squares: wave buoys; red circles: radar stations.

that measure the air gap to the water surface with a frequency of 2 or 4 Hz. The six blue boxes mark surface-following Datawell Directional Waverider buoys of type MkIII that measures at a frequency of 1.28 Hz. The buoy stations are located in the German Bight, while the radar stations are situated in the southern part of the North Sea off the Dutch coast and towards Great Britain. Table 1 provides an overview of the positions of the measurement stations and the water depth at each position.

The buoys delivered their data in the form of surface elevation samples, each of which had a length of 30 min (1800 s). Radar data were available as continuous time series. For comparison, they were also split into half-hour samples. In total, the procedure yielded approximately 797 000 half-hour samples from 6 years of observations at the 11 stations (Table 2). Subsequently, all buoy and radar samples were treated equally.

In the following, a wave was defined as the course of the sea surface elevation in the time interval between two successive zero upcrossings. This way, a total of approximately 329 million individual waves were derived from the 797 000 samples. Parameters describing the distribution of waves are found to be unaffected by the choice of upcrossing or downcrossing approaches (Goda, 1986).

## 2.2 Quality control and rogue wave identification

Both buoy and radar data were delivered in the form of raw surface elevation data. To identify and to eliminate spikes and erroneous data, each time series was checked and tested according to a number of quality criteria. These criteria were selected such that unreasonable spikes and data should be flagged and removed, while at the same time extreme peaks that may qualify as rogue waves should be maintained. In detail, the following procedure was applied to the raw samples.

1. Data within a 30 min sample should be as complete as possible to allow for the robust estimation of sea state parameters and individual waves. Samples missing more than three data points were discarded.

2. Since data were obtained not only during stormy but also in moderate and calm weather conditions, some samples contained a very large number of small waves. It was presumed that each wave in a record should be described by at least five measurement points to be reliably counted. When $n_\mathrm{p}$ denotes the minimum number of measurement points per wave, the maximum number of waves $n_\mathrm{max}$ in a 30 min (1800 s) sample is given by $n_\mathrm{max} = 1800\,\mathrm{s}\; f_\mathrm{s} n_\mathrm{p}^{-1}$, where $f_\mathrm{s}$ denotes the sampling frequency. For data from wave buoys sampled at a frequency of 1.28 Hz, 30 min records containing more than 460 waves were thus discarded. For the radar stations recording with sampling frequencies of 2 and 4 Hz, samples containing more than 720 and 1440 waves, respectively, were excluded.

3. To eliminate influences from tides, the mean of each sample was subtracted. Subsequently, for each record, statistics such as significant wave height $H_\mathrm{s}$, zero upcrossing period $T_z$, and standard deviation $\sigma$ were calculated using the zero upcrossing method. Significant wave height was computed as the average of the highest third of the waves in a 30 min record.

4. Subsequently and based on physical reasoning, a set of error indicators (EIs) adopted from Christou and Ewans (2014) (EI 1–EI 5) and from Baschek and Imai (2011) (EI 6–EI 8) was applied. Time series were discarded if any of the error indicators were true.

   - *EI 1.* A 30 min sample included 10 or more consecutive points of equal value.
   - *EI 2.* A 30 min sample included a wave with a zero upcrossing period longer than $T_z = 25$ s. For such waves to be wind generated, extreme wind speeds exceeding hurricane strength over a fetch of more than 4000 km for several hours would be required (WMO, 1998, p. 44), which appears unrealistic over the North Sea.
   - *EI 3.* The limit rate of change $S_y$ of the water surface was exceeded. According to Christou and Ewans (2014), the limit rate is given by $S_y = 2\pi\sigma\overline{T_z}^{-1}\sqrt{2\ln N_z}$, where $\sigma$ represents the standard deviation of the surface elevation in the 30 min sample and $\overline{T_z} = N(f_\mathrm{s} N_z)^{-1}$ denotes the mean zero upcrossing period. In the latter, $N$ denotes the number of elevation points, $f_\mathrm{s}$ again the sampling rate, and $N_z$ the number of zero upcrossings in the sample.

**Table 1.** Position and water depth $h$ at the measurement sites. In addition, typical ratios between water depth and wavelength $L$ are shown as $kh = 2\pi L^{-1}h$.

| Station name | Abbreviation | Latitude | Longitude | Water depth | $kh$ range |
|---|---|---|---|---|---|
| AWG | AWG | 53.493° | 5.940° | 6.3 m | 0.411–7.913 |
| L9 | L9 | 53.613° | 4.953° | 24 m | 1.140–24.636 |
| K14 | K14 | 53.269° | 3.626° | 26.5 m | 1.157–27.479 |
| Leman | Leman | 53.082° | 2.168° | 34 m | 2.344–40.857 |
| Clipper | Clipper | 53.458° | 1.730° | 21 m | 1.228–24.428 |
| Fino 3 | FN3 | 55.195° | 7.158° | 25 m | 1.141–6.615 |
| Westerland | WES | 54.917° | 8.222° | 13 m | 0.716–3.447 |
| Heligoland North | LTH | 54.219° | 7.818° | 30 m | 1.457–7.937 |
| Heligoland South | HEL | 54.160° | 7.868° | 20 m | 1.135–5.292 |
| Fino 1 | FN1 | 54.015° | 6.588° | 30 m | 1.213–7.937 |
| Norderney | SEE | 53.748° | 7.104° | 10 m | 0.689–2.684 |

**Table 2.** Number of available half-hour samples ($\times 10^4$) in 2011–2016 at each station after quality control (see Sect. 2.2). Measurement frequencies are indicated by font style: 1.28 Hz (normal text), 2 Hz (bold), 4 Hz (italic). The bottom row indicates data availability per year (in %).

| Station/year | 2011 | 2012 | 2013 | 2014 | 2015 | 2016 | Total |
|---|---|---|---|---|---|---|---|
| AWG | **1.70** | *1.76* | *1.72* | *1.74* | *1.75* | *1.75* | 10.42 |
| L9 | **0.96** | *1.46* | *1.75* | *1.75* | *1.75* | *1.75* | 9.42 |
| K14 | **1.74** | *1.75* | *1.75* | *1.75* | *1.75* | *1.75* | 10.49 |
| Leman | **1.73** | *1.60* | *1.74* | *1.75* | *1.75* | *1.75* | 10.32 |
| Clipper | **1.69** | **1.70** | **1.60** | **1.70** | **1.71** | **1.71** | 10.11 |
| FN3 | – | 0.76 | 1.21 | 1.07 | 1.51 | 1.16 | 5.71 |
| WES | – | 0.28 | 0.93 | 1.01 | 1.15 | 1.08 | 4.45 |
| LTH | 0.78 | 1.24 | 1.07 | 1.06 | 0.75 | 0.85 | 5.75 |
| HEL | – | 0.43 | 0.98 | 0.19 | – | 0.39 | 1.99 |
| FN1 | 1.21 | 1.26 | 1.13 | 0.85 | 1.24 | 0.87 | 6.56 |
| SEE | 0.54 | 0.82 | 0.71 | 0.84 | 1.04 | 0.99 | 4.94 |
| Data availability | **54 %** | **68 %** | **76 %** | **71 %** | **75 %** | **73 %** | **69 %** |

The criteria were applied for both the surface elevation and its acceleration.

- *EI 4*. The energy in the wave spectrum at frequencies below 0.04 Hz (periods larger than 25 s) exceeded 5 % of the total wave energy.
- *EI 5*. The energy in the wave spectrum at frequencies above 0.60 Hz exceeded 5 %. These waves are too short to be captured by five or more measurements at sampling frequencies of 1.28 or 2 Hz.
- *EI 6*. The sample included at least one data spike for which the vertical velocity of the surface exceeded $6\,\mathrm{m\,s^{-1}}$.
- *EI 7*. The ratio between the magnitudes of vertical and horizontal displacements exceeded a factor of 1.5 which, in deep water, is indicative of unexpected deviations from the orbital motions of the water particles.
- *EI 8*. At least one wave height in the sample exceeded the water depth.

5. The remaining samples were tested for the presence of rogue waves. They were considered to contain rogue waves if at least one of the waves in the sample fulfilled the criteria of Haver and Andersen (2000):

$$\frac{H}{H_s} \geq 2 \text{ and/or } \frac{C}{H_s} \geq 1.25, \tag{2}$$

   where $H$ and $C$ denote the individual wave and crest height, respectively.

6. The detected rogue wave should again be described by at least five measurement points in order to be considered further.

7. Eventually, all remaining rogues underwent a subjective visual check to ensure that all spurious extremes were removed.

Applying these criteria, in total approximately 28 % of the buoy samples and 15 % of the radar samples were eliminated and discarded from further analyses.

## 3 Results

Rogue waves refer to exceptionally high waves within a given sea state in which the state of the sea is commonly characterized by the significant wave height $H_s$. Whether or not a wave qualifies as a rogue under the definition of Haver and Andersen (2000) thus does not directly depend on its height but on its height relative to the height of the prevailing waves characterized by $H_s$. Rogue waves may hence occur in heavy seas but also during moderate or relatively calm conditions. Because the largest waves have the largest impact, many studies have focused on the analysis of extreme cases only, which is the analysis of rogue waves for large $H_s$ (e.g.,

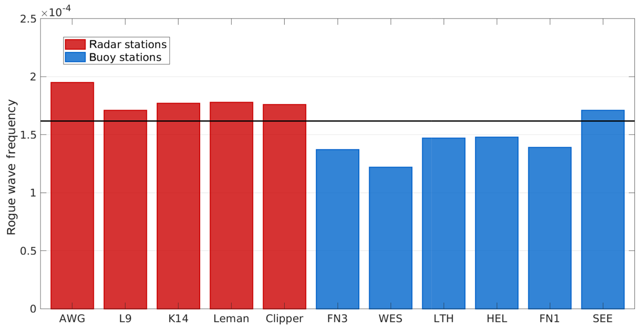


**Figure 2.** Rogue wave frequency in 2011–2016 at the 11 radar (red) and buoy (blue) locations. The solid black line indicates the rogue wave frequency ($1.62 \times 10^{-4}$) derived from the Forristall distribution (Forristall, 1978).

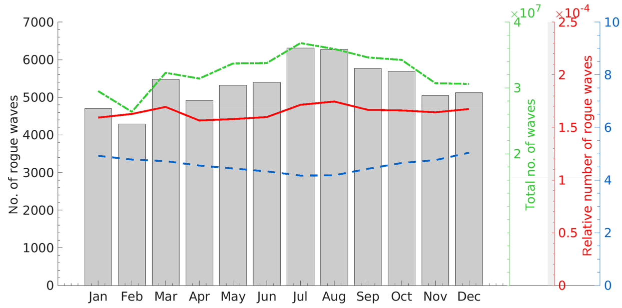


**Figure 3.** Seasonal distribution of rogue wave frequency (red), total number of waves (green), and rogues waves (gray bars) in the period 2011–2016 and of monthly mean zero upcrossing wave periods (blue) based on data from all measurement sites. Note the different scales and $y$ axis for the different parameters.

Forristall, 1978; Soares et al., 2003; Stansell, 2004; Waseda et al., 2011). Unlike these studies, in the following, we use all available data from all sea states, which is to say also cases with rogue waves from small or moderate sea states. In some cases, when only rogue waves during high sea states are considered, this is explicitly mentioned. We generally analyzed the number of rogue waves in relation to the total number of individual waves, which in the following is referred to as rogue wave frequency.

### 3.1 Spatial distribution of rogue wave frequencies

Rogue wave frequency observed at the different stations within the period 2011–2016 varied between $1.24 \times 10^{-4}$ at WES and $1.95 \times 10^{-4}$ at AWG (Fig. 2). This corresponds on average to about 1.24 and 1.95 rogue waves in every 10 000 waves. Generally, rogue waves were detected more frequently in the radar than in the buoy samples. At all radar stations, rogue wave frequency exceeded the values expected from a Forristall distribution (Fig. 2), while, with the exception of SEE, values at buoy locations were below expectations from a Forristall distribution. Rogue wave frequencies are larger in the western part of our analysis domain, but as all radar/buoy stations are located in western/eastern part of the domain, we cannot infer whether this is a result of the different measurement techniques or spatial location. When water depth is considered in addition (Table 1), no clear relation between rogue wave frequency and depth could be inferred.

Spatial coherence between rogue wave frequencies at the different sites was analyzed based on monthly values. Correlations were computed to test for the likelihood of joint occurrences of increased or decreased frequencies at the different stations for a given month. Only data from 2012 to 2016 were used because of larger gaps in 2011. Correlations between monthly rogue wave frequencies at the different stations varied between $-0.15$ for K14 and HEL and $+0.34$ for Leman and FN1 (Table 3). For the given sample size of $N = 60$ monthly values, these correlations are not significantly different from zero at the 95 % confidence level. This indicates that monthly frequencies of rogue waves vary independently at the different stations.

### 3.2 Temporal distribution of rogue wave frequencies

#### 3.2.1 Seasonality

Rogue wave frequency, which is to say the number of rogue waves per number of observed waves, was found to be relatively constant and to vary only little in the course of the year (Fig. 3). Even so, a considerably higher number of rogue waves were observed during late summer and early fall. In absolute numbers, these waves are not necessarily high as significant wave heights in summer and early fall are generally small. In winter, there are fewer rogue waves, but they generally occur during higher sea states and may thus have larger impacts. Moreover, wave periods are shorter in summer than in winter. Therefore, on average a 30 min sample from the winter seasons contains fewer waves than a corresponding sample from summer (Fig. 3). In total, both effects cancel each other out, and rogue wave frequency was found to be remarkably stable in the course of the year. Similar conclusions hold when the different measurement sites are analyzed individually (Fig. 4).

#### 3.2.2 Interannual variability

There was pronounced interannual variability in rogue wave frequency around its long-term mean at each measurement site (Figs. 5 and 6). Variability was found to be somewhat larger at the radar stations in the western part of our domain. The largest fluctuation where found at AWG where rogue wave frequency varied between $-27$ % and 16.5 % around the 2011–2016 mean. Variability derived from the wave buoy data was somewhat smaller with the exception of the two buoys WES and SEE, both located in relatively shallow water (Table 1). Again, there is hardly any correlation between the values at the different stations. While, for example, most

**Table 3.** Correlations between monthly rogue wave frequencies in 2012–2016 at the 11 measurement sites.

| | AWG | L9 | K14 | Leman | Clipper | FN3 | WES | LTH | HEL | FN1 | SEE |
|---|---|---|---|---|---|---|---|---|---|---|---|
| AWG | +1.00 | | | | | | | | | | |
| L9 | −0.01 | +1.00 | | | | | | | | | |
| K14 | +0.25 | +0.24 | +1.00 | | | | | | | | |
| Leman | +0.13 | +0.04 | +0.07 | +1.00 | | | | | | | |
| Clipper | +0.04 | −0.06 | +0.03 | +0.17 | +1.00 | | | | | | |
| FN3 | −0.06 | +0.11 | +0.01 | +0.05 | −0.12 | +1.00 | | | | | |
| WES | −0.07 | −0.05 | −0.07 | +0.01 | −0.13 | +0.31 | +1.00 | | | | |
| LTH | −0.12 | +0.06 | +0.07 | +0.14 | −0.04 | +0.12 | −0.01 | +1.00 | | | |
| HEL | −0.07 | +0.05 | −0.15 | −0.14 | −0.03 | +0.25 | +0.10 | +0.02 | +1.00 | | |
| FN1 | −0.05 | −0.03 | +0.04 | +0.34 | +0.17 | +0.22 | +0.06 | −0.04 | −0.09 | +1.00 | |
| SEE | −0.06 | +0.03 | −0.03 | +0.12 | +0.13 | −0.09 | −0.05 | +0.06 | +0.11 | −0.09 | +1.00 |

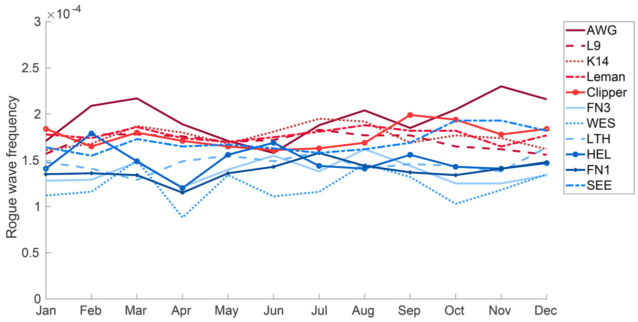


**Figure 4.** Seasonal distribution of rogue wave frequency in 2011–2016 at the 11 measurement sites. Red colors: radar stations; blue colors: wave buoys.

stations suggest a minimum in rogue wave frequency for the year 2011, it was above average at LTH. While LTH in turn showed very small frequencies in 2013, most other stations had values close to their long-term means. Whereas AWG had a maximum in rogue wave frequency in 2014, other stations showed only small anomalies, and SEE even had low values in 2014. Although rogue wave frequency in 2016 was enhanced at most stations, this was not supported by L9, Clipper, and FN1. This further supports the results from the correlation analysis of monthly rogue wave frequencies (Table 3). Despite the small distances between the measurement stations, rogue wave frequencies seem to vary independently. This suggests that mechanisms driving rogue wave variability on larger scales might be difficult to identify.

### 3.3 Comparison of observations with Rayleigh and Forristall distributions

The cumulative frequencies of occurrences of wave heights relative to the significant wave height derived from the measurements were compared to corresponding exceedance probabilities given by Weibull distributions with both Rayleigh and Forristall parameters (Fig. 7). For wave heights up to twice the significant wave height, which corresponds to the threshold used to identify rogue waves, the measurement data are well described by the Forristall distribution. At a height of $H \approx 2H_s$, the data begin to deviate from the Forristall distribution. Both distributions increasingly diverge for larger relative wave heights, $HH_s^{-1}$. This suggests that in our data, rogue waves occurred more frequently than could be expected from the Forristall distribution. The frequency of rogue waves much larger than twice the significant wave height also exceeded expectations given by the Rayleigh distribution. The figure further illustrates that for increasing relative wave heights, these findings are based on increasingly smaller samples.

To assess whether these deviations reflect a common behavior or originate from a few measurement sites only, the analysis was repeated for each station individually (Fig. 8). Substantial differences between the various sites were found. At AWG and Clipper, the frequency of waves higher than about 2 times the significant wave height increasingly deviated from the Forristall distribution, and for waves larger than about 2.7 times the significant wave height, the frequency reached or even exceeded that estimated from a Rayleigh distribution. This behavior was found to be typical for the radar sites. On the other hand and with the exception of SEE, observations from the wave buoys generally followed (e.g., LTH) or underestimated (e.g. WES) frequencies from the Forristall distribution. Thus the radar stations were mostly responsible for the strong deviation of the overall data set from the Forristall distribution for extreme waves. This again may indicate differences arising from the different measurement techniques or the region.

So far the analyses were carried out for all sea states. For design purposes and navigation or other marine operations, rogue waves in high sea states that may cause the greatest damage are generally the most interesting ones. To assess whether a similar behavior is found also for these waves, the analysis was repeated including only cases in which the significant wave height exceeded the long-term 95th percentile at each site (Fig. 9 and Table 4). Again a similar behavior for all waves was found. For smaller waves, the frequency fol-

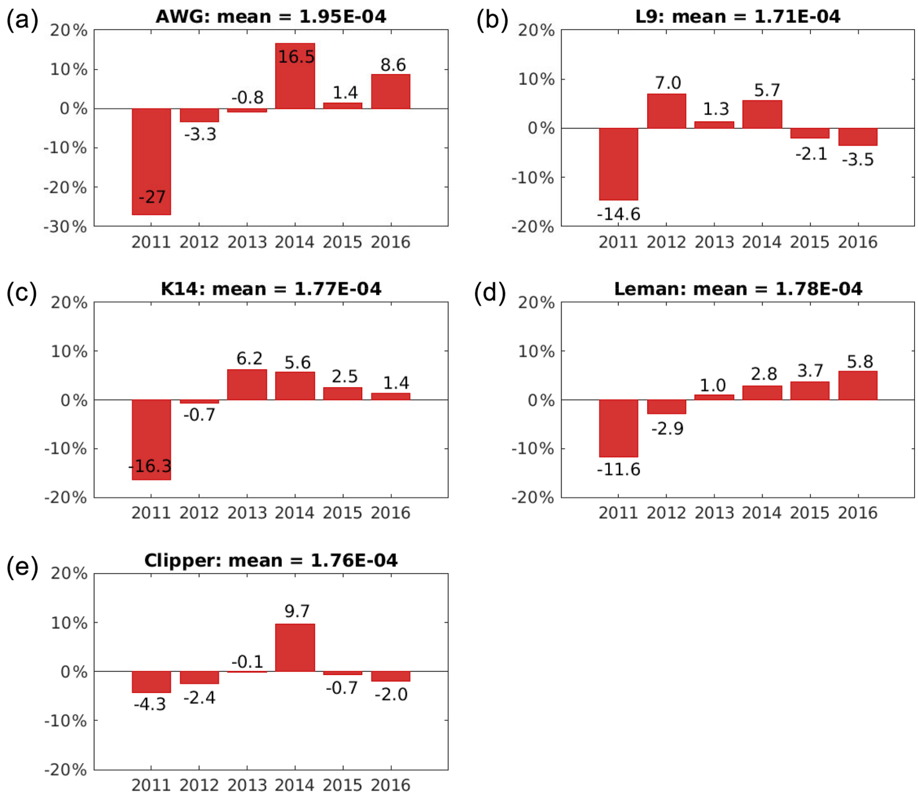


**Figure 5.** Anomalies in percent of annual rogue wave frequency relative to the corresponding long-term mean at each site for the five radar stations: AWG, L9, K14, Leman, and Clipper (from **a** to **d**).

**Table 4.** Long-term 95th percentile of significant wave height at each site.

| Station name | AWG | L9 | K14 | Leman | Clipper | FN3 | WES | LTH | HEL | FN1 | SEE |
|---|---|---|---|---|---|---|---|---|---|---|---|
| $H_s$ | 1.84 m | 3.04 m | 2.95 m | 2.37 m | 2.36 m | 3.18 m | 2.37 m | 2.86 m | 2.47 m | 3.19 m | 2.25 m |

lows a Forristall distribution. The frequency of larger waves is substantially increased, in particular for rogue waves exceeding about 2.2 times the significant wave height. Again, the data from the radar stations accounted for most of the deviation, while data from the buoys followed the Forristall distribution more closely.

In summary, while results from the buoys (with the exception of SEE) suggest that rogue waves did not occur more frequently than could be expected from a Forristall distribution and thus could be considered typical rare realizations within a given sea state, results from the radar measurements pointed towards enhanced rogue wave probability which might be indicative of mechanisms not described by second-order statistics. This holds for rogue waves both in all sea states and in high sea states only.

### 3.4 Analysis of the background wave field

Data from some sites, especially the radar stations, suggested that differences between the frequency distributions derived from observations and the Forristall distribution may exist for higher relative wave heights and in particular for those qualifying as rogue waves. In the following, we distinguish between rogue waves and all other waves in 30 min samples. The latter will be referred to as the background field. The aim was to investigate whether or not in samples with and without rogue waves differences in the distribution of waves in the background field might be identified that may potentially predict rogue waves.

More specifically, the measurement data were divided into two groups of samples: Group 1 comprised all samples including at least one rogue wave exceeding twice the significant wave height, and Group 2 included all other samples. Subsequently, a third group was built from Group 1 by removing the individual rogue waves but retaining all other

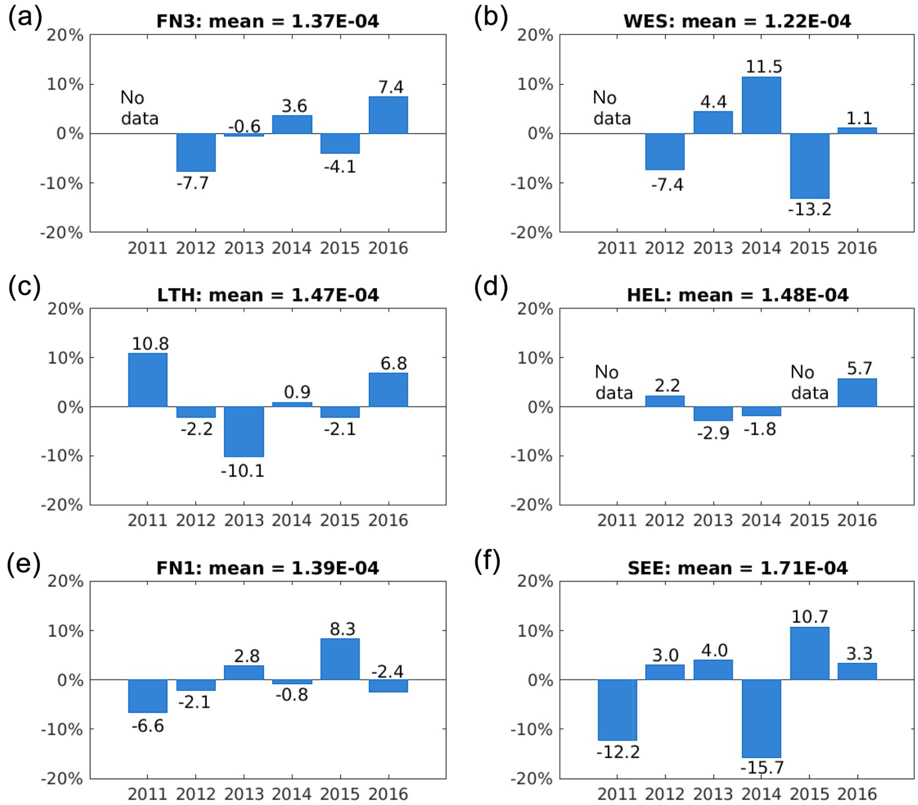


**Figure 6.** Anomalies in percent of annual rogue wave frequency relative to the corresponding long-term mean at each site for the six wave buoys: FN3, WES, LTH, HEL, FN1, and SEE (from **a** to **f**).

waves, which is to say the background field. In the following, to what extent differences in the background fields in groups 2 and 3 can be identified is assessed.

### 3.4.1 Wave height distribution in the background field

The frequency distributions of wave heights in the background field in samples with and without rogue waves were compared (Fig. 10). Visually, both distributions appear to be quite similar, and also the curve representing samples from Group 2 (normal samples not containing rogue waves) is systematically below that of Group 3 (background field of samples containing rogue waves). This is supported by comparing the moments of the distributions, with Group 2 having a slightly larger mean and being marginally more flat-topped than Group 3 (Table 5). Additionally, the skewness of both distributions is positive, with the skewness of Group 3 slightly deviating more from that of a normal distribution than Group 2.

To test whether the differences between the two groups were significant, a Kolmogorov–Smirnov (KS) test (von Storch and Zwiers, 1999) was applied. More specifically, the KS test is a nonparametric test that compares two empirical distributions and tests whether or not the null hypothesis that both distributions represent data from the same population can be rejected. The test is based on the distance $D$ between the two empirical distribution functions $F_{1,n}$ and $F_{2,m}$ (Fig. 10) such that

$$D_{n,m} = \sup_x |F_{1,n}(x) - F_{2,m}(x)|, \tag{3}$$

where sup denotes the supremum function and $n$ and $m$ denote the corresponding sample sizes. For large samples, the null hypothesis is rejected at level $\alpha$ when

$$D_{n,m} > K_\alpha \sqrt{\frac{n+m}{nm}}, \tag{4}$$

where

$$K_\alpha = \sqrt{0.5 \ln \frac{2}{\alpha}}. \tag{5}$$

**Table 5.** Moments of the relative wave height distribution shown in Fig. 10. Note that the relative wave height is nondimensional.

| | Mean | Standard deviation | Kurtosis | Skewness |
|---|---|---|---|---|
| Group 2 | 0.638 | 0.319 | 2.944 | 0.473 |
| Group 3 | 0.628 | 0.320 | 3.027 | 0.516 |

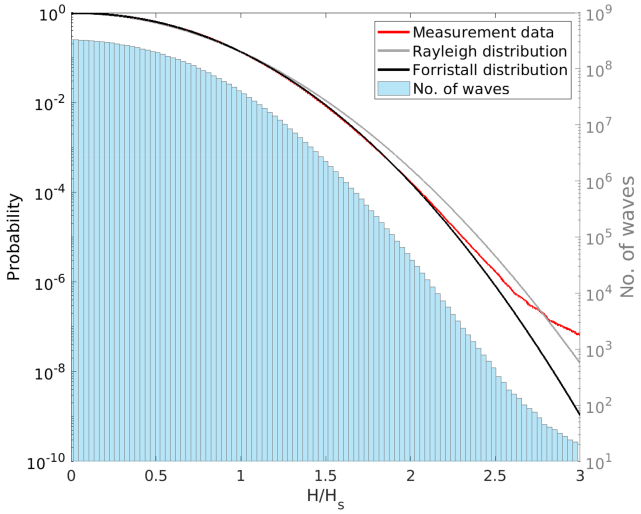


**Figure 7.** Comparison of the exceedance frequency of relative wave heights derived from observations (red) and corresponding exceedance probabilities derived from the Rayleigh (gray) and Forristall (black) distributions, together with a histogram (100 bins) of the number of available relative wave height observations (blue bars). Note the different $y$ axes for exceedance probability (left) and the number of waves ($y$) and that the $x$ axis shows relative wave height, which is to say the height of each wave relative to the significant wave height of its 30 min sample.

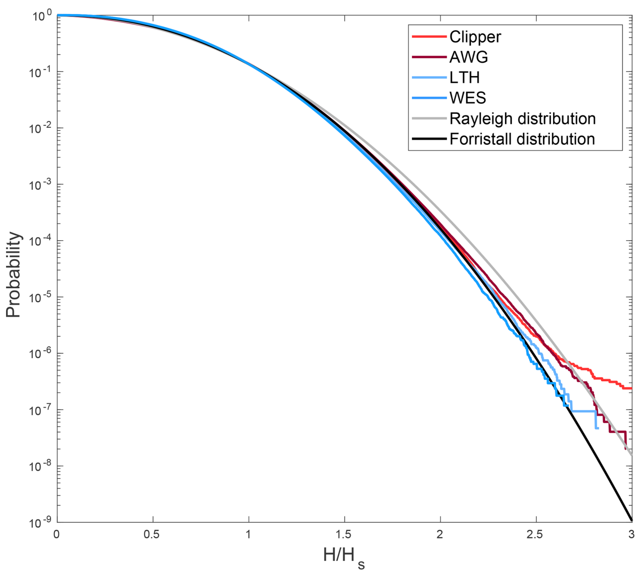


**Figure 8.** Comparison of the distributions of relative wave height at different stations to Rayleigh and Forristall distributions. On the $x$ axis, the height of each individual wave in relation to the significant wave height of its half-hour sample is given. The $y$ axis shows the probability of relative wave heights being exceeded.

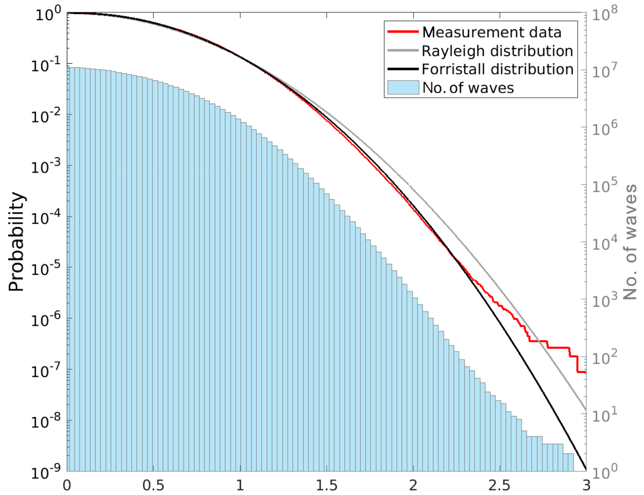


**Figure 9.** As in Fig. 7 but only including samples in which the significant wave height exceeded the corresponding long-term 95th percentile at the different sites.

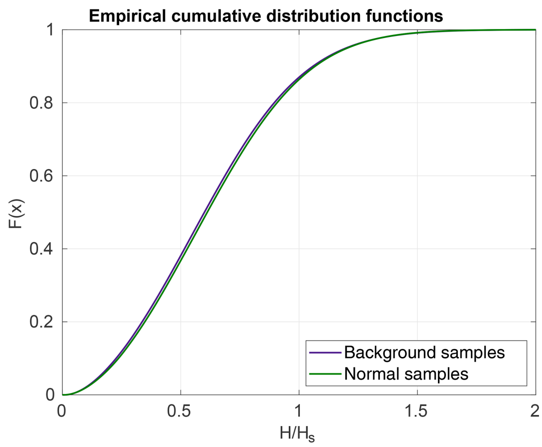


**Figure 10.** Empirical cumulative frequency distributions of relative wave heights in groups 2 (green) and 3 (purple).

For sample sizes of $n = 306\,282\,148$ waves in Group 2 and $m = 23\,073\,717$ waves in Group 3, the null hypothesis is to be rejected at $\alpha = 0.05$ when $D_{n,m}$ is greater than $2.93 \times 10^{-4}$. From the data, $D_{n,m} = 1.42 \times 10^{-2}$ was estimated, suggesting that the null hypothesis that both samples originate from the same population should be rejected at the 95 % confidence level. This indicates that although differences appear to be small, the test identified statistically significant differences between the background wave field from samples with and without rogue waves.

We suppose that this might be a consequence of the large sample sizes in which the test renders even very small differences as being significant at a given significance level. We argue that for the differences to be *relevant*, they should further bear the potential for rogue wave prediction or detection. To test this, a simple prediction/detection scheme was applied and tested for potential efficacy.

1. We split the data from groups 2 and 3 into two halves and recomputed the cumulative distribution function (cdf) of the first half.

2. From the second half, we randomly selected a 30 min sample 10 000 times. In the case of a sample containing a rogue wave, it was removed to only retain the background field. Subsequently, the empirical cdf of these data was computed.

3. Subsequently, the distances between the empirical cdf and those of Group 2 and Group 3 (step 1) were computed.

4. Based on the smaller of these distances, we predicted that a rogue wave was likely or unlikely to occur within the given sample.

5. We assessed whether or not the prediction would have been correct and marked the result accordingly.

The results and the skill of this simple exercise are shown in Fig. 11. It can be inferred that the probability of detecting a rogue wave correctly, given only the knowledge about the distribution of waves in the background field, is only about 55 % (POD $= a(a+c)^{-1}$; Wilks, 2011). The probability of false detection, $b(b+d)^{-1}$ (often referred to as false alarm rate; Barnes et al., 2009), indicating how often a rogue wave would have been detected incorrectly, is about 41 %. While this would still imply some limited skill, the probability of a false alarm, $b(a+b)^{-1}$ (often called the false alarm ratio; Barnes et al., 2009), is extremely large and exceeds 90 %. In total, the overall critical success index, $a(a+b+c)^{-1}$ (Wilks, 2011), which refers to the number of correct yes forecasts divided by the total number of occasions on which the event was forecast and/or observed, is only about 0.08. For a perfect forecast, the critical success index would be unity. This suggests that although the KS test identified statistically significant differences between the distributions of wave heights in the background field of samples with and without rogue waves, these differences appear not to be relevant as they hardly bear any potential for rogue wave detection or prediction. For an extended discussion about statistical significance and relevance, see, e.g., Frost (2017). To test whether analyses done separately for the individual stations yield different results, the exercise was repeated only for stations that showed deviations from the Forristall distributions in the upper tail. In principle, the same results were obtained. For example, the analysis of data from Clipper only yields a probability of detection of about 49 %, a probability of false detection of about 46 %, and a probability of false alarm of 93 %, which are very close to the values derived from the entire data set.

| Rogue wave forecast | Rogue wave observed: Yes | Rogue wave observed: No | Total |
|---|---|---|---|
| Yes | a= 373 | b= 3829 | a+b = 4202 |
| No | c= 310 | d= 5488 | c+d = 5798 |
| Total | a+c = 683 | b+d = 9317 | n = a+b+c+d = 10000 |

**Figure 11.** Contingency table of forecast/event pairs: a is hits, b is false alarms, c is misses, and d is correct negatives.

### 3.4.2 Wave steepness distribution in the background field

#### Mean steepness

Rogue waves are often described as exceptionally steep waves, which is to say waves whose height is large compared to their length or period (Christou and Ewans, 2014; Donelan and Magnusson, 2017). In the following, we investigate whether wave steepness differs in samples with and without rogue waves. Following the approach taken in Christou and Ewans (2014), the mean wave steepness $S$ for each sample was derived from $S = H_{\mathrm{s}}L^{-1}$, where $L$ denotes the mean wavelength in the sample. As both wave buoys and radar devices provide point measurements, $L$ is not directly available but was estimated from the wave period and the water depth by iteratively solving the wave dispersion relation. Similar to Christou and Ewans (2014), the maximum crest height in each sample was plotted as a function of mean wave steepness for samples both with and without rogue waves (Fig. 12). The analysis was performed separately for stations with a water depth of less than and more than 15 m, as well as for radar and buoy stations. Generally, the shape of the scatter plots is in agreement with the findings of Paprota et al. (2003), who showed that for increasingly higher waves, the steepness approaches values of approximately 0.06. Also, in all cases, rogue wave samples appear to be a subset of the samples without rogue waves. In other words, from the analysis, it could not be inferred that the mean steepness in a rogue wave sample exceeds that in samples without rogue waves. This holds for both wave buoys and radar stations. For the most shallow radar station, it is even inferred that while there exists a considerable number of samples with very high wave heights and steepnesses, none of those contained a rogue wave (Fig. 12a). This is consistent with the

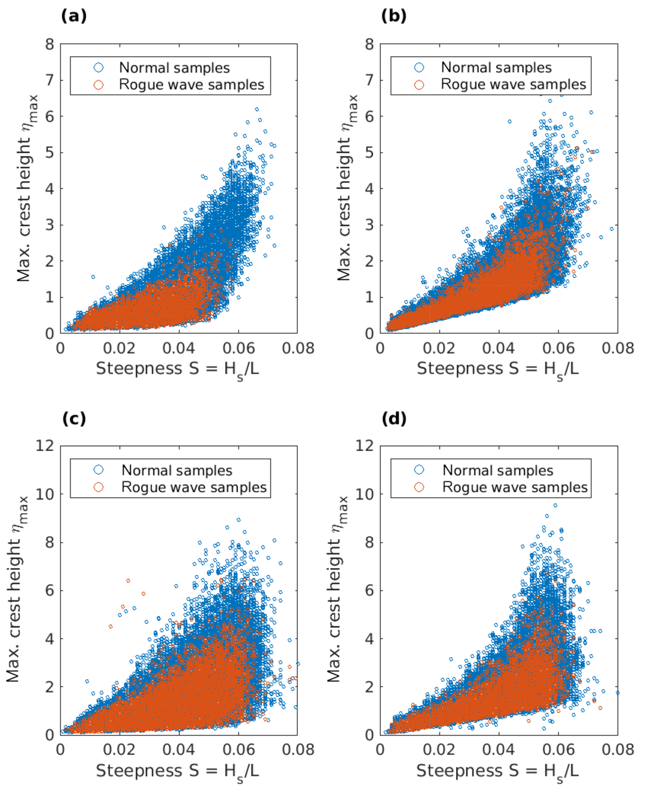


**Figure 12.** Scatter plot between mean wave steepness and maximum crest height in samples with (red) and without (blue) rogue waves. **(a, c)** Data from radar stations. **(b, d)** Data from wave buoys. **(a, b)** Data from stations with a water depth of less than 15 m. **(c, d)** Data from stations with a water depth of more than 15 m.

findings of Christou and Ewans (2014) and Paprota et al. (2003), who, for their data sets, concluded that the steepness in wave records containing a rogue wave is not significantly different from that of other records. The same results as for the entire data set were obtained when only stations that showed deviations from the Forristall distribution in the upper tail were taken into account.

#### Steepness in the vicinity of a rogue wave

While mean wave steepness was not found to systematically deviate between samples with or without rogue waves, such differences might still be limited to waves in the immediate vicinity of the rogue wave. Wilms (2017) investigated breaking waves in a hydrodynamic wave tank and observed increases in wave steepness five to six waves ahead of a breaking wave. To elaborate whether such behavior can also be found ahead of observed rogue waves in the real ocean, 1234 rogue wave samples from radar devices and 716 rogue wave samples from wave buoys were used to derive a distribution of wave steepness of individual waves ahead of the rogue wave (Fig. 13). Only severe sea states were considered; that is, only samples for which the significant wave height exceeded the corresponding long-term 95th percentile at each station were regarded . This was done as determining the shape and steepness of individual waves was more robust and reliable for high waves with large periods.

For both radar and wave stations, the rogue waves themselves stick out as waves of strongly increased wave steepness on the order of about twice that of the preceding waves. The distributions of the 2–10 waves ahead of the rogue wave were not peculiarly noticeable. All of them were characterized by almost constant median steepnesses ranging between about 0.037 and 0.041 at radar and between about 0.032 and 0.034 at wave buoy locations. Only the waves directly ahead of the rogue wave showed a tendency towards increased wave steepness (0.054 and 0.036 for radar and buoy stations, respectively). However, the latter strongly depends on the choice of the method used to define the waves. In our analyses, a zero upcrossing approach was used. In this case, the trough preceding a rogue wave is considered to be part of the wave ahead. If zero downcrossings would have been used instead, the wave trough preceding the rogue wave would have been treated as part of the rogue wave itself. Since the wave trough ahead of a rogue wave is usually not as deep as the one following it, this would have led, in most cases, to a decrease in the steepness of the rogue wave and its preceding wave. Consequently, such a definition would have supported the conclusion that also the steepness of the wave immediately ahead of the rogue wave is not outstanding compared to the others.

### 3.4.3 Asymmetry of waves preceding rogue waves

For steep waves such as rogue waves, due to nonlinear wave–wave interactions, higher wave crests are expected compared to second-order theory (Forristall, 2005; Christou and Ewans, 2014). This results in asymmetric waves in which the asymmetry $\mu$ can be described as the ratio between crest height $C$ and wave height $H$. For linear sine waves, the asymmetry is $\mu = 0.5$; for second-order Stokes waves in deep water, it is $\mu = 0.61$ (Wilms, 2017). The parameter $\mu$ is commonly used for the description of the geometry of breaking waves (Kjeldsen and Myrhaug, 1980). According to Kjeldsen and Myrhaug (1980), the asymmetry of breaking waves may reach values of up to $\mu = 0.84$–$0.95$. For rogue waves, Magnusson and Donelan (2000) stated that they are characterized by pronounced crest-to-trough asymmetries similar to breaking waves. From wave tank experiments, Wilms (2017) concluded that increased asymmetries may occur five to six waves ahead of breaking waves.

Using the same rogue wave samples of 1234 radar and 716 buoy data as above for which the significant wave height exceeded the long-term 95th percentile, the distributions of wave asymmetries of the waves preceding the rogue waves were computed (Fig. 14). Generally and on average, for both radar and wave buoy stations, asymmetries of the 2–10 waves preceding the rogue wave were close to the value of $\mu = 0.5$

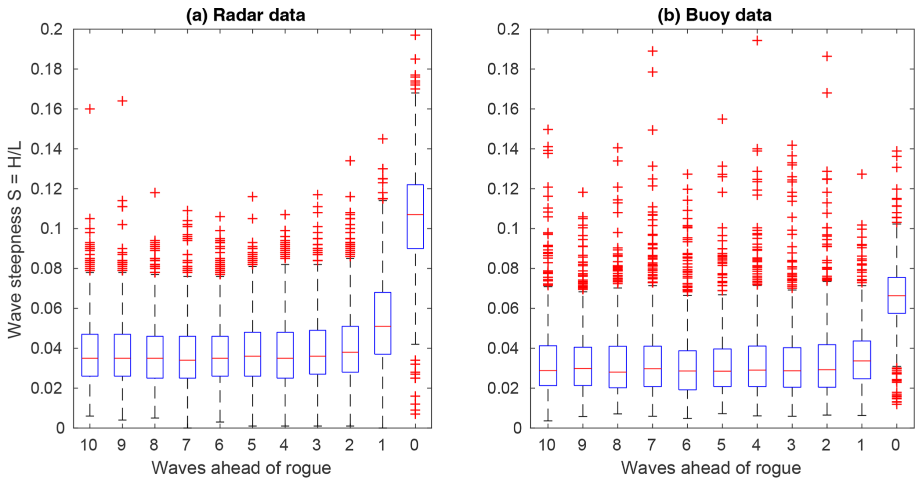


**Figure 13.** Distribution of wave steepness of the 10 individual waves preceding a rogue wave (wave 0) for radar **(a)** and wave buoy **(b)** locations. Distributions were obtained from 1234 (716) rogue wave samples at radar (buoy) locations for which the significant wave height exceeded the corresponding long-term 95th percentile. Distributions are shown as box-and-whisker plots (median: red line; box: interquartile range; whiskers: 1.5 times the interquartile range; red crosses: data outside the whiskers).

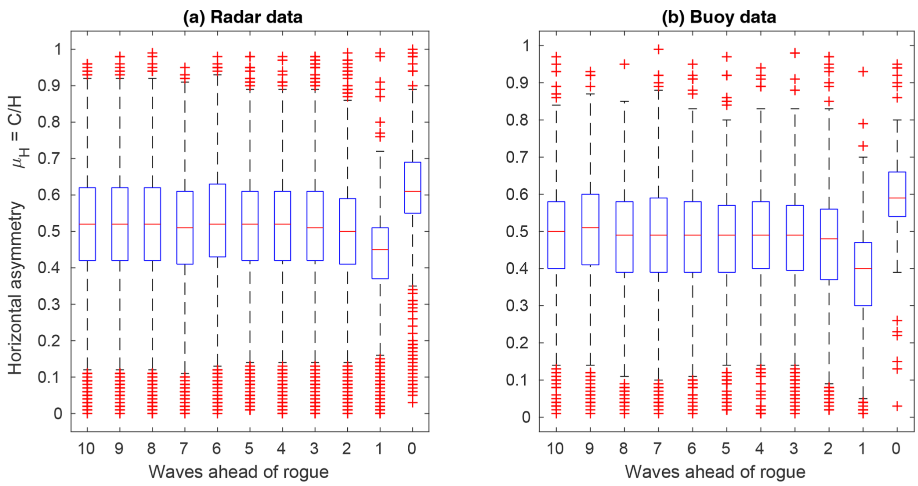


**Figure 14.** Distribution of asymmetry of individual waves ahead of rogue waves (wave 0) for radar **(a)** and wave buoy **(b)** locations. Distributions were obtained from 1234 (716) rogue wave samples at radar (buoy) locations for which the significant wave height exceeded the corresponding long-term 95th percentile. Distributions are shown as box-and-whisker plots (median: red line; box: interquartile range; whiskers: 1.5 times the interquartile range; red crosses: data outside the whiskers).

expected from linear theory. The waves immediately ahead of the rogue waves on average showed a strong decrease in asymmetry, while the asymmetry of the rogue waves themselves was increased, indicating higher crests than troughs. Again, this result strongly depends on how the individual waves were defined. The reduced asymmetry of the wave immediately ahead of the rogue wave is due to the assignment of the relatively deep trough ahead of the rogue to the preceding wave. Using a zero downcrossing analysis, this trough is assigned to the rogue wave, and the mean asymmetry remains constant at approximately 0.5 with the exception of the rogue wave itself. Additionally, it is interesting to note that the average asymmetry of waves ahead of rogue waves in our data set was usually close to $\mu = 0.5$, which represents a typical value for regular first-order waves. Furthermore, it can be inferred that the radar devices measured slightly more asymmetric and steep waves than the wave buoys. The tendency of buoys to underestimate wave crests is recognized in the literature (Allender et al., 1989; Forristall, 2000).

## 4 Discussion

The comparison of rogue wave frequencies in our data set revealed that the radar stations usually identified more rogue waves during the measurement period than the wave buoys.

Generally, all radar stations were located in the western part and all wave buoys in the eastern part of our analysis domain. By means of the available data set, it is therefore not possible to unambiguously assign these differences to either the use of different measurement devices or to the location of measurements in different regions. Generally, it is known that different wave measurement devices yield different results. Compared to other instruments, wave buoys tend to underestimate the statistics of the amplitude (Allender et al., 1989) and yield statistics below the Gaussian curve (Baschek and Imai, 2011). Possible explanations for these effects were given by Forristall (2000), who concluded that wave buoys may, on the one hand, be dragged through or slide away from (short) wave crests, which might result in missing the maximum amplitudes. On the other hand, these devices tend to cancel the second-order nonlinearities by their own Lagrangian movement and thus overestimate the mean water level, which in turn leads to an underestimation of crest heights (Forristall, 2000). Especially for steep waves which are strongly nonlinear, this leads to significant differences compared to fixed Eulerian sensors (Longuet-Higgins, 1986). In addition, it must be taken into account that wave buoys are moored and as such represent a part of a damped mechanical system. The influence of the anchoring is not clear to identify (Forristall, 2000). Radar systems looking down at the water surface, on the other hand, may overestimate crests by misinterpreting spray, breaking waves, or even fog (Grønlie, 2006). Forristall (2005) noted that there is no standard way to calibrate measurement instruments and that it is not possible to decide which instrument yields the "most correct" results. Moreover, differences may arise from different sampling frequencies. It is conceivable that wave buoys which measure at a lower sampling frequency than radar devices miss some of the wave maxima and minima. To test this, we subsampled the radar time series that were originally measured at 4 Hz with a frequency of 1 Hz, which is close to the buoy sampling frequency of 1.28 Hz. In this way, fewer rogue waves were detected than in the original time series. This was especially true for lower significant wave heights (and shorter periods) for which waves are described by fewer measurement points. This indicates that the differences in sampling frequencies can account for differences in the statistics obtained from wave buoys and radars. Because of these obvious differences that may arise from different sensors, we assume that at least large parts of the observed differences were likely caused by the different measurement techniques used. We can, however, not fully rule out that some differences in rogue wave frequencies between the different regions do exist. To address this issue, joint installations of wave buoys and radar devices at a location would be desirable.

While we assume that large parts of the observed differences in rogue wave frequencies might be attributed to the use of different sensors, there are some examples in the literature which indicate that rogue wave statistics may differ regionally, for example, due to different fetch, bathymetry, or proximity to the coast. Baschek and Imai (2011) found that rogue wave frequencies were not significantly different in deep and shallow water but were reduced in sheltered coastal oceans. Cattrell et al. (2018), on the other hand, reported that rogue wave frequencies were not spatially uniform and increased in coastal seas. In our case, there was one buoy (SEE) at which more rogue waves than expected from the Forristall distribution were identified. There are several options that may explain this behavior. These options need to be explored further. At first, the buoy is deployed at a rather shallow average water depth. This may lead to measurement issues as described above, in particular in the presence of breaking waves. Furthermore, the region is characterized by a strongly structured bathymetry with strong gradients and by strong tidal currents, both of which may contribute to a focusing of wave energy. In fact, SEE reveals very particular bathymetry conditions. Located close to the island of Norderney, the measurement buoy is placed directly above a sudden change in water depth. This stimulates shoaling and refraction leading to an increase in wave height (Goda, 2010). Trulsen et al. (2012) have shown experimentally that the propagation of waves over a slope from deep to shallow water may provoke a maximum in kurtosis and skewness. According to Trulsen et al. (2020), the behavior of waves propagating over a shoal is different in various depth regimes. Based on their findings, they anticipate a local maximum of rogue wave probability which would be in accordance with observations at SEE but would need further investigation to be fully confirmed.

We compared the relative wave height distribution in our data set to the Rayleigh and Forristall distributions. Waseda et al. (2011) found that the Forristall distribution fits well with storm wave records from the northern North Sea (190 m water depth) both when regarding the entire data set of 2723 records and when forming subsets along different significant wave heights. Over a range of sea states and from a large data set of 122 million waves in water depths between about 7 and 1311 m, Christou and Ewans (2014) found that the waves possess statistical characteristics in between linear and second-order theory. In our data, which were gathered in comparably shallow water, the distribution of wave heights in the total data set showed a fair agreement with the Forristall distribution up to a relative wave height $HH_s^{-1} \sim 2$. Rogue waves, and especially rogue waves with a very large relative wave height, occurred more often than expected from the Forristall distribution. Deviations from this distribution, however, varied across stations and between buoys and radar stations.

Our results may to some extent be affected by the choice to define a wave as the course of the sea surface elevation between two successive upcrossings or downcrossings. For rogue waves of moderate relative wave heights and wave steepness, numerical studies indicate no fundamental differences between rogue wave frequencies when upcrossing or downcrossing approaches were taken (e.g., Sergeeva and

Slunyaev, 2013). However, for extreme rogue waves whose heights exceed $8\sigma$ in very steep wave conditions, numerical simulations suggested differences in frequencies when upcrossing or downcrossing definitions were used (Slunyaev et al., 2016). For in situ measurements, de Pinho et al. (2004) reported increased rogue wave frequencies when zero upcrossing approaches were taken.

Magnusson et al. (2003) reported deviations in the upper tail of the relative wave height distribution similar to the present study, although they find the statistics of their analyzed individual wave heights from buoy and laser data at 70 m water depth to be in agreement with Rayleigh and Weibull distributions. Forristall (2005) confirmed an underestimation of large individual wave heights by his distribution when single records were considered but could not find such behavior for larger amounts of data. He concluded that "a large wave which stands out as unusual in a short record may be expected if we look long enough. [...] If we wait a long time, Gaussian statistics can produce a very large wave" (Forristall, 2005). In fact, Haver and Andersen (2000), who brought up the question of whether or not rogue waves can be considered part of a typical distribution, stated that a statistical approach based on empirical data may not be sufficient to address this question as empirical records typically contain too few rogue waves. Even in our large data set, there is only the small number of 21 cases in which relative wave heights exceeded a factor of $H H_s^{-1} \gtrsim 3$.

## 5 Conclusions

The 6 years of wave measurements from 11 measurement sites in the southern North Sea were quality controlled and analyzed for rogue wave occurrences and frequency. We found that rogue wave frequencies were relatively constant over seasons and uncorrelated between stations. We found that on average, the distribution of wave heights followed the Forristall distribution with some deviations in the upper tail, in particular for radar sites. However, deviations are based on estimates from a relatively small number of cases. While there appeared to be some differences in the wave height distribution in samples with and without rogue waves, differences were too small to be usable in rogue wave detection. Other properties such as wave steepness or wave asymmetry did not show substantial differences between samples containing a rogue wave or not. From the analyses of their data, Christou and Ewans (2014) suggested that rogue waves may simply represent rare realizations from typical distributions caused by dispersive focusing. Using a different data set, this conclusion is in principle supported by our analyses.

*Data availability.* The underlying wave buoy and radar data are the property of and were made available by the Federal Maritime and Hydrographic Agency, Germany, and Shell, UK, respectively. They can be obtained upon request from these organizations.

*Author contributions.* All authors contributed to the idea and scope of the paper. IT performed the analyses and wrote the paper. RW, JM, and OK provided help with data analysis, discussed the results, and contributed to the writing of the paper. RW supervised the work.

*Competing interests.* The authors declare that they have no conflict of interest.

*Acknowledgements.* This work was supported by the Federal Maritime and Hydrographic Agency (BSH). The buoy data were kindly provided by BSH and the Lower Saxony Water Management, Coastal Defence and Nature Conservation Agency (NLWKN). The authors are grateful to Graham Feld and Shell for providing the radar data. The authors are grateful to Christian Senet for providing Matlab code for the visualization of buoy raw data, and for his valuable input.

*Financial support.* Ina Teutsch received funding for this work from the Federal Maritime and Hydrographic Agency (BSH).

The article processing charges for this open-access publication were covered by a Research Centre of the Helmholtz Association.

*Review statement.* This paper was edited by Ira Didenkulova and reviewed by two anonymous referees.

## References

Allender, J., Audunson, T., Barstow, S., Bjerken, S., Krogstad, H., Steinbakke, P., Vartdal, L., Borgman, L., and Graham, C.: The wadic project: A comprehensive field evaluation of directional wave instrumentation, Ocean Eng., 16, 505–536, https://doi.org/10.1016/0029-8018(89)90050-4, 1989.

Barnes, L. R., Schultz, D. M., Gruntfest, E. C., Hayden, M. H., and Benight, C. C.: CORRIGENDUM: False alarm rate or false alarm ratio?, Weather Forecast., 24, 1452–1454, https://doi.org/10.1175/2009waf2222300.1, 2009.

Baschek, B. and Imai, J.: Rogue wave observations off the US west coast, Oceanography, 24, 158–165, https://doi.org/10.5670/oceanog.2011.35, 2011.

Benjamin, T. B.: Instability of periodic wavetrains in nonlinear dispersive systems, P. Roy. Soc. Lond. A, 299, 59–76, https://doi.org/10.1098/rspa.1967.0123, 1967.

Bitner-Gregersen, E. M. and Gramstad, O.: Rogue waves. Impact on ship and offshore structures, DNV GL, Strategic Research & Innovation Position Paper 05-2015, 60 pp., available at: https://www.dnvgl.com/technology-innovation/rogue-waves/ (last access: 30 September 2020), 2016.

Cattrell, A. D., Srokosz, M., Moat, B. I., and Marsh, R.: Can rogue waves be predicted using characteristic wave parameters?, J. Geophys. Res.-Oceans, 123, 5624–5636, https://doi.org/10.1029/2018jc013958, 2018.

Chien, H., Kao, C.-C., and Chuang, Z. H.: On the characteristics of observed coastal freak waves, Coast. Eng., 44, 301–319, https://doi.org/10.1142/S0578563402000561, 2002.

Christou, M. and Ewans, K.: Field Measurements of rogue water waves, J. Phys. Oceanogr., 44, 2317–2335, https://doi.org/10.1175/jpo-d-13-0199.1, 2014.

de Pinho, U. F., Liu, P., and Ribeiro, C. P.: Freak waves at Campos Basin, Brazil, Geofizika, 21, 53–67, 2004.

Donelan, M. A. and Magnusson, A.-K.: The Making of the Andrea Wave and other rogues, Sci. Rep.-UK, 7, 44124, https://doi.org/10.1038/srep44124, 2017.

Dysthe, K., Krogstad, H. E., and Müller, P.: Oceanic rogue waves, Annu. Rev. Fluid Mech., 40, 287–310, https://doi.org/10.1146/annurev.fluid.40.111406.102203, 2008.

Fedele, F., Brennan, J., de León, S. P., Dudley, J., and Dias, F.: Real world ocean rogue waves explained without the modulational instability, Sci. Rep.-UK, 6, 27715, https://doi.org/10.1038/srep27715, 2016.

Forristall, G. Z.: On the statistical distribution of wave heights in a storm, J. Geophys. Res., 83, 2353, https://doi.org/10.1029/jc083ic05p02353, 1978.

Forristall, G. Z.: Wave crest distributions: observations and second-order theory, J. Phys. Oceanogr., 30, 1931–1943, https://doi.org/10.1175/1520-0485(2000)030<1931:wcdoas>2.0.co;2, 2000.

Forristall, G. Z.: Understanding rogue waves: are new physics really necessary?, in: Proc. 14th Aha Hulikoà Winter Workshop, 25–28 January 2005, Honolulu, Hawaii, available at: http://www.soest.hawaii.edu/PubServices/2005pdfs/Forristall.pdf (last access: 30 September 2020), 2005.

Frost, I.: Statistische Testverfahren, Signifikanz und p-Werte, Springer Fachmedien Wiesbaden, Wiesbaden, https://doi.org/10.1007/978-3-658-16258-0, 2017.

Goda, Y.: Effect of wave tilting on zero-crossing wave heights and periods, Coast. Eng. Jpn., 29, 79–90, https://doi.org/10.1080/05785634.1986.11924429, 1986.

Goda, Y.: Random seas and design of maritime structures, World Scientific, World Scientific, 708 pp., https://doi.org/10.1142/7425, 2010.

Grønlie, O.: Wave radars: techniques and technologies, Sea Technol., 47, 39–43, 2006.

Haver, S.: Evidences of the existence of freak waves, in: Proc. Rogue Waves, Brest, France, available at: http://www.ifremer.fr/web-com/molagnon/bv/haver_w.pdf (last access: 30 September 2020), 2000.

Haver, S.: A possible freak wave event measured at the Draupner Jacket, 1 January 1995, in: Rogue Waves Workshop, Brest, France, 1–8, available at: http://www.ifremer.fr/web-com/stw2004/rogue/fullpapers/walk_on_haver.pdf (last access: 30 September 2020), 2004.

Haver, S. and Andersen, O. J.: Freak waves: rare realizations of a typical population or typical realizations of a rare population?, in: vol. III, Proc. International Offshore and Polar Engineering Conference, Seattle, 27 May–2 June 2000, Washington, USA, 123–130, 2000.

Holthuijsen, L. H.: Waves in oceanic and coastal waters, Cambridge University Press, Cambridge, United Kingdom, https://doi.org/10.1017/cbo9780511618536, 2007.

Janssen, P. A. E. M.: Nonlinear four-wave interactions and freak waves, J. Phys. Oceanogr., 33, 863–884, 2003.

Kharif, C., Pelinovsky, E., and Slunyaev, A.: Rogue waves in the ocean, Springer-Verlag, Berlin, Heidelberg, https://doi.org/10.1007/978-3-540-88419-4, 2009.

Kjeldsen, S. P. and Myrhaug, D.: Wave-wave interactions, current-wave interactions and resulting extreme waves and breaking waves, in: Coastal Engineering 1980, American Society of Civil Engineers, 17th International Conference on Coastal Engineering, 23–28 March 1980, Sydney, Australia, https://doi.org/10.1061/9780872622647.137, 1980.

Longuet-Higgins, M. S.: Eulerian and Lagrangian aspects of surface waves, J. Fluid Mech., 173, 683–707, https://doi.org/10.1017/s0022112086001325, 1986.

Magnusson, A. K. and Donelan, M. A.: Extremes of waves measured by a wave rider buoy and vertical lasers, in: Proc. Rogue Waves 2000, Brest, France, 17, 231–245, available at: http://www.ifremer.fr/metocean/conferences/stw_abstracts/magnusson.pdf (last access: 30 September 2020), 2000.

Magnusson, A. K. and Donelan, M. A.: The Andrea wave characteristics of a measured North Sea rogue wave, J. Offshore Mech. Arct., 135, 031108, https://doi.org/10.1115/1.4023800, 2013.

Magnusson, A. K., Jenkins, A., Niedermayer, A., and Nieto-Borge, J. C.: Extreme wave statistics from time-series data, in: Proceedings of MAXWAVE Final Meeting, 8–10 October 2003, Geneva, 231–245, available at: https://www.researchgate.net/publication/238621373_EXTREME_WAVE_STATISTICS_FROM_TIME-SERIES_DATA (last access: 30 September 2020), 2003.

Mori, N., Liu, P., and Yasuda, T.: Analysis of freak wave measurements in the Sea of Japan, Ocean Eng., 29, 1399–1414, https://doi.org/10.1016/S0029-8018(01)00073-7, 2002.

Naess, A.: The joint crossing frequency of stochastic processes and its application to wave theory, Appl. Ocean Res., 7, 35–50, https://doi.org/10.1016/0141-1187(85)90016-1, 1985.

Olagnon, M. and van Iseghem, S.: Some observed characteristics of sea states with extreme waves, in: Proc. 10th Int. Offshore Polar Engineering Conf., International Society of Offshore and Polar Engineers, 28 May–2 June 2000, Seattle, Washington, USA, 84–90, 2000.

Onorato, M., Osborne, A. R., and Serio, M.: Extreme wave events in directional, random oceanic sea states, Phys. Fluids, 14, L25–L28, https://doi.org/10.1063/1.1453466, 2002.

Paprota, M., Przewłócki, J., Sulisz, W., and Swerpel, B. E.: Extreme waves and wave events in the Baltic Sea, in: Proceedings of MAXWAVE Final Meeting, GKSS Research Center, Geesthacht, Germany, 2003.

Sergeeva, A. and Slunyaev, A.: Rogue waves, rogue events and extreme wave kinematics in spatio-temporal fields of simulated sea states, Nat. Hazard Earth Syst Sci., 13, 1759–1771, https://doi.org/10.5194/nhess-13-1759-2013, 2013.

Skourup, J. K., Andreassen, K., and Hansen, N. H. O.: Non-Gaussian extreme waves in the central North Sea, J. Offshore Mech. Arct. Eng. Aug., 119, 146–150, https://doi.org/10.1115/1.2829061, 1997.

Slunyaev, A., Sergeeva, A., and Didenkulova, I.: Rogue events in spatio-temporal numerical simulations of unidirectional waves in basins of different depth, Nat. Hazards, 84, 549–565, https://doi.org/10.1007/s11069-016-2430-x, 2016.

Soares, C. G., Cherneva, Z., and Antão, E.: Characteristics of abnormal waves in North Sea storm sea states, Appl. Ocean Res., 25, 337–344, https://doi.org/10.1016/j.apor.2004.02.005, 2003.

Stansell, P.: Distributions of freak wave heights measured in the North Sea, Appl. Ocean Res., 26, 35–48, https://doi.org/10.1016/j.apor.2004.01.004, 2004.

Tayfun, M. A.: Distribution of large wave heights, J. Waterw. Port. C., 116, 686–707, https://doi.org/10.1061/(ASCE)0733-950X(1990)116:6(686), 1990.

Trulsen, K., Zeng, H., and Gramstad, O.: Laboratory evidence of freak waves provoked by non-uniform bathymetry, Phys. Fluids, 24, 097101, https://doi.org/10.1063/1.4748346, 2012.

Trulsen, K., Raustøl, A., Jorde, S., and Rye, L. B.: Extreme wave statistics of long-crested irregular waves over a shoal, J. Fluid Mech., 882, R2, https://doi.org/10.1017/jfm.2019.861, 2020.

von Storch, H. and Zwiers, F. W.: Statistical analysis in climate research, Cambridge University Press, Cambridge, United Kingdom, https://doi.org/10.1017/cbo9780511612336, 1999.

Waseda, T., Hallerstig, M., Ozaki, K., and Tomita, H.: Enhanced freak wave occurrence with narrow directional spectrum in the North Sea, Geophys. Res. Lett., 38, L13605, https://doi.org/10.1029/2011gl047779, 2011.

Wilks, D. S.: Statistical methods in the atmospheric sciences, Elsevier, Amsterdam, Academic Press, Boston, USA, available at: https://www.elsevier.com/books/statistical-methods-in-the-atmospheric-sciences/wilks/978-0-12-385022-5 (last access: 30 September 2020) 2011.

Wilms, M.: Criteria of wave breaking onset and its variability in irregular wave trains, PhD thesis, Gottfried Wilhelm Leibniz Universität, Hannover, Germany, https://doi.org/10.15488/3520, 2017.

WMO: Guide to Wave Analysis and Forecasting, WMO-No. 702, Secretariat of the World Meteorological Organization, Geneva, Switzerland, available at: https://www.wmo.int/pages/prog/amp/mmop/documents/WMONo702/WMO702.pdf (last access: 30 September 2020), 1998.

# B Intermediate-water rogue waves

This appendix contains a paper, which has been submitted to "Journal of Physical Oceanography" as

**Teutsch, I., and Weisse, R., 2022:**

**Intermediate-Water Rogue Waves in the Southern North Sea- Generated by a Modulational Instability?**



The contribution of Ina Teutsch and the co-author to this paper is as follows.

Both authors contributed to the idea and scope of the paper. Ina Teutsch prepared the data such that only deep-water samples were included in the analysis, and decided to analyse different categories of rogue waves separately. This way, differences in wave spectral parameters for height and crest rogue samples could be identified. Both authors discussed the implications of different measurement frequencies and the benefits of sub-sampling. Ina Teutsch selected the bandwidth parameters of interest and decided upon the method to calculate directional spectra from buoy data. Ralf Weisse suggested statistical methods to deal with the discrepancy in data availability between normal and radar samples. Ina Teutsch calculated the directional spectra and the spectral parameters, and compared these to rogue wave occurrence frequencies that were identified in the first paper. Both authors discussed the results. Ina Teutsch prepared the manuscript. Ralf Weisse reviewed the manuscript and supervised the work.

# Intermediate-Water Rogue Waves in the Southern North Sea-
# The Role of Modulational Instability

Ina Teutsch,[a] Ralf Weisse,[a]

[a] *Helmholtz-Zentrum Hereon, Max-Planck-Str. 1, 21502 Geesthacht, Germany*

*Corresponding author*: Ina Teutsch, ina.teutsch@hereon.de

ABSTRACT: The role of the modulational instability for rogue wave generation in the ocean is still under debate. We investigated a continuous data set, consisting of buoy and radar wave elevation data of different frequency resolutions, from eight intermediate-water stations in the southern North Sea. For periods with rogue waves, we evaluated the presence of conditions for the modulational instability to work, that is, a narrow wave spectrum in both, frequency and angular direction. We found rogue waves exceeding twice the significant wave height indeed to occur at slightly lower frequency bandwidths than usual. For rogue waves that are defined only by high crests, this was, however, not the case. The results were dependent on the measurement frequency. The directional spreading of the buoy spectra yielded no information on the presence of a rogue wave. In general, all spectra estimated from the data set were found to be broad in frequency and angular direction, while the Benjamin–Feir index yielded no indication on a high nonlinearity of the sea states. These are unfavorable conditions for the evolution of a rogue wave through modulational instability. We conclude that the modulational instability did not play a substantial role in the formation of the rogue waves identified in our data set from the southern North Sea.

SIGNIFICANCE STATEMENT: This work investigates whether rogue waves measured at intermediate-water depths in the southern North Sea may have been generated by a modulational instability. The latter is a nonlinear mechanism of wave energy focusing that has been proven mathematically and confirmed in laboratory experiments. However, it is still unclear whether this mechanism is responsible for rogue wave generation under realistic ocean conditions. The modulational instability primarily arises when waves have similar frequencies and directions. In our data, these conditions were not satisfied. This finding leads to the insight that the modulational instability is not the most probable mechanism to generate rogue waves in this part of the ocean.

## 1. Introduction

In numerical and physical experiments, nonlinear focusing has been identified as a possible mechanism for rogue wave generation. Its role for the formation of rogue waves in the real ocean, however, remains unclear. Nonlinear focusing was first described by Benjamin and Feir (1967): due to a modulational instability, a uniform wave train in deep water may dissolve into groups, which subsequently produce one large wave that is growing at the expense of the surrounding waves. Ten years later, Lake et al. (1977) demonstrated this so-called Benjamin–Feir instability to work in wave tank experiments. Onorato et al. (2004) showed- also in a wave flume- that as the instability develops, the rogue wave occurrence frequency increases. The Benjamin–Feir instability has therefore been proposed as a possible explanation for the formation of rogue waves (Janssen 2003).

Onorato et al. (2001) investigated the effects of modulational instability numerically by applying the cubic Nonlinear Schroedinger (NLS) equation. Their results showed a dependency of rogue wave occurrence on the ratio of wave steepness to spectral bandwidth. This ratio quantifies the importance of nonlinear interactions, relative to that of dispersion in deep water, equally to the role of the Ursell number in shallow water. Based on the experimental results by Benjamin and Feir (1967) and Lake et al. (1977), Janssen (2003) introduced the so-called Benjamin–Feir index (BFI) as

$$\mathrm{BFI} = \frac{\sqrt{2}\epsilon}{\Delta\omega/\omega_0} \tag{1}$$

where $\sqrt{2}\epsilon$ represents steepness defined by the slope parameter $\epsilon = k_0 \cdot \sqrt{m_0}$. Here, $k_0$ is the mean wave number estimated from the mean frequency $f_0$ in the dispersion relation in deep water,

$k_0 = (2\pi f_0)^2/g$ with gravity $g$, and $m_0$ is the 0th moment of the frequency spectrum. $\Delta\omega$ denotes the frequency bandwidth, while $\omega_0$ is the angular frequency at $k_0$. For BFI $<< 1$, a sea state may be described by the linear superposition of sinusoidal waves, while for BFI $\geq 1$, nonlinear interactions are expected to dominate the evolution of the wave train (Alber and Saffman 1978; Onorato et al. 2001). The "BFI has been suggested as an indicator for the probability of occurrence of freak waves in the sense that large BFI means larger probability of freak waves" (Gramstad and Trulsen 2007).

Alber (1978) showed mathematically that the requirement for a Benjamin Feir–type instability to occur in a random wave field in deep water, is a sufficiently low bandwidth and small directional spreading of the wave spectrum. This has been substantiated numerically (Yuen and Ferguson 1978) and experimentally (Stansberg 1995). Waseda et al. (2009) showed in wave tank experiments that narrow-banded conditions favor an increased rogue wave occurrence.

Several authors have discussed the effect of broadening of the frequency spectrum on the distribution of wave heights and crests (Tayfun 1983; Naess 1985; Karmpadakis et al. 2020). Accounting for the spectral bandwidth in wave height and crest distributions influences the estimate of the significant wave height and the prediction of the largest wave in a wave train (Naess 1985), which both are important figures for the investigation of rogue waves. A number of parameters have been defined to describe the bandwidth of a spectrum in the frequency domain. Cartwright and Longuet-Higgins (1956) were the first to take the broadness of the frequency spectrum into account in the development of a distribution of the maximum surface elevation $\eta_{\max}$ in a time series. They introduced the parameter

$$\varepsilon = \sqrt{\frac{m_0 m_4 - m_2^2}{m_0 m_4}} : 0 < \varepsilon < 1 \tag{2}$$

with the spectral moments

$$m_n = \int_0^\infty f^n S(f) df \tag{3}$$

as a measure of the root mean square width of the (non-directional) energy spectrum $S(f)$. A wave spectrum is considered narrow-banded if $\varepsilon$ approaches zero (Cartwright and Longuet-Higgins 1956). In that case, the individual waves in the considered time series have similar frequencies and the wave energy is concentrated near the peak frequency (Cattrell et al. 2018). For an infinitely narrow spectrum with $\varepsilon = 0$, $\eta_{\max}$ is Rayleigh-distributed (Cartwright and Longuet-Higgins 1956).

In the case of a broad-banded spectrum, in which the wave energy is distributed over a wide range of frequencies and $\varepsilon \rightarrow 1$, $\eta_{\max}$ is Gaussian-distributed (Cartwright and Longuet-Higgins 1956). When describing a probability density function of the wave period, Longuet-Higgins (1975) additionally introduced the narrowness parameter

$$\nu = \sqrt{\frac{m_0 m_2}{m_1^2} - 1} : 0 < \nu < 1 \tag{4}$$

as a measure of the bandwidth. For a narrow spectrum, $\nu \approx 0.5 \cdot \varepsilon$ (Longuet-Higgins 1975). Typical values for wave conditions during a storm are $\nu \approx 0.3 - 0.5$ (Cattrell et al. 2018).

Some authors have stated a disadvantage of the parameters $\varepsilon$ and $\nu$, which is their sensitivity to high-frequency noise in the spectrum, represented by the higher spectral moments (Vandever et al. 2008; Janssen and Bidlot 2009, e.g.). This becomes problematic at low sampling rates like the buoy and radar sampling rates of $f_s$ =1.28 Hz and 2 Hz, as investigated in this study (Häfner et al. 2021a). It has also been criticized that $\varepsilon$ for a spectrum of real sea waves describes the resolution of the data sampling rather than the spectral width (Goda 1988a,b). Rye (1977) found that Goda's peakedness parameter (Goda 1970)

$$Q_p = \frac{2}{m_0^2} \int_0^{\infty} f \left[ \int_0^{2\pi} S(f, \Theta) d\Theta \right]^2 df, \tag{5}$$

as opposed to $\varepsilon$ and $\nu$, is independent of the high-frequency cutoff $f_c$. $Q_p$ is to some extent related to the spectral width parameter $\varepsilon$, but not by a simple function. While a small $\varepsilon$ is associated with a large value of $Q_p$, the value of $\varepsilon \approx 0.7$ is associated with a variety of $Q_p$ values (Goda 1970). Due to the dependency of Eq. 5 on the square of the frequency spectrum, peaks in the spectrum are emphasized. This means that the weight is transferred to wave components with a higher contribution to the total wave energy (Janssen and Bidlot 2009). Values of $Q_p$ range between 2 for fully developed wind seas and > 4 for swell (Saulnier et al. 2011).

A narrow and peaked frequency spectrum indicates regular wave conditions and more pronounced wave groups than a broad-banded spectrum. The bandwidth parameters described above are thus also a measure of wave groupiness (Holthuijsen 2007). High $Q_p$ values and low $\varepsilon$ and $\nu$ values are therefore expected in swell-dominated sea states or wave fields including wave groups.

Janssen and Bidlot (2009) showed that under the assumption of a Gaussian shape of the frequency spectrum, the BFI may also be expressed in terms of $Q_p$. Then,

$$\Delta\omega/\omega_0 = \frac{1}{Q_p\sqrt{\pi}} \tag{6}$$

and

$$\mathrm{BFI} = k_0 \cdot \sqrt{m_0} \cdot Q_p\sqrt{2\pi}. \tag{7}$$

Casas-Prat et al. (2009) successfully applied this formulation to buoy measurement data.

Besides a narrow bandwidth, another prerequisite for the modulational instability to occur is a narrow directional spreading. Numerical calculations have shown that unidirectional seas may result in much higher waves than predicted by second-order theory (Gibson and Swan 2006). This has been interpreted as an increase in the probability for rogue wave occurrences due to the modulational instability in unidirectional waves (Gramstad and Trulsen 2007). A broadening of the spectrum on the contrary leads to a reduction in rogue wave occurrence probability (Onorato et al. 2002; Waseda 2006; Janssen and Bidlot 2009). Latheef and Swan (2013) reported from a laboratory study that higher-order nonlinear effects can be important in directionally spread seas as well, provided the waves are sufficiently steep and not too short-crested. In Onorato et al. (2009)'s laboratory experiments in a 3D wave basin, waves with a directional spreading larger than $\sigma_\Theta = 15°$ showed an almost Gaussian distribution, thus, a rogue wave occurrence frequency close to the expectations of second-order theory. Waseda et al. (2009) concluded from hindcast data in the northwest Pacific that the directional spreading must be extremely low for quasi-resonant wave-wave interactions to happen. Such a formation of an extremely narrow-banded sea state has been observed, for example, when wind waves interacted with swell (Tamura et al. 2009). Waseda (2006) showed in tank experiments that the BFI was only informative on the non-Gaussianity of a sea state in very narrow-banded waves, which in the real ocean would correspond, for example, to prevailing swell conditions. From their results, it can be seen that in typical wind-wave conditions, a high BFI did not necessarily indicate the presence of a modulational instability.

Gramstad and Trulsen (2007) stated that the probability of large waves depends on both, the spectral bandwidth and the directional spreading, and recommended including both parameters in the rogue wave probability prediction. Waseda et al. (2009) also performed a combined investigation of the effects of frequency bandwidth and directional spreading. They summarized from their studies in a wave tank that while for uni-directional waves, the occurrence frequency of rogue waves increased due to quasi-resonant wave-wave interactions as the frequency bandwidth narrowed, the rogue wave probability reduced for an increased directional spreading.

Prevosto (1998) distinguished between deep and shallow water in his study based on a second-order directional irregular wave model. In deep water, he found the wave characteristics changed significantly for an increase in bandwidth, while he did not identify this effect in shallow water. He further concluded that in deep water, the unidirectional case produced the highest wave and crest heights. In shallow water, with the bottom affecting the nonlinear behaviour of waves, unidirectional conditions yielded the largest wave heights, crest heights might however be higher in directionally spread waves. Forristall (2000) supported these results. He found that in deep water, simulations taking the directional spreading into account, produced crests about 2 % lower than unidirectional simulations. In shallow water, however, waves with a narrow directional spreading were in some cases more nonlinear than unidirectional waves.

The bandwidth parameters described by Eq. 2-5 did not take the directional spreading of waves into account. Janssen and Bidlot (2009) introduced a parameter to quantify the importance of the angular width, compared to the frequency width, which may be applied as a "measure of short-crestedness for the dominant waves" (Fedele 2015):

$$R = \frac{1}{2}\frac{\sigma_\Theta^2}{\nu^2} \tag{8}$$

with the spectral bandwidth $\nu$ (Eq. 4), following Fedele et al. (2016), and the directional spreading

$$\sigma_\Theta = \sqrt{2(1-C_1)}, \tag{9}$$

using the spectrally-weighted, thus frequency-independent, averages of the first-order Fourier coefficients $a_1$ and $a_2$ with $C_1 = \sqrt{a_1^2 + b_1^2}$. Janssen and Bidlot (2009) found that when the directional spreading is larger than $\sqrt{2}$ times the frequency width (corresponding to $R = 1$, according to Eq. 8), the sea state is de-focussing and rogue waves occur less frequently than expected. They concluded that the occurrence probability of rogue waves is highest for almost unidirectional waves with a high BFI.

Dysthe et al. (2008) argued that the preconditions for a modulational instability are unlikely to occur in wind waves conditions. Also Orzech and Wang (2020) came to the conclusion that nonlinear focusing effects are "expected to reduce in the open ocean". Waseda et al. (2009) interpreted the region for quasi-resonant wave-wave interaction as a frequency bandwidth below 0.14 and a directional spreading of approximately 30° and found that these values are possible, based on hindcast data from the Sea of Japan, which include Typhoon conditions. A number of studies based on measurement data have been carried out that evaluated the broadness of wave spectra during rogue wave occurrence. Indeed, a number of authors found that the occurrence frequency of rogue waves was dependent on the spectral bandwidth in the underlying wave field. Karmpadakis et al. (2020) described, based on radar measurements in the North Sea, a reduction in wave heights with an increase in spectral bandwidth. Cattrell et al. (2018) investigated buoy data from the US coast and found that the spectral bandwidth parameters of rogue seas displayed different probability distributions than those estimated from normal seas. Christou and Ewans (2014) stated, based on radar and laser data from the North Sea and other locations, that the spectral bandwidth might be an indicator for distinguishing rogue waves from high normal waves. Most recent findings by Häfner et al. (2021b), based on machine learning algorithms applied to buoy data from the US coast, showed that the spectral bandwidth was much more informative about rogue wave probability than the BFI as a measure of nonlinear effects. They commented, however, that the spectral bandwidth acted through its correlation with the crest-trough correlation, which they identified as the key control parameter for rogue wave occurrence: a high crest-trough correlation implies that crest heights and trough depths are of comparable size, which naturally corresponds to a narrow frequency bandwidth. Since the crest-trough correlation is not applicable to crest heights, they stated that bandwidth effects were not relevant for crest rogue waves.

On the other hand, some authors have found that the rogue wave occurrence frequency was not or only weakly dependent on the spectral bandwidth (Stansell 2004, e.g.). Goda (1970) wrote, supported by numerical experiments, that wave heights defined by the zero-upcrossing method practically followed the Rayleigh distribution, independently of the spectral bandwidth. When examining the broadness parameter $\varepsilon$, Christou and Ewans (2014) found little difference between rogue wave samples and the highest normal samples. They explained the similarity with the difference between the shapes of rogue waves and the highest normal waves being nearly identical for crest and trough, and $\varepsilon$ being related to both, the local maxima and minima of the surface elevation.

Also concerning the directional spreading during rogue wave occurrence, investigations have come to different conclusions in different parts of the ocean. While Waseda et al. (2011) confirmed, based on radar measurement data from a platform in the North Sea, that on days with a high occurrence of rogue waves, the directional spreading of the wave spectrum was narrower than on other days, Christou and Ewans (2014) found no significant differences between normal samples and rogue wave samples and concluded that the environmental conditions generating normal waves, were also able to form rogue waves.

As a result, a number of authors have come to the conclusion that the modulational instability was not the main reason for the formation of rogue waves in their measurement data (Cattrell et al. 2018, e.g.). Christou and Ewans (2014) found that the difference in shape between rogue waves and the highest normal waves was not explained by nonlinear transformations. This is in agreement with theoretical work and measurements by Tayfun (2008), who concluded that the random superposition of spectral components enhanced by the presence of second-order bound modes is the most likely mechanism of the formation of rogue waves in the real ocean. Fedele et al. (2016) found, based on a large collection of field data from various locations in Europe, that the main generation mechanism of rogue waves is the constructive interference of elementary waves [dispersive and directional focusing], enhanced by second-order bound nonlinearities and not the modulational instability. They concluded that rogue waves are likely to be rare occurrences of weakly nonlinear random seas. Orzech and Wang (2020) found the BFI for rogue wave samples to be only slightly higher than for normal samples, confirming a minor role of nonlinear modulation.

Based on a field measurement data set of approximately 123.000 samples from radar stations and 63.000 samples from wave buoys in the intermediate water of the southern North Sea, our aim is to investigate whether the requirements for a modulational instability, that is, narrow bandwidth in both frequency and angular direction, is given during rogue wave occurrence. This is done in terms of the bandwidth parameters (Eq. 2-5), the directional spreading (Eq. 9) and the combined parameter $R$ for directional spreading and spectral bandwidth (Eq. 8). Finally, the BFI (Eq. 1) in our data set is evaluated and compared for time series with and without rogue wave occurrence.

The measurement area and the data set, as well as the estimation method of the directional spectrum, are described in section 2. The results of the evaluation of the bandwidth parameters and the BFI are described in section 3. In section 4, our results are related to previous experimental studies, and differences in the findings from the two different measurement devices are discussed. From the results and discussions, we draw our conclusions in section 5.

## 2. Data and Methods

### *a. Data*

Surface elevation measurement data from 2011-2016 at eight measurement stations in the southern North Sea were investigated (Fig. 1). At four of the stations, the data were provided by fixed radar devices, measuring the air-gap to the sea surface at a sampling frequency of either $f_s = 2$ Hz or $f_s = 4$ Hz. The remaining four stations are equipped with surface-following buoys of type MkIII, measuring at a sampling rate of $f_s = 1.28$ Hz. The buoy data were delivered in samples of 30 minutes duration. The radar data, which were available as continuous time series, were split into 30 minute samples accordingly.

To exclude low-energy sea states, only samples with a significant wave height $H_s$ above the long-term 70th percentile of the significant wave height at each station, $H_{s,70}$, were included in the analysis. The significant wave height $H_s$ is here defined as the mean of the highest 30 % of the wave heights in a 30 minute sample. $H_{s,70}$ was calculated from the significant wave heights $H_s$ of all 30 minute samples during the six years of available measurement data. On the one hand, this excludes possible measurement uncertainties caused by small waves that are only described by a few points, and on the other hand, it includes only rogue waves of heights relevant for offshore activities. $H_{s,70}$ is presented for each station in Table 1.

One of the requirements for the formation of a modulational instability is deep water. Unidirectional waves are expected to be modulationally unstable above a threshold of $kh = 1.363$, in which k is the wave number and h is the water depth (Benjamin 1967). In deep water, where $k = 2\pi(L)^{-1}$, the condition becomes $h(L)^{-1} > 0.22$. Inserting $L = g(2\pi)^{-1} \cdot T_p^2$, leads to the condition for the peak period

$$T_p < \sqrt{\frac{\pi \cdot h}{0.11g}} \tag{10}$$

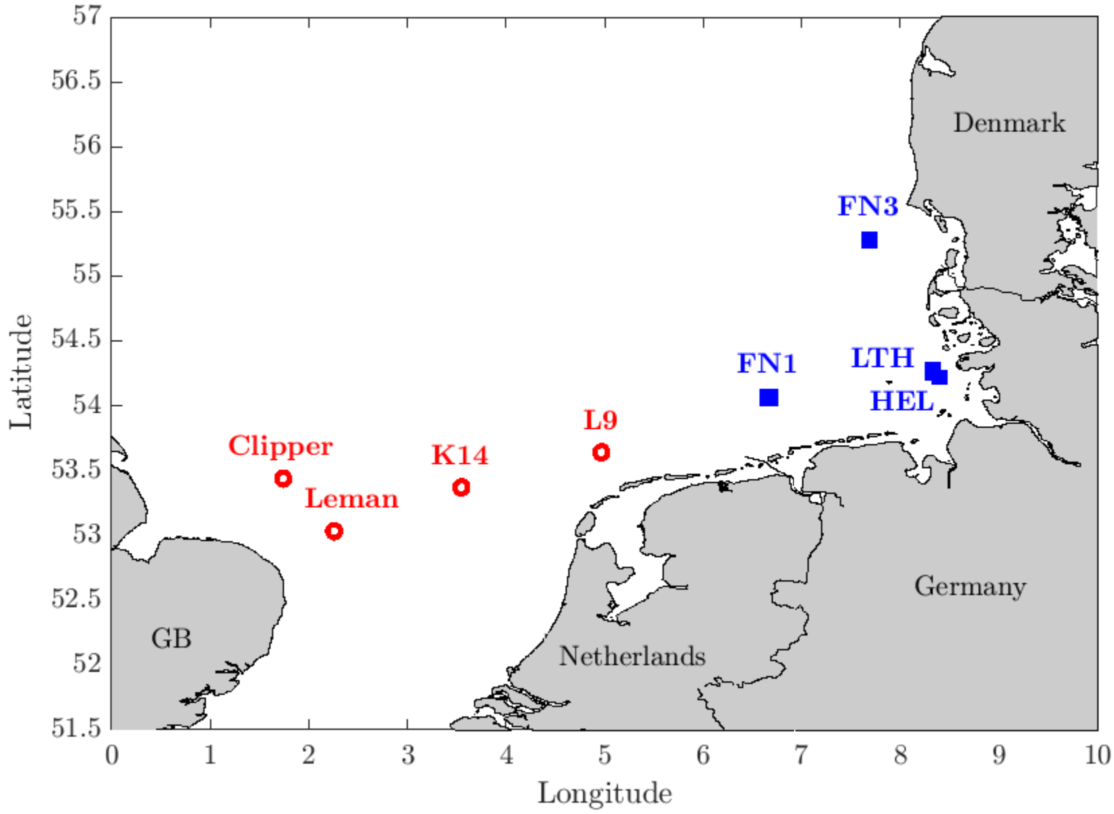


FIG. 1. Measurement sites considered in the study. Red circles: radar stations; blue squares: wave buoys.

TABLE 1. Water depth $h$ and long-term 70th percentile of the significant wave height, $H_{s,70}$, at all stations included in the analysis.

| Station type | Station name | $h$ | $H_{s,70}$ |
|---|---|---|---|
| Radar | L9 | 24 m | 1.55 m |
| | K14 | 26.5 m | 1.53 m |
| | Leman | 34 m | 1.26 m |
| | Clipper | 21 m | 1.28 m |
| Buoy | FN3 | 25 m | 1.88 m |
| | LTH | 30 m | 1.61 m |
| | HEL | 20 m | 1.47 m |
| | FN1 | 30 m | 1.79 m |

with gravity $g$ and the peak period $T_p = 1 f_p^{-1}$ of each sample, with $f_p$ representing the peak frequency in the linear fast Fourier transform (FFT) spectrum of the sample. Table 2 shows the maximum accepted peak period for deep-water samples at each station, according to Eq. 10. It is compared to the 99th percentile of peak periods $T_{p,99}$ for samples above $H_{s,70}$ at each station.

Since the great part of samples satisfies deep-water conditions according to their peak periods, we assume it reasonable to treat the selected stations as deep-water stations. The number of available samples above $H_{s,70}$ is shown in Table 3. A quality control, followed by the identification of rogue waves, was applied to these samples, as described in Teutsch et al. (2020).

TABLE 2. 99th percentile of the peak period $T_{p,99}$,in all samples above $H_{s,70}$, compared to the peak period threshold $T_p$, below which samples are classified as deep-water samples.

| Station | L9 | K14 | Leman | Clipper | FN3 | LTH | HEL | FN1 |
|---|---|---|---|---|---|---|---|---|
| $T_p$-threshold | 8.4 s | 8.8 s | 9.9 s | 7.8 s | 8.5 s | 9.3 s | 7.6 s | 9.3 s |
| $T_{p,99}$ | 8.0 s | 8.2 s | 6.8 s | 7.5 s | 8.3 s | 7.9 s | 7.7 s | 8.5 s |

TABLE 3. Number of available 30 minute measurement samples with $H_s$ above the long-term 70th percentile of the significant wave height, $H_{s,70}$. The data are classified according to the station and the sampling frequency $f_s$ of the recording.

| Station/ $f_s$ | 4 Hz | 2 Hz | 1.28 Hz | Total |
|---|---|---|---|---|
| L9 | 26.565 | 2368 | - | 28.933 |
| K14 | 26.266 | 6585 | - | 32.851 |
| Leman | 25.816 | 3883 | - | 29.699 |
| Clipper | 3438 | 28.111 | - | 31.549 |
| FN3 | - | - | 17.757 | 17.757 |
| LTH | - | - | 17.754 | 17.754 |
| HEL | - | - | 7175 | 7175 |
| FN1 | - | - | 20.333 | 20.333 |

### *b. Methods*

For all 30 minute samples in Table 3, the spectral bandwidth was estimated from the FFT spectrum in terms of the broadness parameter $\varepsilon$ (Eq. 2), the narrowness parameter $\nu$ (Eq. 4) and Goda's peakedness parameter $Q_p$ (Eq. 5). In addition, the BFI was calculated for each sample, according to Eq. 7. As described in Teutsch et al. (2020), each sample was assigned to one of the following categories:

- **"normal samples"**- measurement samples that did not contain a rogue wave.

- **"height rogue samples"**- measurement samples that contained a rogue wave according to the height criterion (Haver and Andersen 2000)

$$2.3\ H_s > H \geq 2.0\ H_s, \tag{11}$$

  with $H$ denoting the height of the rogue wave from crest to trough.

- **"extreme rogue samples"**- measurement samples that contained a rogue wave according to a more strict height criterion of

$$H \geq 2.3\ H_s. \tag{12}$$

- **"crest rogue samples"**- measurement samples that contained a rogue wave according to the crest criterion (Haver and Andersen 2000)

$$C \geq 1.25\ H_s, \tag{13}$$

  with $C$ denoting the crest height of the rogue wave above still water level.

- **"double rogue samples"**- measurement samples that contained a rogue wave according to both the criteria defined in Eq. 11 and Eq. 13. Double rogue samples were excluded in the groups of height and crest rogue samples.

Table 4 shows the number and percentage of available samples in each category.

TABLE 4. Number of samples in each category, for the groups of radar and buoy stations.

| Station type | Normal | Height | Crest | Double | Extreme | Total |
|---|---|---|---|---|---|---|
| Radar | 115.065 | 4810 | 941 | 1450 | 446 | 122.712 |
| | (93.8%) | (3.9%) | (0.8%) | (1.2%) | (0.4%) | (100%) |
| Buoy | 59.218 | 2291 | 485 | 806 | 219 | 63.019 |
| | (94.0%) | (3.6%) | (0.8%) | (1.3%) | (0.3%) | (100%) |

The Datawell Waverider buoys provide information on their position on the water surface in heave, North and West directions. Based on the three-dimensional information, it is possible to estimate a directional wave spectrum for each 30 minute sample. We calculated the wave spectrum from buoy data according to Huntley et al. (1977), who applies the Iterated Maximum Likelihood

Method (IMLM) developed by Pawka (1983). Based on the directional spectrum, the directional spreading of each sample, and subsequently the parameter $R$, which relates the directional spreading to the spectral bandwidth, were calculated (Eq. 8 and Eq. 9).

## 3. Results

### *a. Spectral bandwidth*

The measurement data analyzed in this study, were recorded by different measurement instruments and at different sampling rates (Table 3). When comparing spectral bandwidth parameters and BFI at all stations, we observed that the parameter range differed with the measurement frequency $f_s$ (Fig. 2 and 3). This became most obvious for the broadness parameter $\varepsilon$, whose median value showed to be approximately 30% higher in radar samples measured at $f_s = 4$ Hz than in buoy samples with $f_s = 1.28$ Hz (Fig. 2). To test the hypothesis that the investigated spectral parameters are sensitive to the measurement frequency, we sub-sampled the 4 Hz data at station L9 at 2 Hz and at 1 Hz, respectively. The result demonstrates that the same time series yield different spectral parameters when sampled at different frequencies (Fig. 4). The changes are most pronounced for the broadness parameter $\varepsilon$. The reason for this dependency of the parameters on the sampling frequency is a change in spectral shape with the measurement frequency (Fig. 5). This results in a change in spectral moments (Table 5). A change in sampling frequency strongly affects those bandwidth parameters which are dependent on the higher moments of the spectrum (Eq. 2 and Eq. 4). This issue has already been raised by Goda (1988a,b), who introduced a peakedness parameter which is independent of the higher moments of the frequency spectrum (Eq. 5). Indeed, the peakedness parameter $Q_p$ is least of all bandwidth parameters affected by the measurement frequency (Fig. 2).

TABLE 5. Spectral moments $m_n$, bandwidth parameters and BFI, calculated from the same time series, measured on 01 January 2016, starting at 00:00. It was originally sampled at $f_s = 4$ Hz and sub-samples at 2 Hz and 1 Hz.

| Sampling frequency | $m_0$ | $m_1$ | $m_2$ | $m_4$ | $\varepsilon$ | $\nu$ | $Q_p$ | BFI |
|---|---|---|---|---|---|---|---|---|
| 4 Hz | 0.287 | 0.0259 | 0.0032 | 3.75E-04 | 0.953 | 0.591 | 2.185 | 0.384 |
| 2 Hz | 0.287 | 0.0511 | 0.0111 | 0.0014 | 0.836 | 0.467 | 2.372 | 0.406 |
| 1 Hz | 0.285 | 0.0990 | 0.0393 | 0.0103 | 0.687 | 0.380 | 2.527 | 0.410 |

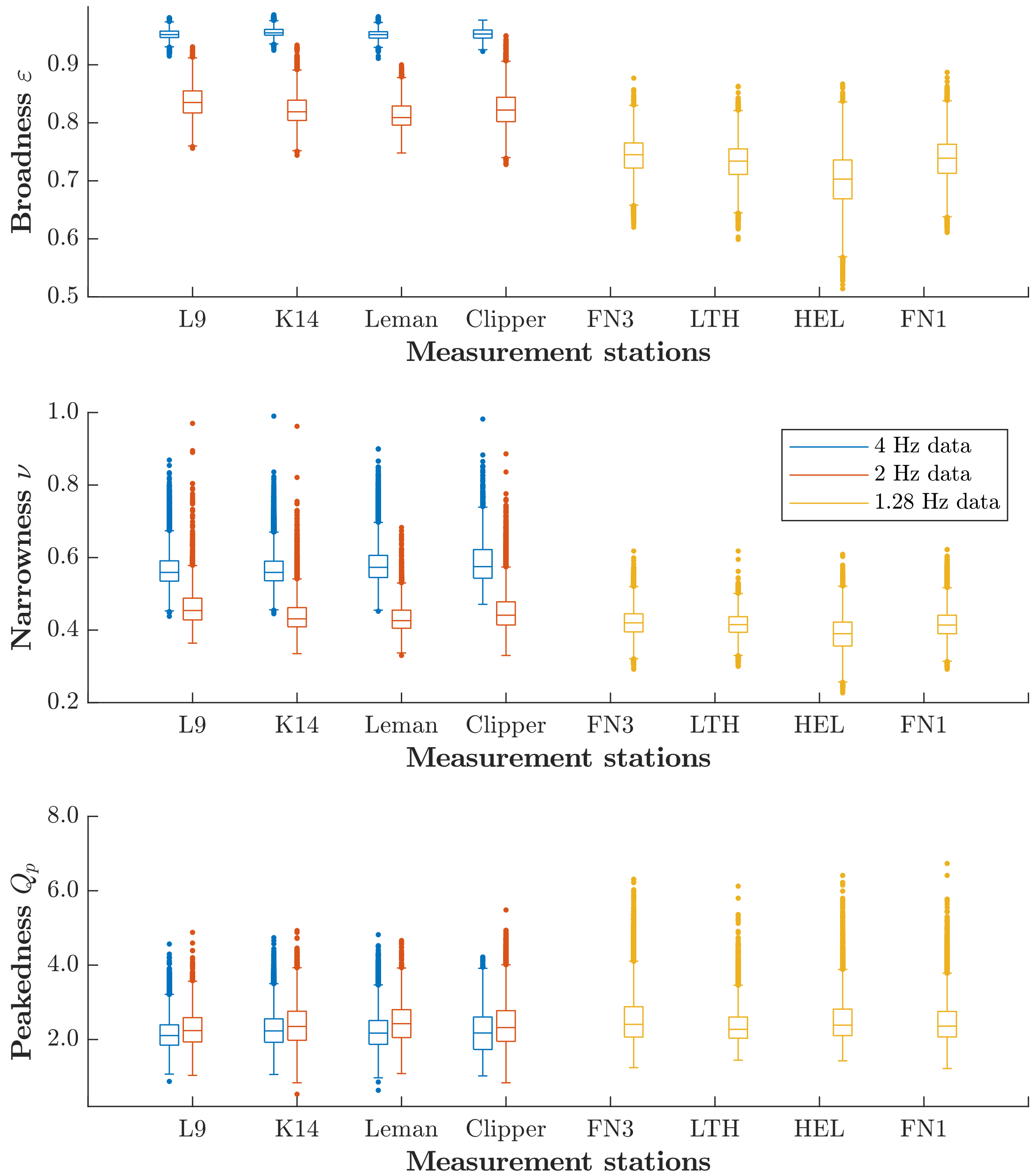


FIG. 2. Bandwidth parameters $\varepsilon$, $\nu$ and $Q_p$, calculated from the available data at all measurement stations.

Since our data set consists of buoy and radar measurement data, which have been sampled at different frequencies, buoy and radar data will be treated separately throughout this study. Within the set of radar measurements, we sub-sampled all time series recorded at 4 Hz with $f_s = 2$ Hz. This way, we still retain measurement data at a high frequency, while enlarging the set of 2 Hz

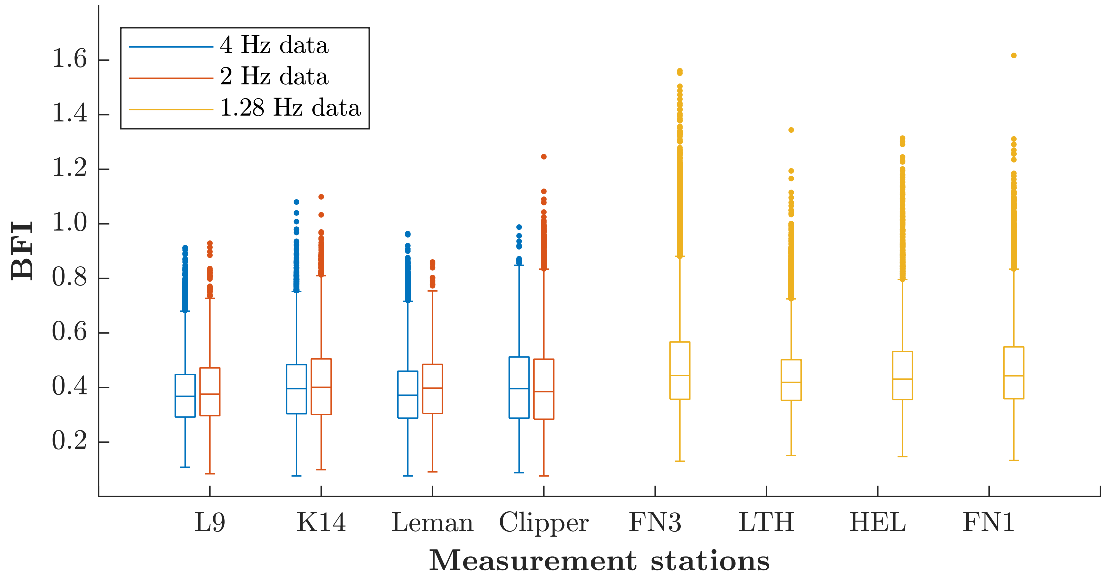


FIG. 3. Benjamin–Feir index, calculated from the available data at all measurement stations.

samples and obtaining bandwidth parameters in a range that is more comparable to the buoy data than the 4 Hz data. Figure 6 is a repetition of Fig. 2, but with all 4 Hz radar data sub-sampled at 2 Hz. The BFI for 2 Hz radar data and 1.28 Hz buoy data is shown in Fig. 7.

The differences between the respective stations are insignificant. Within the sub-set of radar measurement samples, one could infer an increased broadness of the frequency spectrum in terms of both, $\varepsilon$ and $\nu$, with a decrease in water depth, with L9 and Clipper situated in water depths much shallower than Leman (see Table 1). This trend, however, is not seen in the peakedness parameter $Q_p$, and it is not confirmed by the buoy stations, with the deepest stations being FN1 and LTH with a water depth of $h = 30$ m (Fig. 6). The BFI does not display any relation to the water depth in which the samples were recorded (Fig. 7).

Figure 8 shows the broadness parameter $\varepsilon$, combined for each instrument category, but separated into the different sample categories defined in section. 2. From the box plot and the figures in Table 6, it appears that the spectral bandwidth is equal or slightly higher than normal in crest rogue samples and slightly lower than normal in height and extreme rogue samples. This result becomes more evident when displayed in a histogram, comparing normal to height and extreme rogue samples, and normal to crest rogue samples (Fig. 9 and 10). Double rogue samples display a lower bandwidth than normal (Table 6), but they will not be treated further, as they belong to both, height and crest rogue categories.

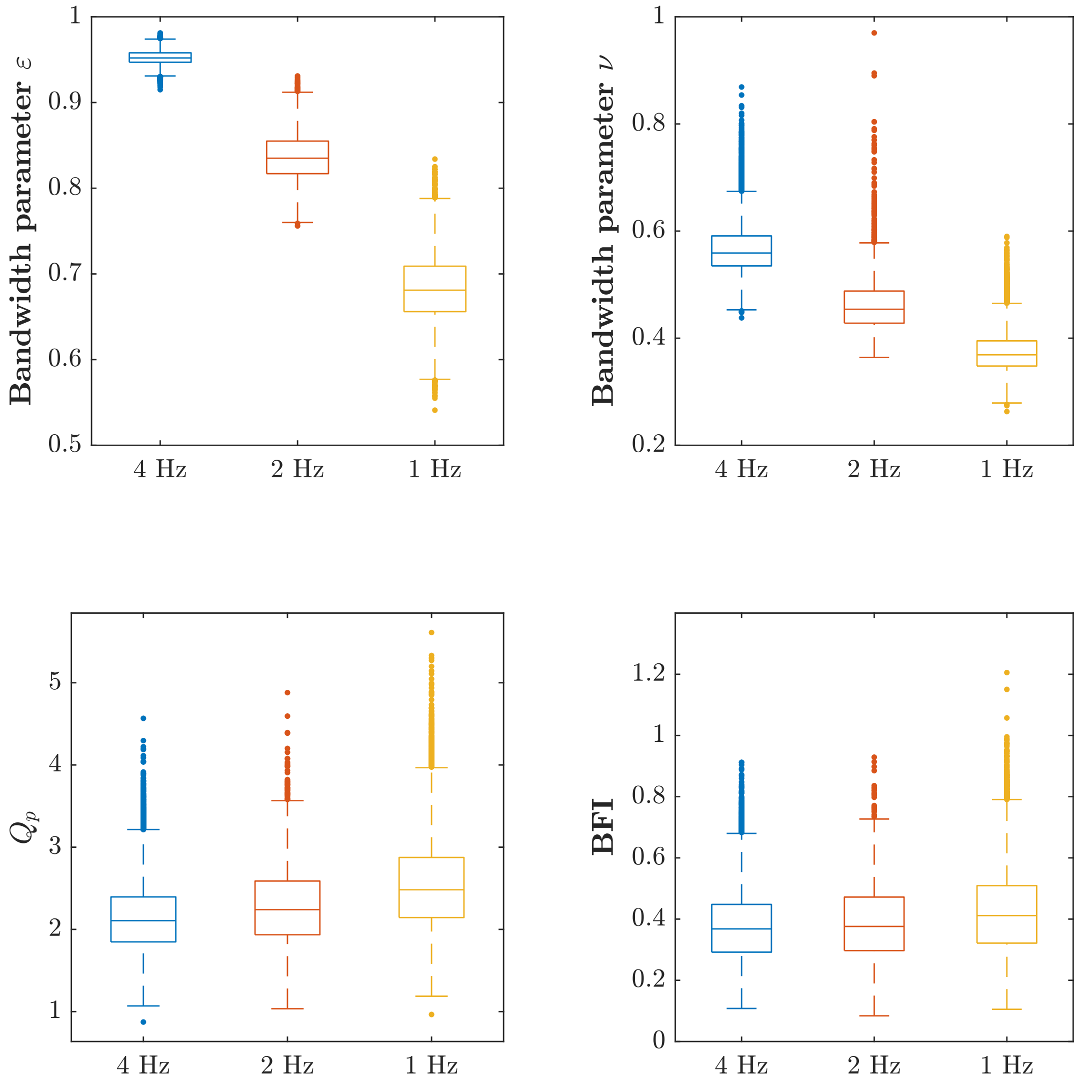


FIG. 4. Data from station L9, originally sampled at 4 Hz, and the same data sub-sampled at 2 Hz and 1 Hz.

TABLE 6. Median values of the distributions of $\varepsilon$ in the different categories, as shown in Fig. 8.

| Station type | Normal | Height | Crest | Double | Extreme |
|---|---|---|---|---|---|
| Radar | 0.819 | 0.816 | 0.819 | 0.814 | 0.817 |
| Buoy | 0.736 | 0.728 | 0.737 | 0.731 | 0.726 |

To test whether the difference between the $\varepsilon$ distributions in the different sample categories is statistically significant, a Monte Carlo simulation was performed for $\varepsilon$, and subsequently for all

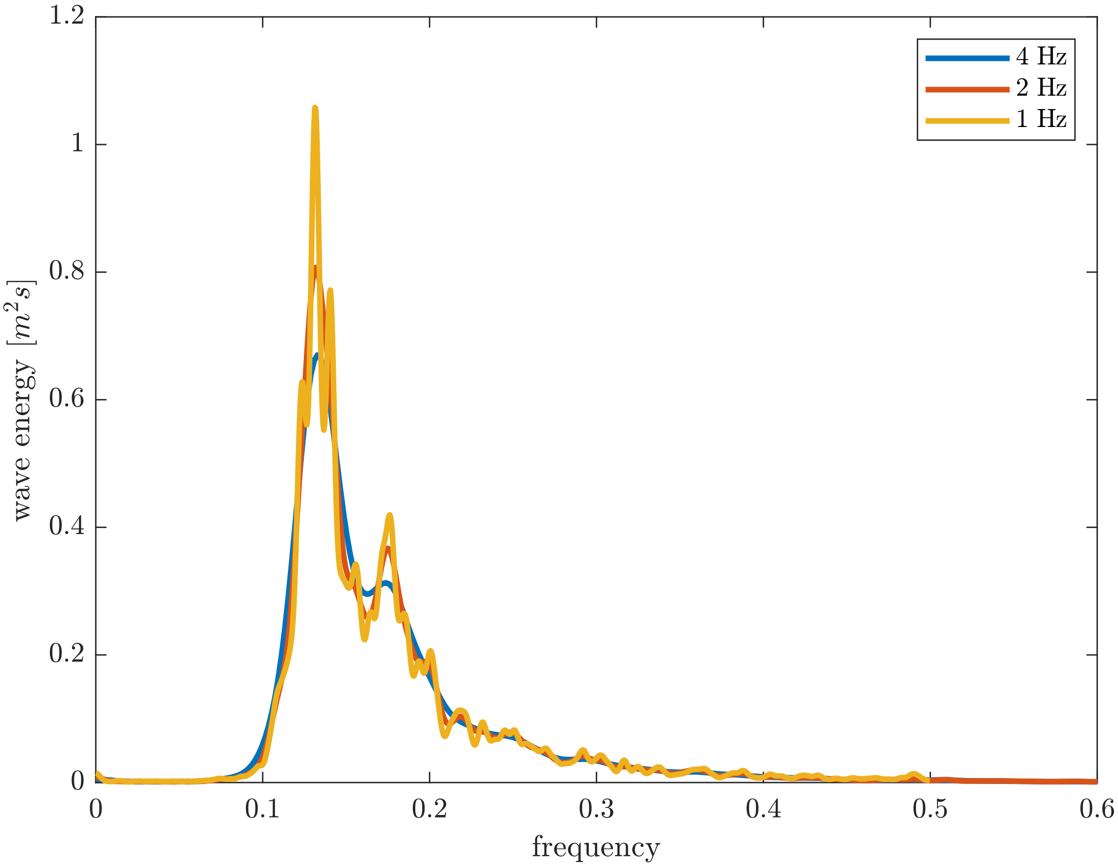


FIG. 5. Change in spectral shape with a change in sampling frequency.

bandwidth parameters and the BFI, comparing the parameters calculated from normal samples to height and extreme rogue samples on the one hand and to crest rogue samples on the other hand. An overview of the Monte Carlo calculations that were performed, is given in Table 7. In each execution of the Monte Carlo simulation, 10.000 samples of the length of the comparison population (height and extreme or crest rogue time series) were drawn with replacement from the population of normal time series. For these samples, the respective parameters in Table 7 were calculated. The mean and standard deviation of the 10.000 parameter distributions is displayed and compared to the comparison population in Fig. 11-14. A significant difference between normal time series and the comparison population is given if the distribution of the comparison population is located outside of two standard deviations of the distribution calculated from the normal time series.

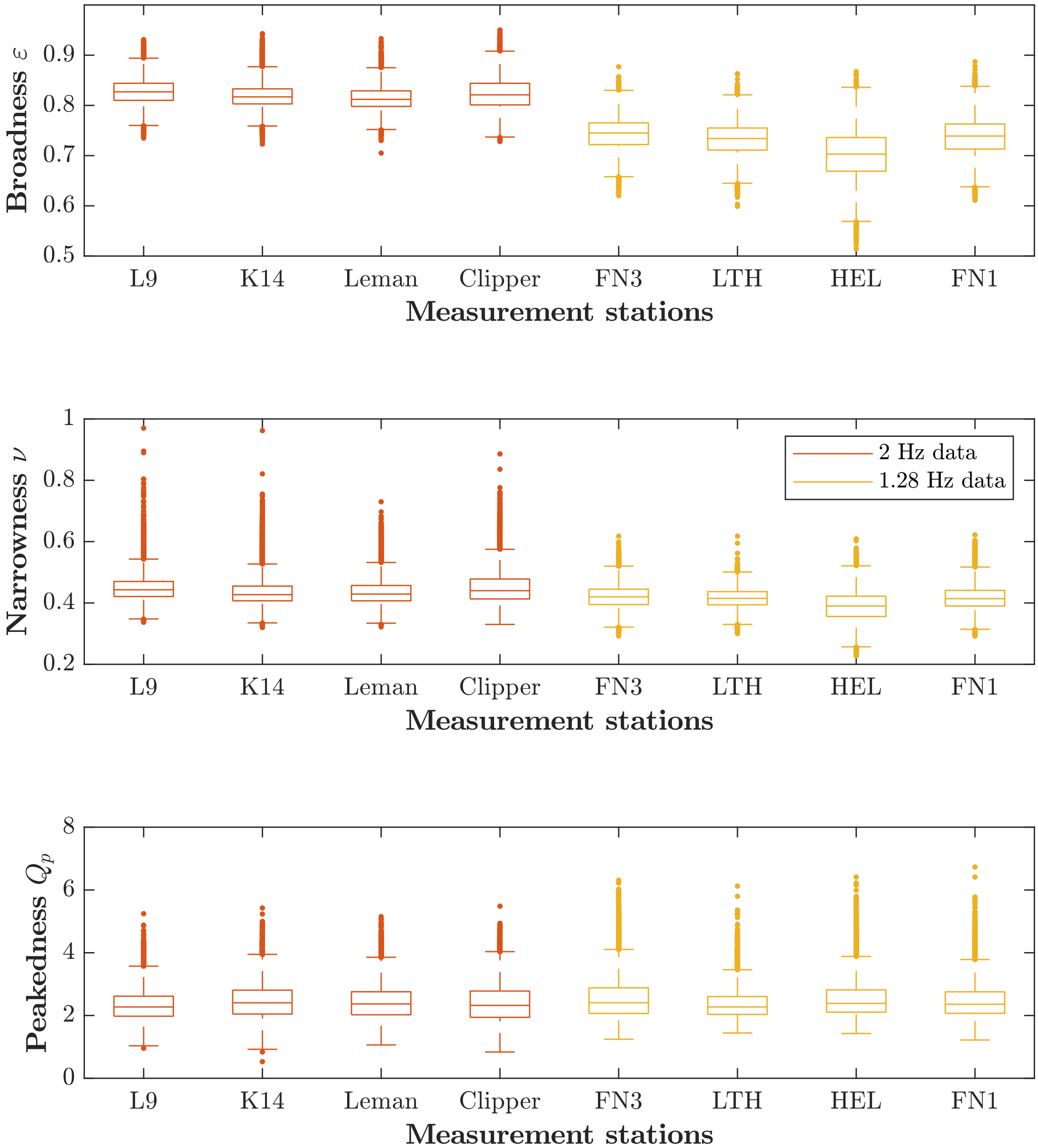


FIG. 6. Bandwidth parameters $\varepsilon$, $\nu$ and $Q_p$, calculated from the available data at all measurement stations. The 4 Hz time series measured at radar stations have been sub-sampled at $f_s$ =2 Hz for comparability.

From the result of the Monte Carlo simulation of the broadness parameter $\varepsilon$, it can be inferred that the frequency spectra calculated from height and extreme rogue samples at the investigated

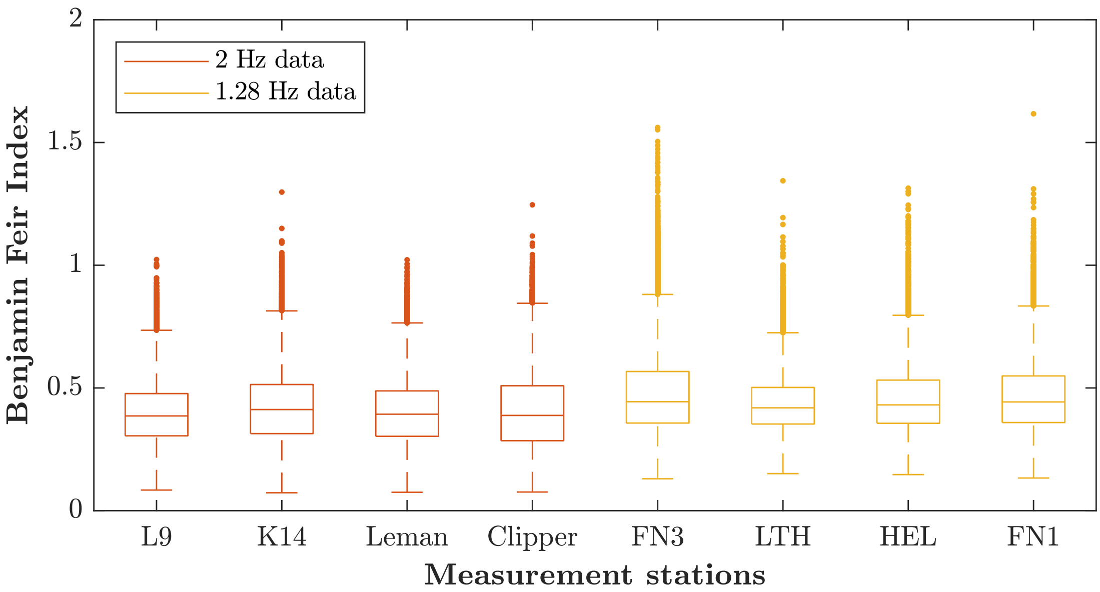


FIG. 7. Benjamin–Feir index, calculated from the available data at all measurement stations. The 4 Hz time series measured at radar stations have been sub-sampled at $f_s$ =2 Hz for comparability.

TABLE 7. Matrix showing for which station type and sample category parameters were compared in Monte Carlo simulations.

| Parameter | Station type | Normal to height/ extreme | Normal to crest |
|---|---|---|---|
| $\varepsilon$ | Radar and Buoy | ✓ | ✓ |
| $\nu$ | Radar and Buoy | ✓ | ✓ |
| $Q_p$ | Radar and Buoy | ✓ | ✓ |
| BFI | Radar and Buoy | ✓ | ✓ |
| $\sigma_\Theta$ | Buoy only | ✓ | ✓ |
| R | Buoy only | ✓ | ✓ |

radar and buoy stations were significantly more narrow than the frequency spectra calculated from time series without rogue waves (Fig. 11). It can be concluded that in our case, height and extreme rogue waves typically occurred in slightly more narrow sea states than expected. For crest rogue samples, Fig. 11 shows a different result: these did not differ significantly from normal time series. The standard deviation in the 10.000 samples drawn from radar data, is very small, due to a narrow $\varepsilon$ distribution in radar samples, as seen in Fig. 9.

The result of the Monte Carlo simulation for the narrowness parameter $\nu$ is slightly different. A significantly more narrow frequency spectrum for height and extreme rogue samples can only be

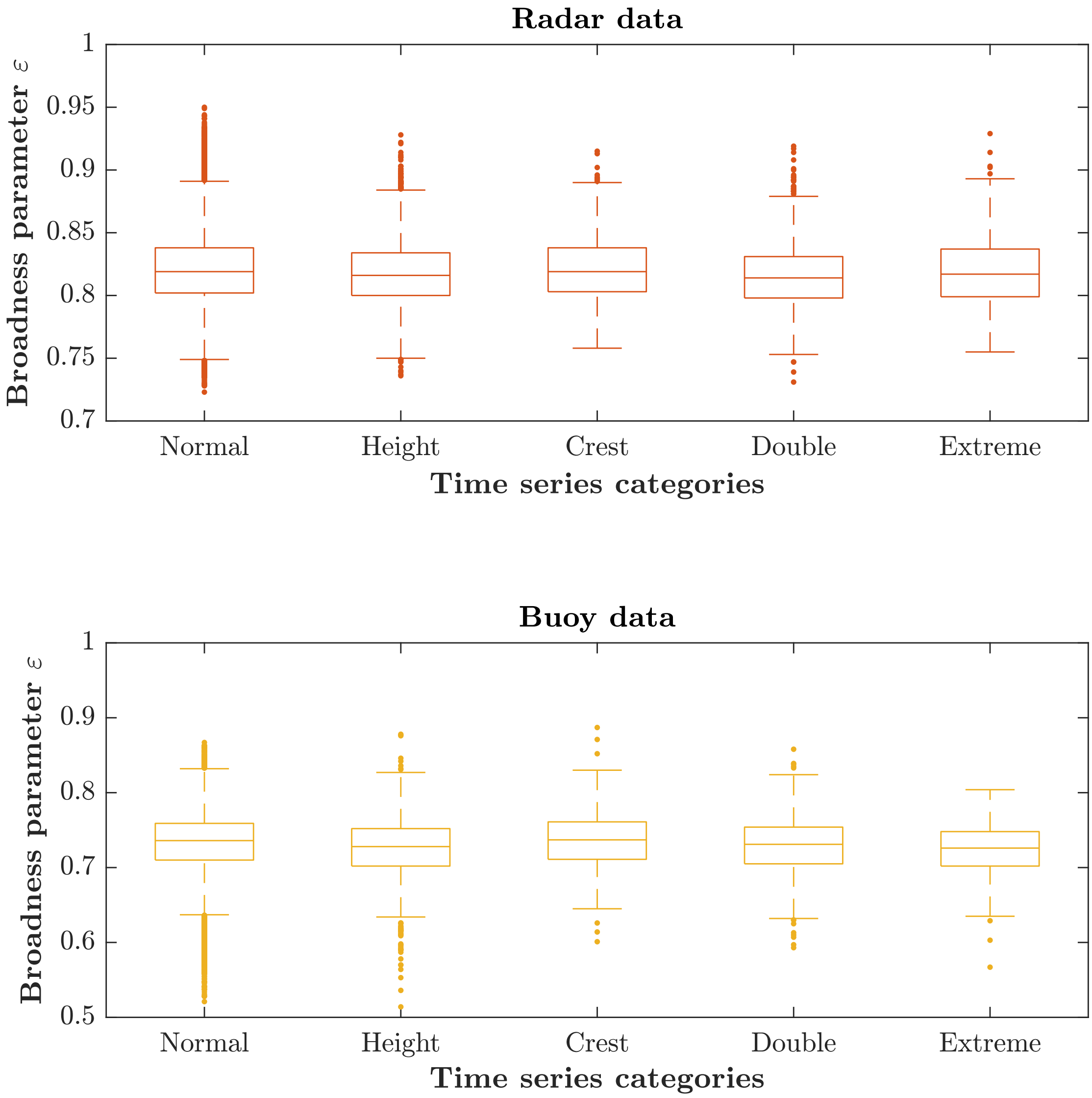


FIG. 8. Broadness parameter $\varepsilon$, calculated from the different time series categories. Distributions are shown as box-and-whisker plots (box: interquartile range; whiskers: 1.5 times the interquartile range; horizontal line inside the box: median; dots: data outside the whiskers).

identified at the buoy stations (Fig. 12). The distribution of $\nu$ for height and extreme rogue samples at radar stations is situated within two standard deviations of the $\nu$ distribution calculated from 10.000 normal sample realizations. For crest rogue samples at both, radar and buoy stations, the

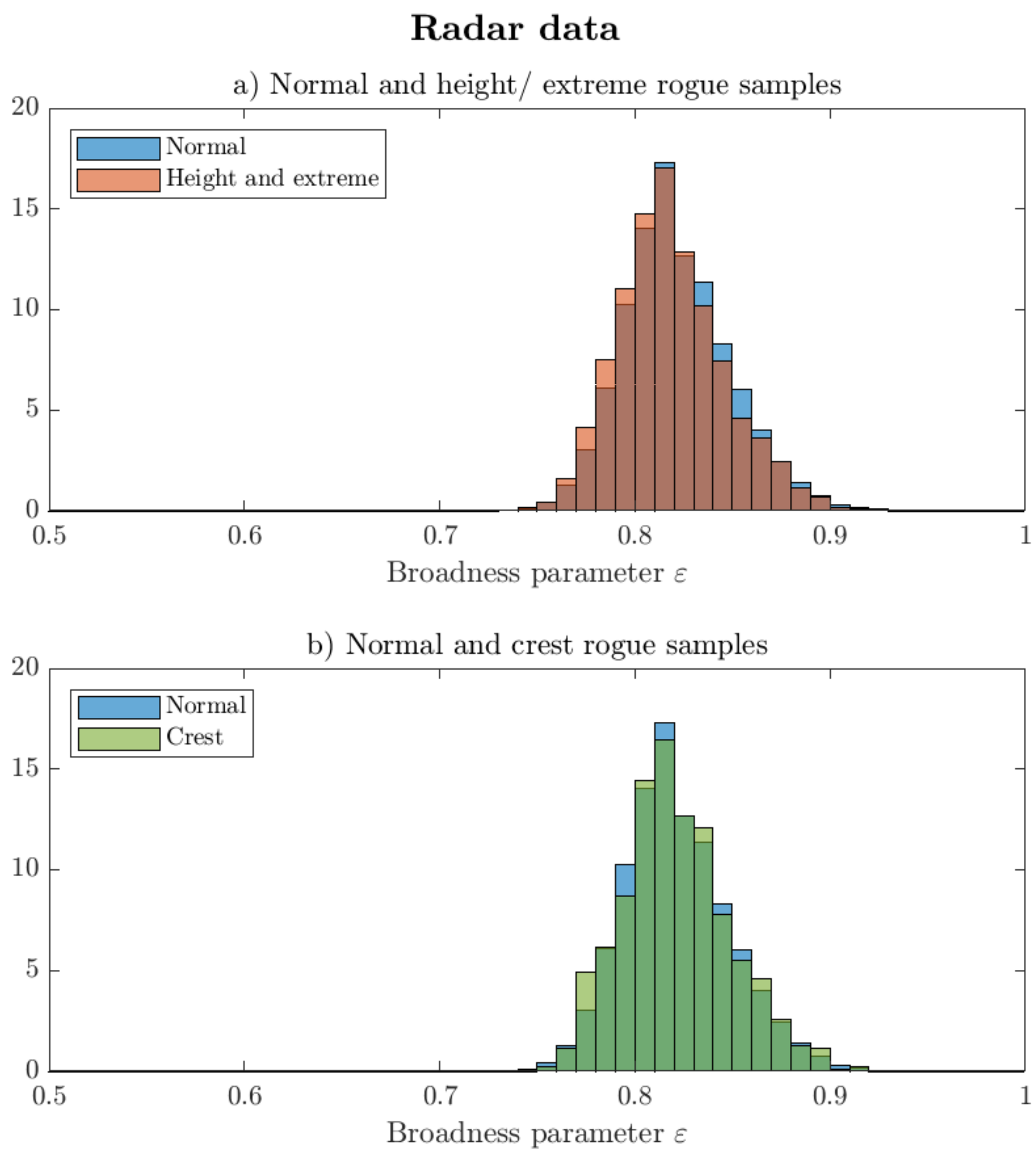


FIG. 9. Broadness parameter $\varepsilon$, calculated at the buoy stations, comparing normal to a) height and extreme rogue samples and b) crest rogue samples.

result remains that the distribution of $\nu$ is not significantly different from the $\nu$ values in normal samples.

In terms of the peakedness parameter $Q_p$, for which a mean value slightly above $Q_p = 2$ is typical at all stations, no significant difference between normal and rogue wave samples was identified (Fig. 13). Although the peakedness/ groupiness of the wave spectrum appears slightly lower for

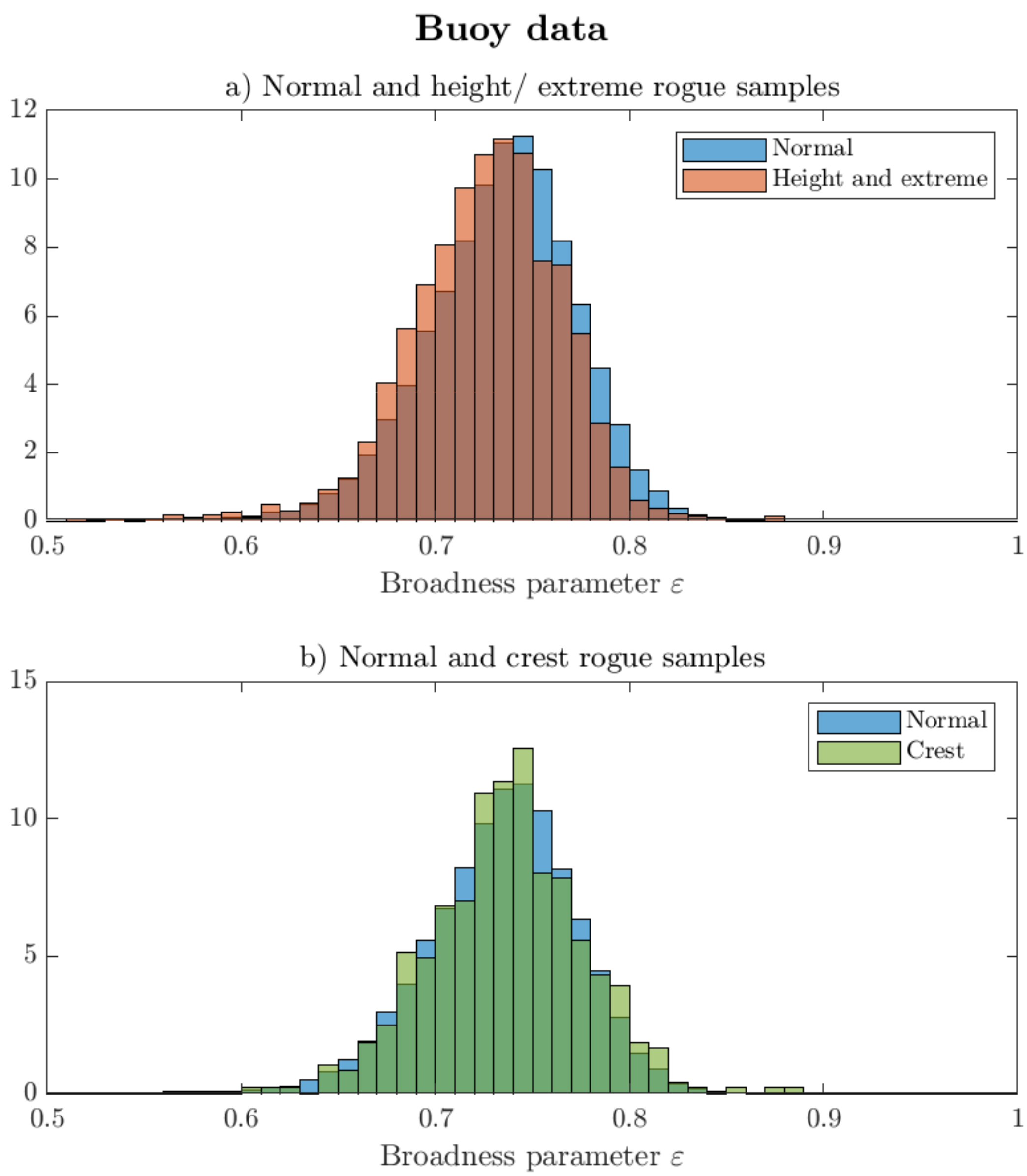


FIG. 10. Broadness parameter $\varepsilon$, calculated at the buoy stations, comparing normal to a) height and extreme rogue samples and b) crest rogue samples.

crest rogue samples than normal and slightly higher for extreme rogue samples than normal, the curves of the comparison populations are within two standard deviations of the distribution from normal samples. The same result applies to the BFI. Under the hypothesis that the modulational instability caused the rogue waves measured at our stations, a higher BFI would be expected in rogue wave samples. However, this does not seem to be the case (Fig. 14). Although within two

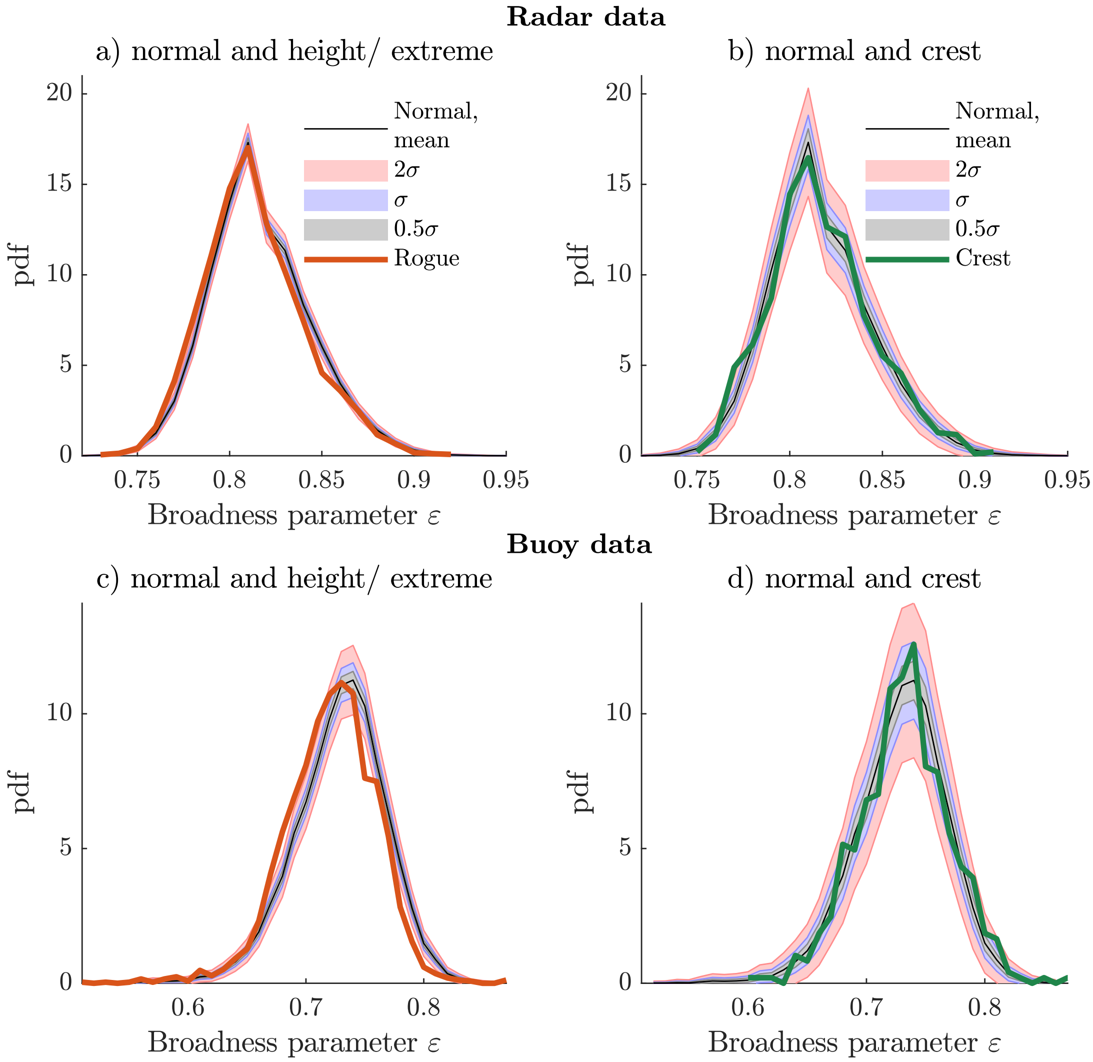


FIG. 11. Result of the Monte Carlo simulation for the broadness parameter $\varepsilon$. Results from height and extreme rogue samples (left column) and from crest rogue samples (right column) are compared to results from 10.000 samples, drawn from the population of normal time series. For these samples, the mean and the standard deviations of the distributions are plotted (Campbell 2022).

standard deviations, low BFI values (BFI≈0.2) seem to be more unusual in height and extreme rogue samples than in normal samples.

### *b. Directional spreading*

The directional spreading of the wave energy in each sample is only available at the buoy stations, which provide three-dimensional information on their location, but not at the radar

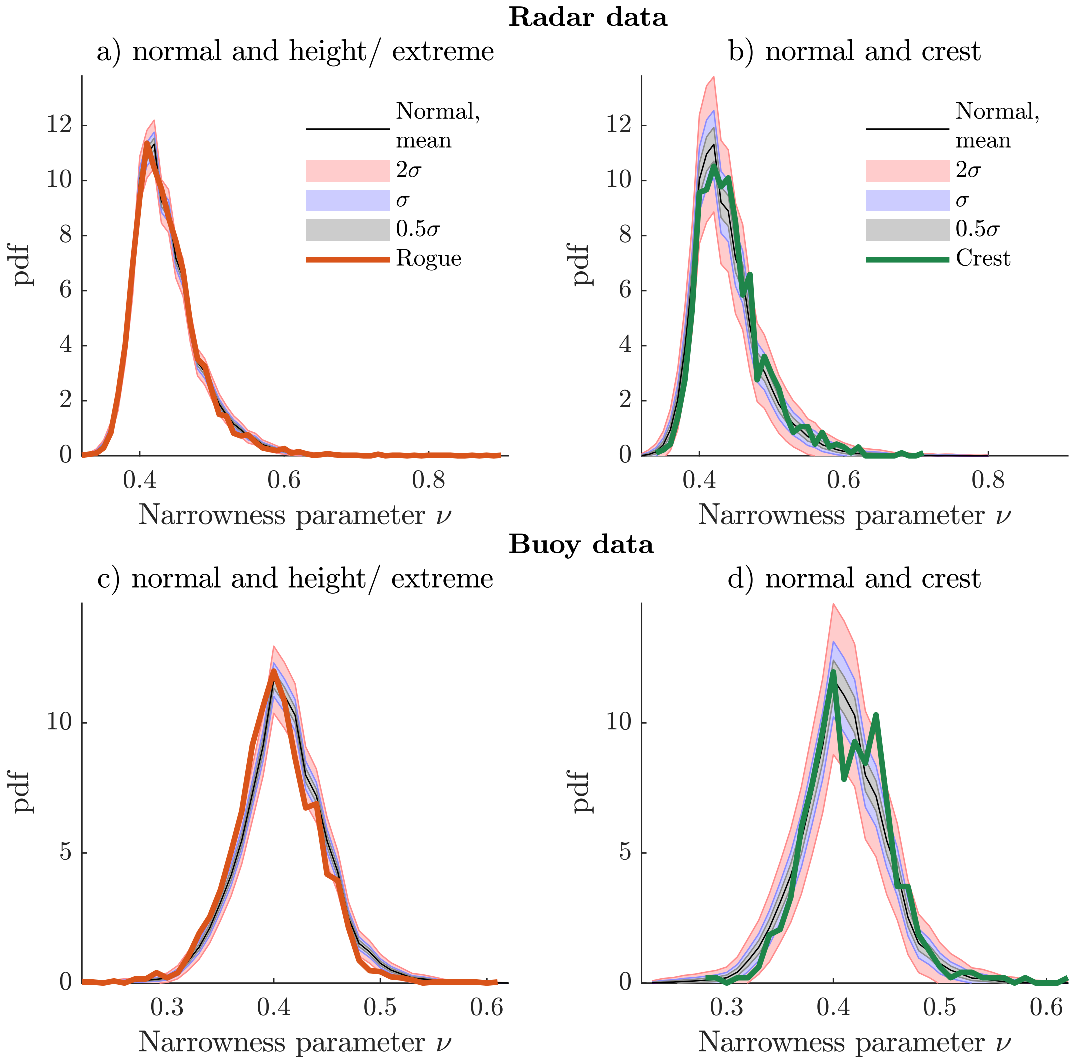


FIG. 12. Result of the Monte Carlo simulation for the narrowness parameter $\nu$. Results from height and extreme rogue samples (left column) and from crest rogue samples (right column) are compared to results from 10.000 samples, drawn from the population of normal time series. For these samples, the mean and the standard deviations of the distributions are plotted (Campbell 2022).

stations with only one-dimensional information on the air gap. Since a narrow directional spreading represents a requirement for the process of the modulational instability to occur, we investigated the directional spreading at all buoy stations and compared it for time series with and without rogue waves. Following the reasoning in the previous section, this was done by means of Monte Carlo simulations, in which a sample of 10.000 time series was drawn from the population of normal time series. Fig. 15 shows that the directional spreading in the measured rogue wave samples was

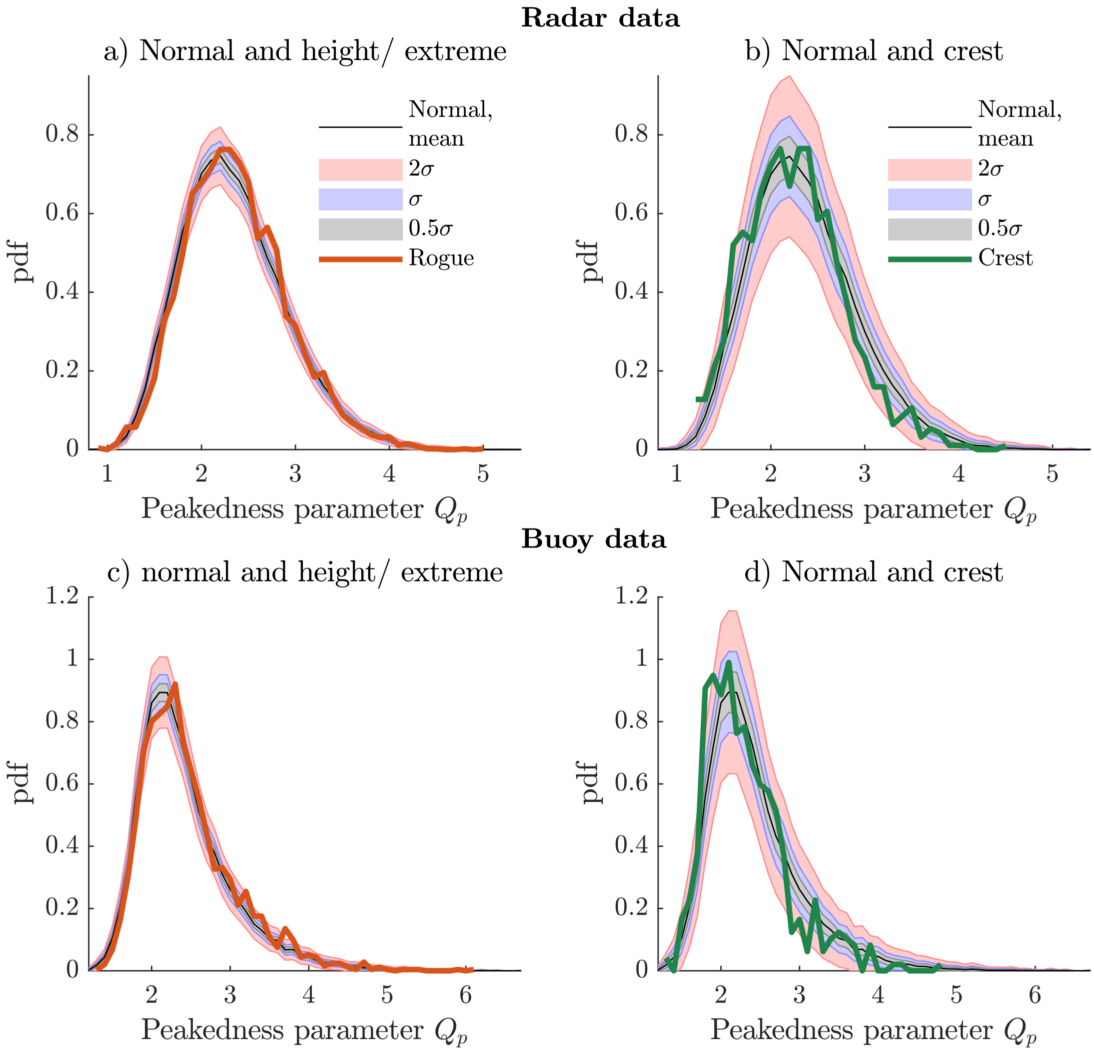


FIG. 13. Result of the Monte Carlo simulation for the peakedness parameter $Q_p$. Results from height and extreme rogue samples (left column) and from crest rogue samples (right column) are compared to results from 10.000 samples, drawn from the population of normal time series. For these samples, the mean and the standard deviations of the distributions are plotted (Campbell 2022).

not significantly different from the directional spreading in samples without rogue waves. Thus, the condition of a specifically low directional spreading in rogue wave samples as a prerequisite for the modulational instability to operate, was not present in our buoy data.

Finally, the combination of spectral bandwidth and directional spreading was examined. This was done because the favoring condition for the formation of a modulational instability has been formulated as a narrow spectrum in both direction and frequency (Alber 1978; Stansberg 1995,

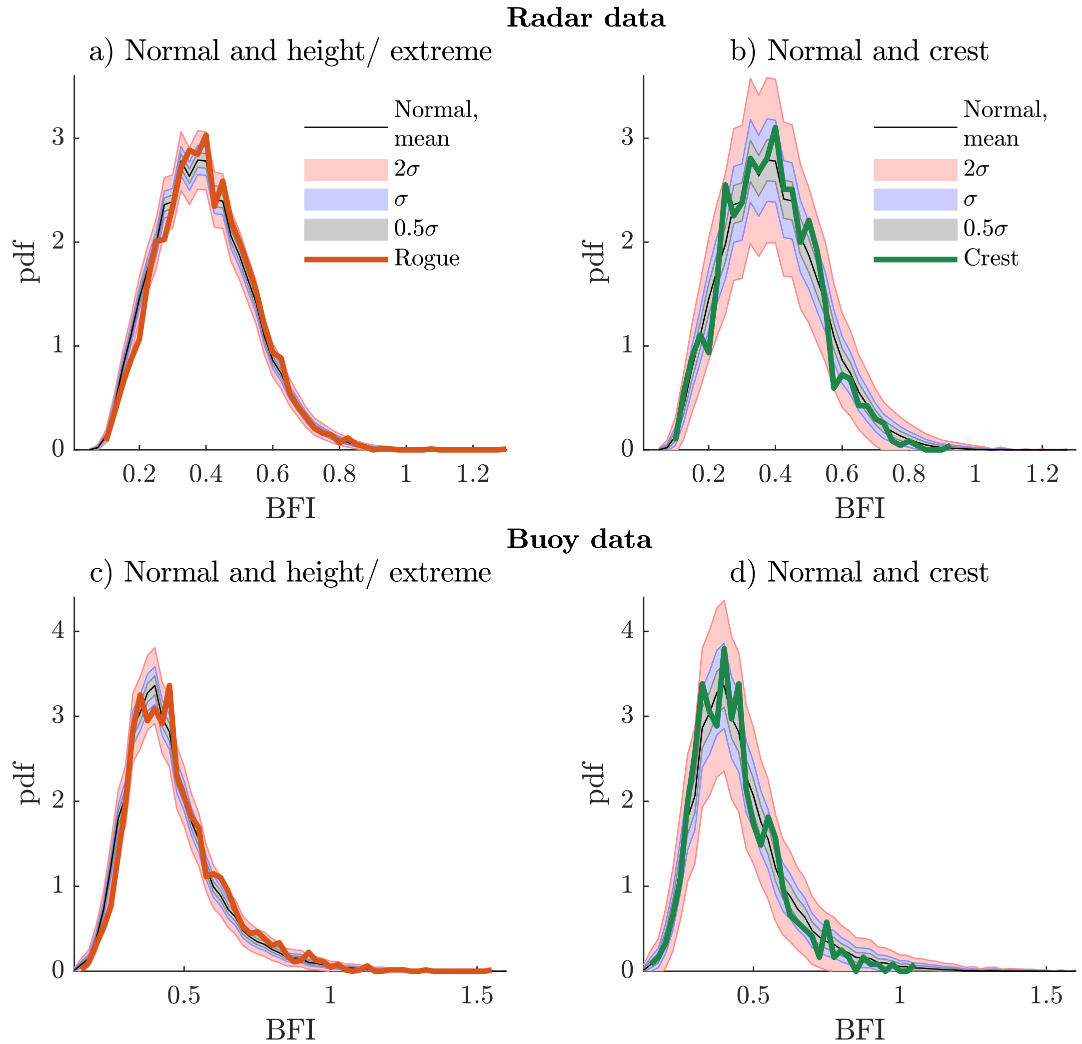


FIG. 14. Result of the Monte Carlo simulation for the BFI. Results from height and extreme rogue samples (left column) and from crest rogue samples (right column) are compared to results from 10.000 samples, drawn from the population of normal time series. For these samples, the mean and the standard deviations of the distributions are plotted (Campbell 2022).

e.g.). Figure 16 shows bandwidth- directional spreading pairs for all buoy samples. It shows that normal samples, as well as the plotted rogue wave samples, cluster around medium bandwidth and directional spreading values. No specific accumulation of rogue wave samples at low bandwidth and directional spreading is seen, which would point towards favorable conditions for the modulational instability.

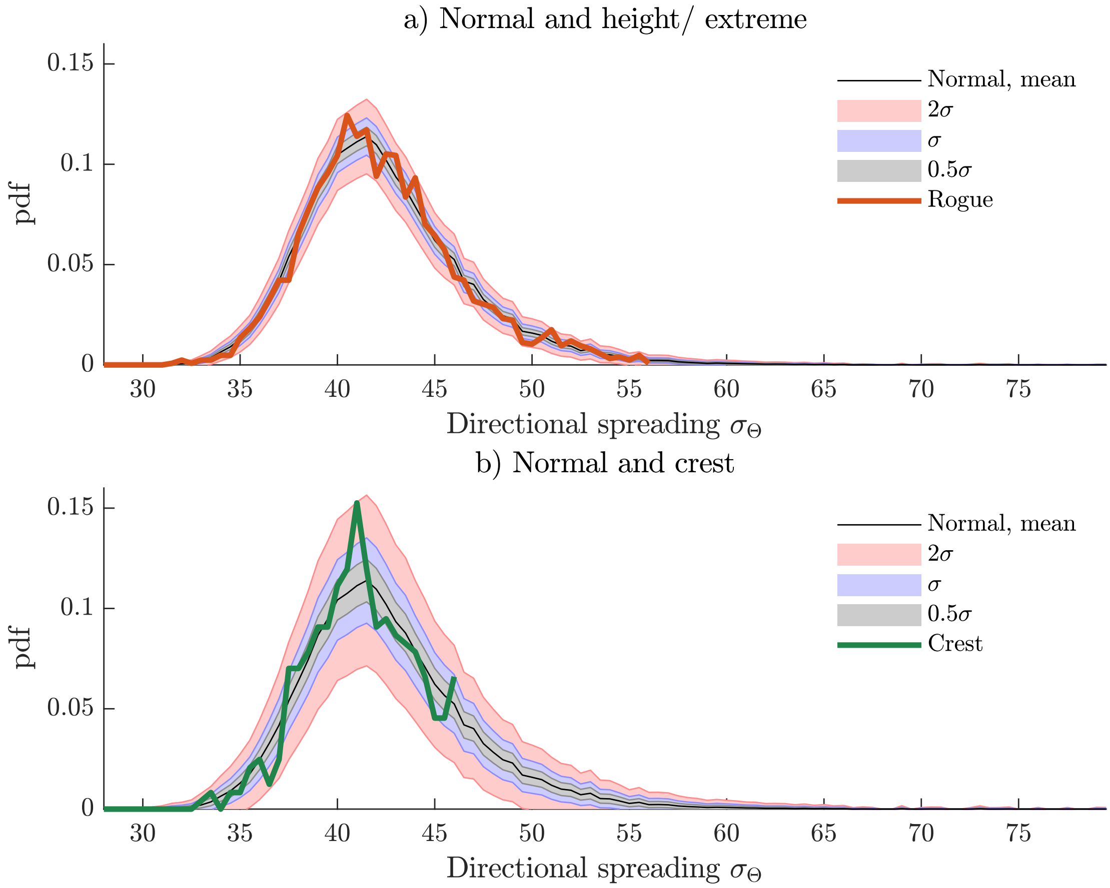


FIG. 15. Result of the Monte Carlo simulation for the directional spreading. Results from height and extreme rogue samples (left column) and from crest rogue samples (right column) are compared to results from 10.000 samples, drawn from the population of normal time series. For these samples, the mean and the standard deviations of the distributions are plotted (Campbell 2022).

Additionally, the Monte Carlo simulation was repeated for parameter R (Eq. 8) in buoy measurement samples, which quantifies the importance of the directional spreading with respect to the spectral bandwidth. Although it appears that the maximum in the rogue wave distributions is shifted towards a higher $R$ value, compared to normal samples, the comparison with the standard deviation reveals that there are no significant differences apparent between rogue wave samples and normal samples (Fig. 17). We conclude that rogue waves in our buoy data set did not occur in sea states that are narrow-banded in frequency and angular direction. This indicates that the modulational instability is an unlikely mechanism for the formation of these rogue waves.

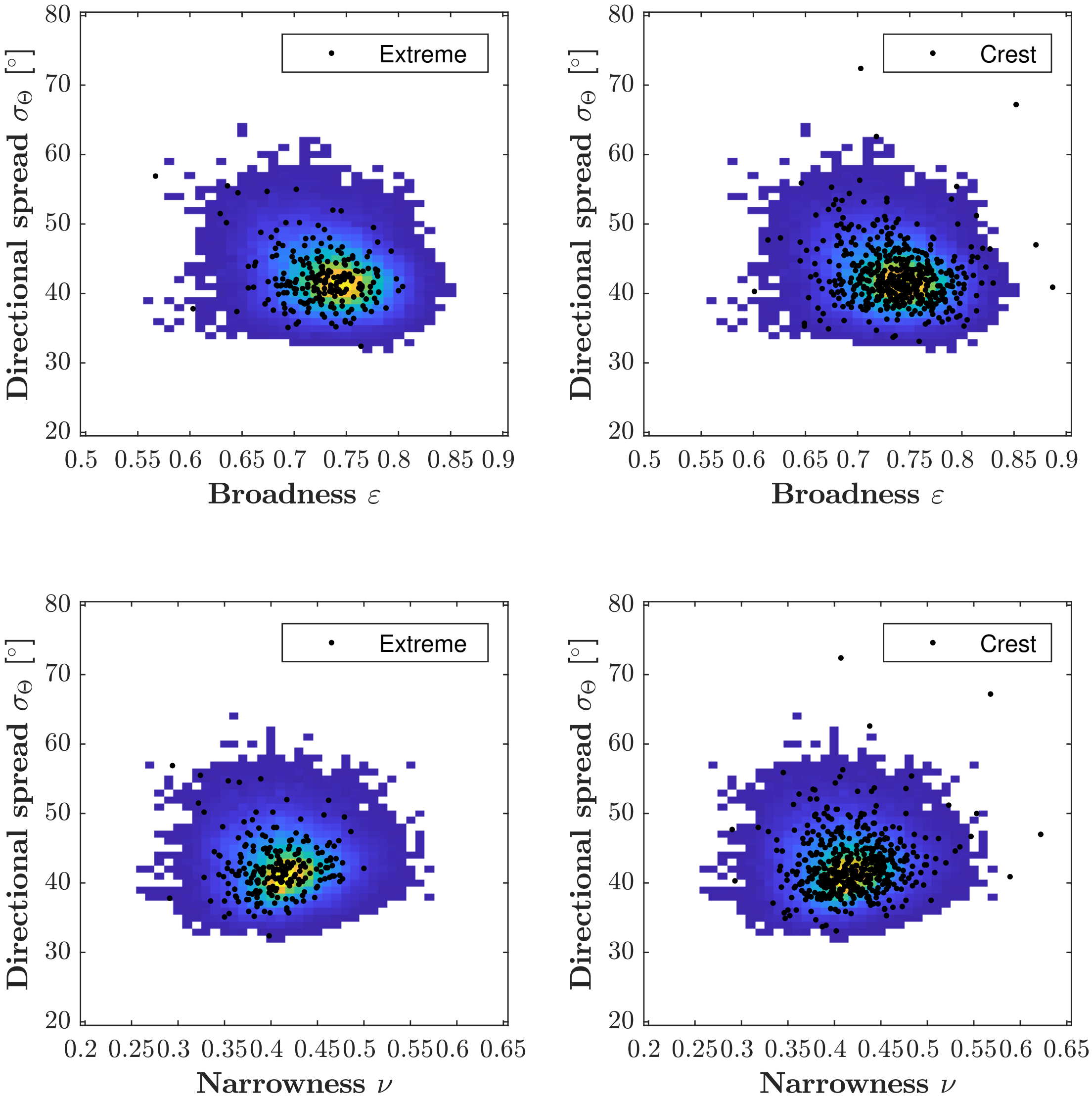


FIG. 16. Comparison of the bandwidth- directional spreading pairs calculated from normal and from rogue wave samples. The bandwidth is quantified in terms of the parameters $\varepsilon$ and $\nu$. Color coding: density of normal samples. Black dots: rogue wave samples, as defined in the legend to each panel.

## 4. Discussion

Wave measurement time series from the southern North Sea that were evaluated in the present study, generally showed a high spectral bandwidth, which is an unlikely condition for nonlinear focusing to occur (Alber 1978; Fedele et al. 2016). A similar observation of unfavorable condi-

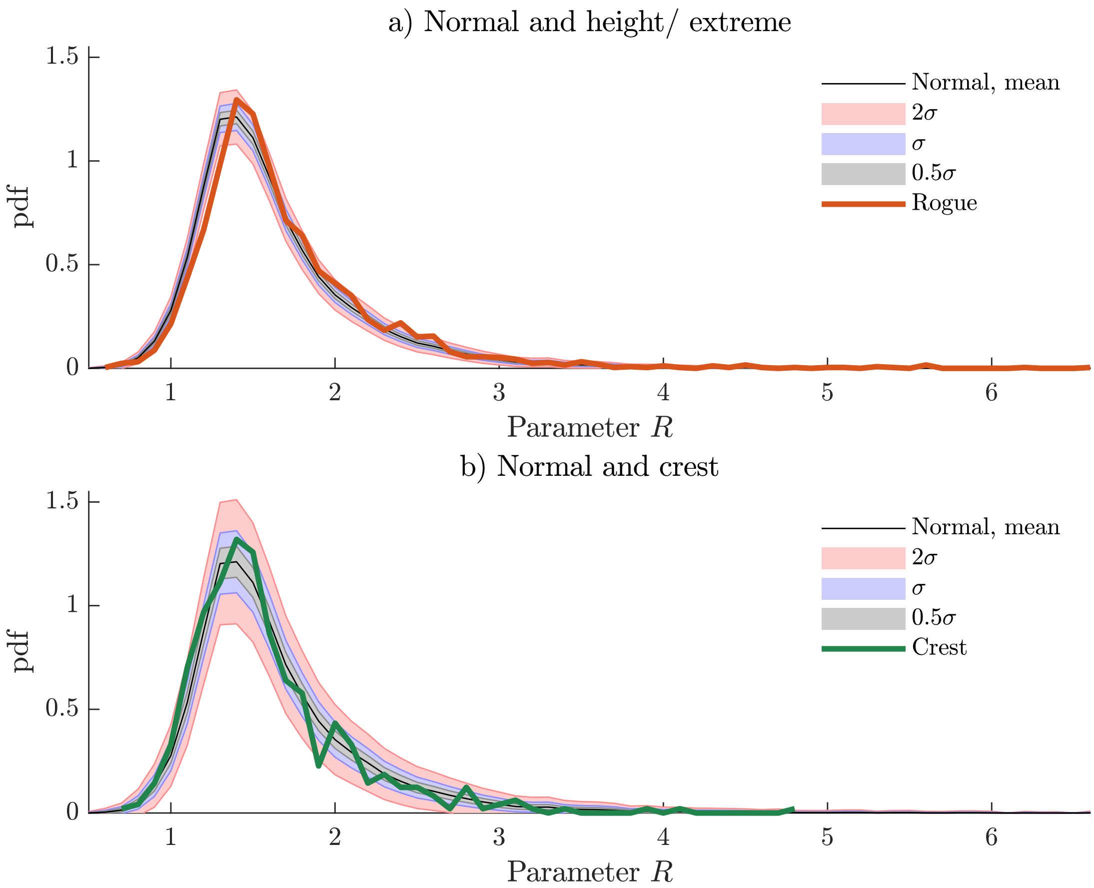


FIG. 17. Result of the Monte Carlo simulation for the combination parameter R. Results from height and extreme rogue samples (left column) and from crest rogue samples (right column) are compared to results from 10.000 samples, drawn from the population of normal time series. For these samples, the mean and the standard deviations of the distributions are plotted (Campbell 2022).

tions for the modulational instability was made by Fedele et al. (2016), who presented sea state parameters for three historical rogue wave occurrences in the North Sea. Due to a high bandwidth parameter $\nu$ and a large directional spreading $\sigma_\Theta$, they came to the conclusion that these rogue waves were probably not the result of nonlinear focusing. This conclusion is transferable to our data set, which displays high spectral bandwidth and directional spreading values for a substantially larger number of rogue waves in the North Sea.

Theoretical considerations and experimental results clearly confirm an increased rogue wave occurrence in narrow bandwidth and directional spreading (Waseda et al. 2009). Observations of field measurement data, however, have come to contradictory conclusions. In our data, the spectral bandwidth was significantly lower than normal in height and extreme rogue wave samples, when quantified by the broadness parameter $\varepsilon$ (Eq. 2). This result is basically consistent with a finding by Christou and Ewans (2014), who discovered, mainly based on radar data from the North Sea, recorded at $f_s = 2$ Hz or 4 Hz, that rogue wave samples are more narrow-banded than the highest samples of normal waves, and concluded that the spectral bandwidth might be an indicator for distinguishing time series with rogue waves from time series with high normal waves. Christou and Ewans (2014) did not distinguish between height and crest rogue waves, but given that in our data, the sample of height rogue samples is approximately five times larger than that of crest rogue samples (Table 4), our results are still comparable to theirs. One major difference in the result, however, is that Christou and Ewans (2014) based their observation on the narrowness parameter $\nu$. In terms of the broadness parameter $\varepsilon$, where we detected the strongest deviations, Christou and Ewans (2014) found little difference between rogue wave samples and the highest normal samples. The data set of Christou and Ewans (2014) included data from the same radar stations as we used in our study, however, for a different time period. Another difference to our dataset is the use of additional data from other regions from a large range of water depths (7-1311 m). The differences in the investigated data could be the reason for our discrepancies from their study. At the buoy stations, we also recognized differences between normal and rogue wave samples in the narrowness parameter $\nu$. Also Karmpadakis et al. (2020) described a clear influence of the spectral bandwidth $\nu$ on the wave height distribution in radar measurements in the North Sea. They found wave heights to decrease with increasing bandwidth. Most of their time series were recorded at $f_s = 2$-4 Hz. Also the data set of Karmpadakis et al. (2020) includes the radar stations we used in the present study, with the time series starting somewhat earlier and continuing until February 2017. In addition to the difference in measurement period, it should be noted that Karmpadakis et al. (2020) did not exclude any $H_s$ values, which makes our study not exactly comparable to theirs. However, Karmpadakis et al. (2020) distinguish between deep and shallow water in their results. Most recent findings by Häfner et al. (2021b) revealed, based on machine learning algorithms applied to Coastal Data Information Program (CDIP) buoy data from the US coast with $H_s > 1$ m, that the spectral bandwidth ($\nu$ and $Q_p$) provides some information on the probability of rogue waves according to the height criterion. Furthermore, their study revealed that bandwidth effects are not relevant for wave crests. Based on our measurement data, we can confirm these results:

although we observed slightly higher bandwidths than normal in crest rogue wave time series, these differences showed to be statistically insignificant. The CDIP data set includes data from water depths between aproximately 10 and 4500 m. Häfner et al. (2021b) supposed that the influence of second-order nonlinearities on wave crests might be higher than estimated on the basis of buoy measurement data, because wave buoys are known to underestimate crest heights (Allender et al. 1989; Forristall 2000). With our data set consisting of both, buoy and radar time series, we had the possibility to compare the results for wave crests based on both instruments, and came to the conclusion that the influence of spectral bandwidth on crest rogue waves is similarly negligible in both types of time series. Also Cattrell et al. (2018) stated an influence of the spectral bandwidth on rogue wave occurrence. However, they came to different conclusions. In their investigation of 80 of the 161 CDIP buoys that were available to Häfner et al. (2021b), the distributions of the spectral bandwidth parameters $\varepsilon$ and $\nu$ indicated that the probability of observing a height rogue wave increased in seas with a higher bandwidth, while that of observing a crest rogue wave increased in seas with a narrow spectral bandwidth. As opposed to Häfner et al. (2021b), Cattrell et al. (2018) investigated the entire range of $H_s$ values, which could lead to the difference in findings. Our data from the southern North Sea seem to resemble the results of Häfner et al. (2021b). Finally, Stansell (2004) claimed, based on a statistical analysis of storm waves at the North Alwyn platform in the North Sea, measured by laser altimeters ($H_s > 3$ m, $h = 130$ m, $f_s = 5$ Hz), that the occurrence probability of rogue waves is only weakly dependent on the spectral bandwidth $\nu$, which confirms our results regarding the narrowness parameter $\nu$ at the radar stations.

It is possible that the results on the influence of spectral bandwidth on rogue wave occurrence are dependent on the sampling frequency of the measurement device: while buoy measurements at $f_s = 1.28$ Hz identified strong dependencies of at least height rogue wave occurrence on the spectral bandwidth (Häfner et al. 2021b; Cattrell et al. 2018), and these results were still valid (Karmpadakis et al. 2020) or less pronounced (Christou and Ewans 2014) in 2-4 Hz radar measurements, the influence of the spectral bandwidth was described as insignificant in a study based on 5 Hz laser measurements (Stansell 2004). We can confirm that in our data set, the influence of spectral bandwidth on height rogue waves was more pronounced in the time series recorded at $f_s = 1.28$ Hz than in the 2 Hz and sub-sampled at 2 Hz, radar data. This leads to the question to what extent the influence of the spectral bandwidth on rogue wave occurrence is actually a physical mechanism and how much of the effect should be attributed to the measurement instrument. Measurement instruments with low sampling frequencies are known to underestimate the occurrence frequency and the heights of the largest waves (Stansell et al. 2002). A false estimation of the spectral bandwidth could be a consequence. For further investigations on this issue, it would be valuable to have a radar device and a wave buoy installed not only in the same area, but at exactly the same place and compare measurement results.

Other reasons for differences in measurement results could be the restriction to specific $H_s$ ranges applied by some authors, or a different behavior of waves at shallow water stations, which were not considered separately in all studies.

In our data, the BFI as the commonly accepted indicator for the modulational instability, was not characteristic during rogue wave occurrence. This again confirms a result of Häfner et al. (2021b), who showed for their data that the BFI as a measure of nonlinear effects does not play a role for the prediction of rogue waves. Also Orzech and Wang (2020) found in buoy measurement data from the US coast the BFI in rogue wave samples only slightly increased, although they identified a higher probability of narrower directional spreading in rogue wave samples- the mean directional spreading during rogue wave events being 5 % lower than in normal samples. They inferred from seasonal narrowing of the directional spreading in their measurement area a locally increased rogue wave probability.

Also in terms of the directional spreading, we could not identify any characteristic tendency during rogue wave occurrence, which agrees with findings by Christou and Ewans (2014) and Häfner et al. (2021b). We agree with Christou and Ewans (2014), who conclude from this observation that "the environmental conditions generating normal waves, are also able to form rogue waves". On the other hand, Waseda et al. (2011) observed in a hindcast that on days with a high occurrence of height rogue waves, as identified by radar measurements at a platform in the North Sea, the directional spreading of the wave spectrum was narrower than on other days. In our combined analysis of directional spreading and spectral bandwidth, we found that our rogue waves did not occur in sea states that were narrow-banded in frequency and angular direction.

We ensured for all parameters in rogue wave samples, by reducing the height of each identified rogue wave by 50 %, that the bandwidth parameters were not influenced by the presence of the rogue wave itself. In fact, this test showed that while the significant wave height of the samples decreased as a result of the reduction of the rogue wave height, the bandwidth parameters and the BFI did not change. Thus, the influence of one rogue wave on the spectral parameters of a 30 minute time series was small, as opposed to the 20 minute windows investigated by Stansell (2004). He found that the difference in spectral bandwidth disappeared when the rogue wave was removed. In our 30 minute time series, it appeared that the information in the bandwidth on the possible presence of a rogue wave was contained within the wave spectrum, not in the rogue wave itself.

The measurement data from the eight stations in the southern North Sea have been part of an earlier study (Teutsch et al. 2020). In that study, the rogue wave frequency was documented with respect to the total number of measured waves at each station (although without the $H_{s,70}$ restriction). When comparing the bandwidth parameters $\varepsilon$ and $\nu$, as presented in Fig. 6, with the rogue wave frequencies from the previous study, it is seen that a high rogue wave occurrence corresponds to a narrow frequency spectrum (Fig. 18).

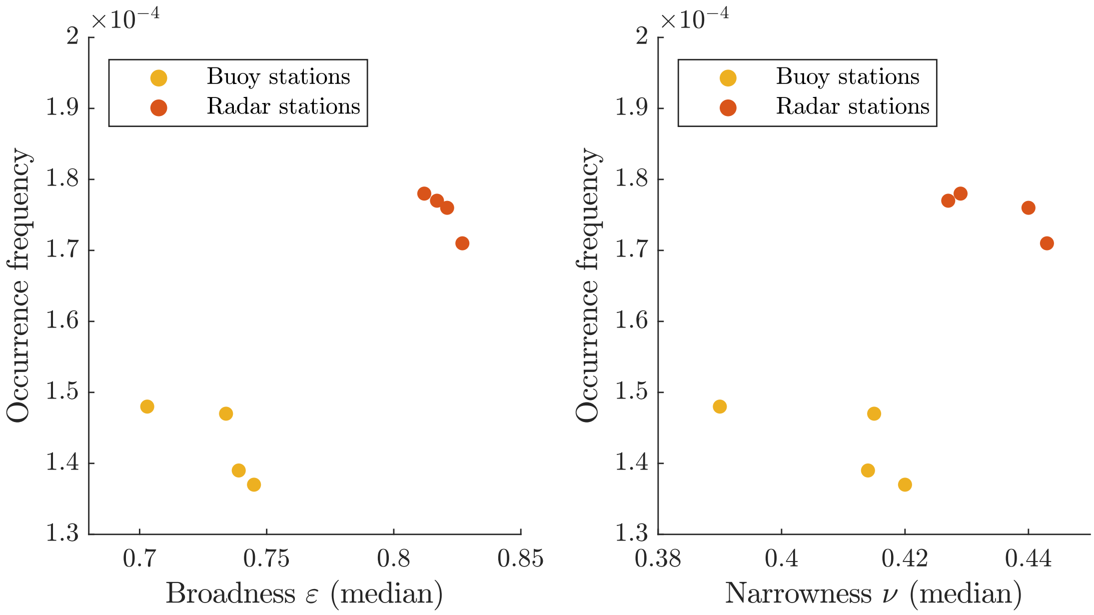


Fig. 18. Comparison of the bandwidth parameters $\varepsilon$ and $\nu$ with rogue wave occurrence frequencies from Teutsch et al. (2020).

The parameters $Q_p$ and BFI did not show any correlation with the rogue wave frequency. The directional spreading could not be compared at all stations, since the radar measurements are one-dimensional. From Teutsch et al. (2020), it is noted that all buoy stations showed rogue wave frequencies below the expectation from second-order theory. Here, Janssen and Bidlot (2009) should be cited, who state that the sea state de-focusses above a certain threshold of $\sigma_\Theta$, which yields even fewer rogue waves than expected according to second-order theory. Having the thresholds of 14-15° in wave tank experiments (Waseda 2006; Onorato et al. 2009) and 30° in the ocean (Waseda et al. 2009) in mind, this could indeed be the case in our measurement data.

## 5. Conclusions

In a data set consisting of radar and buoy measurements from the southern North Sea, we identified lower values of spectral bandwidth than usual during height rogue wave occurrence. Samples with rogue waves according to the crest criterion in turn could not be attributed to specific bandwidth conditions. The directional spreading did not give any indication on the occurrence of rogue waves of any kind, neither did the BFI as a commonly applied indicator for the modulational instability. We conclude that the majority of rogue waves in our data set were probably not generated by a modulational instability, since high spectral bandwidth and directional spreading are unfavorable conditions for nonlinear focusing.

*Acknowledgments.* Ina Teutsch received funding for this work from the Federal Maritime and Hydrographic Agency (BSH). The buoy data were kindly provided by BSH. The authors are grateful to Graham Feld and Shell for providing the radar data. The authors are grateful to Jens Möller and Christian Senet for their valuable input. The article processing charges for this publication were covered by a Research Centre of the Helmholtz Association.

*Data availability statement.* The underlying wave buoy and radar data are the property of and were made available by the Federal Maritime and Hydrographic Agency, Germany, and Shell, UK, respectively. They can be obtained upon request from these organizations.

## References

Alber, I. E., 1978: The effects of randomness on the stability of two-dimensional surface wavetrains. *Proceedings of the Royal Society of London. A. Mathematical and Physical Sciences*, **363 (1715)**, 525–546, https://doi.org/10.1098/rspa.1978.0181, URL https://doi.org/10.1098/rspa.1978.0181.

Alber, I. E., and P. G. Saffman, 1978: Stability of random nonlinear deepwater waves with finite bandwidth spectra. TRW Defense and Space System Group Rep.

Allender, J., and Coauthors, 1989: The wadic project: A comprehensive field evaluation of directional wave instrumentation. *Ocean Engineering*, **16 (5-6)**, 505–536, https://doi.org/10.1016/0029-8018(89)90050-4, URL https://doi.org/10.1016/0029-8018(89)90050-4.

Benjamin, T. B., 1967: Instability of periodic wavetrains in nonlinear dispersive systems. *Proceedings of the Royal Society of London. Series A. Mathematical and Physical Sciences*, **299 (1456)**, 59–76, https://doi.org/10.1098/rspa.1967.0123, URL https://doi.org/10.1098/rspa.1967.0123.

Benjamin, T. B., and J. E. Feir, 1967: The disintegration of wave trains on deep water. *Journal of Fluid Mechanics*, **27 (3)**, 417–430, https://doi.org/10.1017/s002211206700045x, URL https://doi.org/10.1017/s002211206700045x.

Campbell, R., 2022: raacampbell/shadederrorbar. GitHub, URL https://github.com/raacampbell/shadedErrorBar.

Cartwright, D. E., and M. S. Longuet-Higgins, 1956: The statistical distribution of the maxima of a random function. *Proceedings of the Royal Society of London. Series A. Mathematical and Physical Sciences*, **237 (1209)**, 212–232, https://doi.org/10.1098/rspa.1956.0173, URL https://doi.org/10.1098/rspa.1956.0173.

Casas-Prat, M., L. Holthuijsen, and P. Gelder, 2009: Short-term statistics of 10,000,000 waves observed by buoys. *Proceedings of the Coastal Engineering Conference*, 560–572, https://doi.org/10.1142/9789814277426_0047.

Cattrell, A. D., M. Srokosz, B. I. Moat, and R. Marsh, 2018: Can rogue waves be predicted using characteristic wave parameters? *Journal of Geophysical Research: Oceans*, **123 (8)**, 5624–5636, https://doi.org/10.1029/2018jc013958, URL https://doi.org/10.1029/2018jc013958.

Christou, M., and K. Ewans, 2014: Field measurements of rogue water waves. *Journal of Physical Oceanography*, **44 (9)**, 2317–2335, https://doi.org/10.1175/jpo-d-13-0199.1, URL https://doi.org/10.1175/jpo-d-13-0199.1.

Dysthe, K., H. E. Krogstad, and P. Müller, 2008: Oceanic rogue waves. *Annual Review of Fluid Mechanics*, **40 (1)**, 287–310, https://doi.org/10.1146/annurev.fluid.40.111406.102203, URL https://doi.org/10.1146/annurev.fluid.40.111406.102203.

Fedele, F., 2015: On the kurtosis of deep-water gravity waves. *Journal of Fluid Mechanics*, **782**, 25–36, https://doi.org/10.1017/jfm.2015.538, URL https://doi.org/10.1017/jfm.2015.538.

Fedele, F., J. Brennan, S. P. de León, J. Dudley, and F. Dias, 2016: Real world ocean rogue waves explained without the modulational instability. *Scientific Reports*, **6 (1)**, https://doi.org/10.1038/srep27715, URL https://doi.org/10.1038/srep27715.

Forristall, G. Z., 2000: Wave crest distributions: Observations and second-order theory. *Journal of Physical Oceanography*, **30 (8)**, 1931–1943, https://doi.org/10.1175/1520-0485(2000)030<1931:wcdoas>2.0.co;2, URL https://doi.org/10.1175/1520-0485(2000)030<1931:wcdoas>2.0.co;2.

Gibson, R., and C. Swan, 2006: The evolution of large ocean waves: the role of local and rapid spectral changes. *Proceedings of the Royal Society A: Mathematical, Physical and Engineering Sciences*, **463 (2077)**, 21–48, https://doi.org/10.1098/rspa.2006.1729, URL https://doi.org/10.1098/rspa.2006.1729.

Goda, Y., 1970: Numerical experiments on wave statistics with spectral simulation. *Report of the Port and Harbour Research Institute*, **9 (3)**, 3–57.

Goda, Y., 1988a: Numerical investigation on plotting formulas and confidence intervals of return values in extreme statistics. *Report of the Port and Harbour Research Institute*, **27 (1)**, 31–92 (in Japanese).

Goda, Y., 1988b: ON THE METHODOLOGY OF SELECTING DESIGN WAVE HEIGHT. *Coastal Engineering Proceedings*, **1 (21)**, 67, https://doi.org/10.9753/icce.v21.67, URL https://doi.org/10.9753/icce.v21.67.

Gramstad, O., and K. Trulsen, 2007: Influence of crest and group length on the occurrence of freak waves. *Journal of Fluid Mechanics*, **582**, 463–472, https://doi.org/10.1017/s0022112007006507, URL https://doi.org/10.1017/s0022112007006507.

Häfner, D., J. Gemmrich, and M. Jochum, 2021a: FOWD: A free ocean wave dataset for data mining and machine learning. *Journal of Atmospheric and Oceanic Technology*, https://doi.org/10.1175/jtech-d-20-0185.1, URL https://doi.org/10.1175/jtech-d-20-0185.1.

Häfner, D., J. Gemmrich, and M. Jochum, 2021b: Real-world rogue wave probabilities. *Scientific Reports*, **11 (1)**, https://doi.org/10.1038/s41598-021-89359-1, URL https://doi.org/10.1038/s41598-021-89359-1.

Haver, S., and O. J. Andersen, 2000: Freak waves: rare realizations of a typical population or typical realizations of a rare population? *The Tenth International Offshore and Polar Engineering Conference*, International Society of Offshore and Polar Engineers.

Holthuijsen, L. H., 2007: *Waves in Oceanic and Coastal Waters*. Cambridge University Press, https://doi.org/10.1017/cbo9780511618536, URL https://doi.org/10.1017/cbo9780511618536.

Huntley, D. A., R. T. Guza, and A. J. Bowen, 1977: A universal form for shoreline run-up spectra? *Journal of Geophysical Research*, **82 (18)**, 2577–2581, https://doi.org/10.1029/jc082i018p02577, URL https://doi.org/10.1029/jc082i018p02577.

Janssen, P. A. E. M., 2003: Nonlinear four-wave interactions and freak waves. *Journal of Physical Oceanography*, **33 (4)**, 863–884.

Janssen, P. A. E. M., and J.-R. Bidlot, 2009: On the extension of the freak wave warning system and its verification. **(588)**, 42, https://doi.org/10.21957/uf1sybog, URL https://www.ecmwf.int/node/10243.

Karmpadakis, I., C. Swan, and M. Christou, 2020: Assessment of wave height distributions using an extensive field database. *Coastal Engineering*, **157**, 103 630, https://doi.org/10.1016/j.coastaleng.2019.103630, URL https://doi.org/10.1016/j.coastaleng.2019.103630.

Lake, B. M., H. C. Yuen, H. Rungaldier, and W. E. Ferguson, 1977: Nonlinear deep-water waves: theory and experiment. part 2. evolution of a continuous wave train. *Journal of Fluid Mechanics*, **83 (1)**, 49–74, https://doi.org/10.1017/s0022112077001037, URL https://doi.org/10.1017/s0022112077001037.

Latheef, M., and C. Swan, 2013: A laboratory study of wave crest statistics and the role of directional spreading. *Proceedings of the Royal Society A: Mathematical, Physical and Engineering Sciences*, **469 (2152)**, 20120 696, https://doi.org/10.1098/rspa.2012.0696, URL https://doi.org/10.1098/rspa.2012.0696.

Longuet-Higgins, M. S., 1975: On the joint distribution of the periods and amplitudes of sea waves. *Journal of Geophysical Research*, **80 (18)**, 2688–2694, https://doi.org/10.1029/jc080i018p02688, URL https://doi.org/10.1029/jc080i018p02688.

Naess, A., 1985: On the distribution of crest to trough wave heights. *Ocean Engineering*, **12 (3)**, 221–234, https://doi.org/10.1016/0029-8018(85)90014-9, URL https://doi.org/10.1016/0029-8018(85)90014-9.

Onorato, M., A. R. Osborne, and M. Serio, 2002: Extreme wave events in directional, random oceanic sea states. *Physics of Fluids*, **14 (4)**, L25–L28, https://doi.org/10.1063/1.1453466, URL https://doi.org/10.1063/1.1453466.

Onorato, M., A. R. Osborne, M. Serio, and S. Bertone, 2001: Freak waves in random oceanic sea states. *Physical Review Letters*, **86 (25)**, 5831–5834, https://doi.org/10.1103/physrevlett.86.5831, URL https://doi.org/10.1103/physrevlett.86.5831.

Onorato, M., A. R. Osborne, M. Serio, L. Cavaleri, C. Brandini, and C. T. Stansberg, 2004: Observation of strongly non-gaussian statistics for random sea surface gravity waves in wave flume experiments. *Physical Review E*, **70 (6)**, https://doi.org/10.1103/physreve.70.067302, URL https://doi.org/10.1103/physreve.70.067302.

Onorato, M., and Coauthors, 2009: Statistical properties of mechanically generated surface gravity waves: a laboratory experiment in a three-dimensional wave basin. *Journal of Fluid Mechanics*, **627**, 235–257, https://doi.org/10.1017/s002211200900603x, URL https://doi.org/10.1017/s002211200900603x.

Orzech, M. D., and D. Wang, 2020: Measured rogue waves and their environment. *Journal of Marine Science and Engineering*, **8 (11)**, 890, https://doi.org/10.3390/jmse8110890, URL https://doi.org/10.3390/jmse8110890.

Pawka, S. S., 1983: Island shadows in wave directional spectra. *Journal of Geophysical Research*, **88**, 2579–2591.

Prevosto, M., 1998: Effect of directional spreading and spectral bandwidth on the nonlinearity of the irregular waves.

Rye, H., 1977: The stability of some currently used wave parameters. *Coastal Engineering*, **1**, 17–30, https://doi.org/10.1016/0378-3839(77)90004-7, URL https://doi.org/10.1016/0378-3839(77)90004-7.

Saulnier, J.-B., A. Clément, A. F. de O. Falcão, T. Pontes, M. Prevosto, and P. Ricci, 2011: Wave groupiness and spectral bandwidth as relevant parameters for the performance assessment of wave energy converters. *Ocean Engineering*, **38 (1)**, 130–147, https://doi.org/10.1016/j.oceaneng.2010.10.002, URL https://doi.org/10.1016/j.oceaneng.2010.10.002.

Stansberg, C. T., 1995: Effects from directionality and spectral bandwidth on non-linear spatial modulations of deep-water surface gravity wave trains. *Coastal Engineering 1994*, American Society of Civil Engineers, https://doi.org/10.1061/9780784400890.044, URL https://doi.org/10.1061/9780784400890.044.

Stansell, P., 2004: Distributions of freak wave heights measured in the north sea. *Applied Ocean Research*, **26 (1-2)**, 35–48, https://doi.org/10.1016/j.apor.2004.01.004, URL https://doi.org/10.1016/j.apor.2004.01.004.

Stansell, P., J. Wolfram, and B. Linfoot, 2002: Effect of sampling rate on wave height statistics. *Ocean Engineering*, **29 (9)**, 1023–1047, https://doi.org/10.1016/s0029-8018(01)00066-x, URL https://doi.org/10.1016/s0029-8018(01)00066-x.

Tamura, H., T. Waseda, and Y. Miyazawa, 2009: Freakish sea state and swell-windsea coupling: Numerical study of theSuwa-maruincident. *Geophysical Research Letters*, **36 (1)**, https://doi.org/10.1029/2008gl036280, URL https://doi.org/10.1029/2008gl036280.

Tayfun, M. A., 1983: Effects of spectrum band width on the distribution of wave heights and periods. *Ocean Engineering*, **10**, 107–118.

Tayfun, M. A., 2008: Distributions of envelope and phase in wind waves. *Journal of Physical Oceanography*, **38 (12)**, 2784–2800, https://doi.org/10.1175/2008jpo4008.1, URL https://doi.org/10.1175/2008jpo4008.1.

Teutsch, I., R. Weisse, J. Moeller, and O. Krueger, 2020: A statistical analysis of rogue waves in the southern north sea. *Natural Hazards and Earth System Sciences*,

**20 (10)**, 2665–2680, https://doi.org/10.5194/nhess-20-2665-2020, URL https://doi.org/10.5194/nhess-20-2665-2020.

Vandever, J. P., E. M. Siegel, J. M. Brubaker, and C. T. Friedrichs, 2008: Influence of spectral width on wave height parameter estimates in coastal environments. *Journal of Waterway, Port, Coastal, and Ocean Engineering*, **134 (3)**, 187–194, https://doi.org/10.1061/(ASCE)0733-950X(2008)134:3(187).

Waseda, T., 2006: Impact of directionality on the extreme wave occurrence in a discrete random wave system. *9th International Workshop on Wave Hindcasting and Forecasting, September 24-29*, American Society of Civil Engineers.

Waseda, T., M. Hallerstig, K. Ozaki, and H. Tomita, 2011: Enhanced freak wave occurrence with narrow directional spectrum in the north sea. *Geophysical Research Letters*, **38 (13)**, n/a–n/a, https://doi.org/10.1029/2011gl047779, URL https://doi.org/10.1029/2011gl047779.

Waseda, T., T. Kinoshita, and H. Tamura, 2009: Evolution of a random directional wave and freak wave occurrence. *Journal of Physical Oceanography*, **39 (3)**, 621–639, https://doi.org/10.1175/2008jpo4031.1, URL https://doi.org/10.1175/2008jpo4031.1.

Yuen, H. C., and W. E. Ferguson, 1978: Relationship between benjamin–feir instability and recurrence in the nonlinear schroedinger equation. *Physics of Fluids*, **21 (8)**, 1275, https://doi.org/10.1063/1.862394, URL https://doi.org/10.1063/1.862394.

# C Shallow-water rogue waves

This appendix contains a paper, which has been submitted to the journal "Natural Hazards and Earth System Sciences" as

**Teutsch, I., Brühl, M., Weisse, R., and Wahls, S., 2022:**
**Contribution of solitons to enhanced rogue wave occurrence in shallow water: a case study in the southern North Sea.**
***Natural Hazards and Earth System Sciences Discussions*** **[preprint], https://doi.org/10.5194/nhess-2022-28**, in review
under the Creative Commons Attribution 4.0 License.

The contribution of Ina Teutsch and the other authors to this paper is as follows.
All authors contributed to the idea and scope of the paper. Ina Teutsch pursued the procedure of analysing different rogue wave categories separately. Ina Teutsch performed the analyses, using MATLAB code provided by Sander Wahls. Ralf Weisse supervised the work. Markus Brühl and Sander Wahls provided help with the code and further explanations concerning nonlinear theory. Ina Teutsch presented the comparison between rogue wave heights and soliton amplitudes to the other authors, who provided help with the interpretation of the results and suggested further parameters to investigate, such as the Ursell number. Ina Teutsch discovered in a sub-set of the data, that time series containing rogue waves typically yielded a discrete spectrum with an outstanding soliton, and defined a criterion for this "outstandingness" for the application to the larger data set. Ina Teutsch repeated the analysis for different depth assumptions and for samples with a small directional spread, as to check the sensitivity of the results to the water depth and the directional spread of the waves, respectively. All authors discussed the results and their limitations like the restriction to the measurement window size of 30 minutes, and contributed to the interpretation. Ina Teutsch prepared the draft of the paper. All authors contributed to its revision and improvement.

https://doi.org/10.5194/nhess-2022-28
Preprint. Discussion started: 4 March 2022


Natural Hazards and Earth System Sciences
Discussions

# Contribution of solitons to enhanced rogue wave occurrence in shallow water: a case study in the southern North Sea

Ina Teutsch[1], Markus Brühl[2], Ralf Weisse[1], and Sander Wahls[2]

[1]Helmholtz-Zentrum Hereon, Max-Planck-Str. 1, 21502 Geesthacht, Germany
[2]Delft Center for Systems and Control, Delft University of Technology, 2860 Delft, South Holland, Netherlands

**Correspondence:** Ina Teutsch (ina.teutsch@hereon.de)

**Abstract.** The shallow waters off the coast of Norderney in the southern North Sea are characterised by a higher frequency of rogue wave occurrences than expected according to second-order theory. The role of nonlinear processes for the generation of rogue waves at this location is currently unclear. Within the framework of the Korteweg–de Vries (KdV) equation, we investigated the discrete soliton spectra of measured time series at Norderney to determine differences between time series with and without rogue waves. For this purpose, we applied a nonlinear Fourier transform for the Korteweg–de Vries equation with vanishing boundary conditions (vKdV-NLFT). For each time series containing a rogue wave, we were able to identify at least one soliton in the discrete nonlinear vKdV-NLFT spectrum that contributed to the occurrence of the rogue wave in that time series. The amplitudes of these solitons were generally found to be smaller than the crest height of the corresponding rogue wave and interaction with the continuous wave spectrum is needed to fully explain the observed rogue wave. Time series with and without rogue waves showed different characteristic soliton spectra. In most of the spectra calculated from rogue wave time series, most of the solitons clustered around similar heights, while the largest soliton was outstanding with an amplitude significantly larger than all other solitons. The presence of a clearly outstanding soliton in the spectrum was found to be an indicator pointing towards enhanced probability for detecting a rogue wave in the time series. Similarly, when the discrete spectrum appears as a cluster of solitons without the presence of a clearly outstanding soliton, the presence of a rogue wave in the observed time series is unlikely. Under the hypothesis that the KdV describes the evolution of the sea state around the measurement site well, these results suggest that solitons and nonlinear processes substantially contribute to the enhanced occurrence of rogue waves off Norderney.

## 1 Introduction

There has been a lively discussion on whether the occurrence frequency of rogue waves in the open ocean is well described by second-order models. Both Rayleigh (Longuet-Higgins, 1952) and Weibull distributions (Forristall, 1978) have been used to describe the distributions of wave and crest heights. Distributions were assessed for measurement data collected by surface-following buoys (e.g., Baschek and Imai, 2011; Pinho et al., 2004; Cattrell et al., 2018), by radar devices (e.g., Olagnon and v. Iseghem, 2000; Christou and Ewans, 2014; Karmpadakis et al., 2020), and laser altimeters (e.g., Soares et al., 2003; Stansell, 2004), as well as by ADCPs (Fedele et al., 2019). Independent of the measurement device, some authors found measured

https://doi.org/10.5194/nhess-2022-28
Preprint. Discussion started: 4 March 2022



wave heights to agree well with the established distributions, while others found the frequency of rogue wave occurrences over- or underestimated. For example, for the northern North Sea, all three inferences have been made: While Olagnon and v. Iseghem (2000) found rogue wave occurrences to be overpredicted by the classical distributions, they appeared to be in agreement with a Weibull distribution in data of Waseda et al. (2011) and to be underestimated in the dataset of Stansell (2004). Rogue wave occurrences in buoy data from the US coast, recorded in shallow, intermediate and deep water, were found to be strongly overestimated by a Rayleigh distribution. Furthermore, the respective authors describe local differences in rogue wave occurrence frequency between their measurement stations (Baschek and Imai, 2011), depending on the wave climate and especially in coastal waters, where waves interact with the seabed (Cattrell et al., 2018; Orzech and Wang, 2020). In a previous study, we have analysed measurement data from various stations in the southern North Sea (Teutsch et al., 2020) and found rogue wave frequencies to vary spatially and by measurement device. For data obtained from wave buoy measurements, we generally found rogue wave frequencies slightly overestimated by the Forristall distribution, which is a special form of the Weibull distribution, fit to wave data recorded during hurricanes (Forristall, 1978). An exception was one measurement buoy, which was located in the shallow waters off the coast of the island Norderney, Germany (Fig. 1). For this buoy, enhanced rogue wave occurrence, which could not be explained by the Forristall distribution, was observed. This suggests that nonlinear processes and interactions may play a role in explaining the increase in rogue wave occurrence frequency at this specific location.

https://doi.org/10.5194/nhess-2022-28
Preprint. Discussion started: 4 March 2022

Natural Hazards and Earth System Sciences
Open Access
Discussions

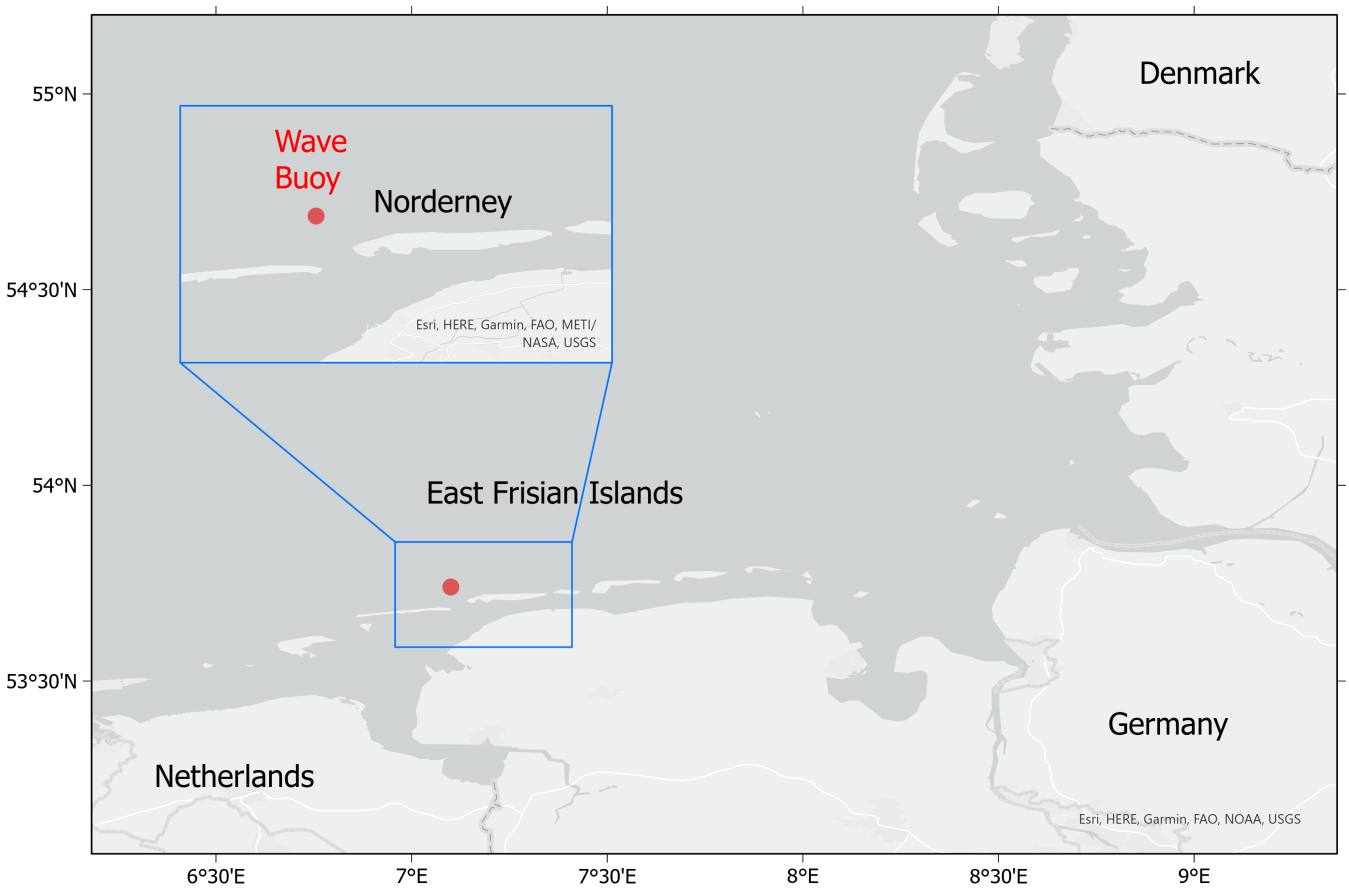


**Figure 1.** Map of the German Bight, showing the location of the measurement buoy close to the island Norderney.

So far, the nonlinear behaviour of deep-water rogue waves has received considerably more attention than that of shallow-water rogue waves. The evolution of the complex envelope of unidirectional wave trains in deep water can be described by the cubic nonlinear Schroedinger (NLS) equation (Onorato et al., 2001; Slunyaev, 2005). Deep water in this context is defined in terms of the wave number $k$ and the water depth $h$ as $k\ h > 1.36$, which represents the lower limit for the application of the NLS equation (Osborne, 2010). The NLS equation is a weakly nonlinear, narrow-banded approximation of the fully nonlinear water wave equations, including both nonlinearity and dispersion (Serio et al., 2006). In deep water, rogue-wave occurrence beyond the second-order model has been explained, for example, by a nonlinear instability that was also found in numerical simulations and tank experiments (Dysthe et al., 2008). Here, uniform wave trains are modulationally unstable to small oblique perturbations and disintegrate into groups, in which the highest wave becomes significantly larger than the wave height in the original train (Benjamin and Feir, 1967). This nonlinear focusing mechanism does not only increase the maximum wave height, but also the probability of rogue wave occurrence (Slunyaev and Shrira, 2013). Alber (1978) derived a stability criterion for such narrow-banded random waves, which later became known as the Benjamin-Feir index (BFI) (Janssen, 2003). A large BFI corresponds to enhanced nonlinearity (de León and Soares, 2014) and has been suggested as an indicator for enhanced rogue

https://doi.org/10.5194/nhess-2022-28
Preprint. Discussion started: 4 March 2022

Natural Hazards and Earth System Sciences
Discussions

wave probability in deep water (Gramstad and Trulsen, 2007). The NLS equation has some exact solutions (known as breathers) that explain the modulational instability, which have been suggested as an analytical model of rogue waves in a unidirectional case (Dysthe and Trulsen, 1999). Here a uniform wave train develops into a number of breathers, and then relaxes back to a uniform wavetrain (Clamond et al., 2006; Gramstad and Trulsen, 2007). Each breather solution represents the modulational instability growth for a specific initial perturbation. In the framework of the NLS equation, a large part of the dynamics of nonlinear waves can be described in terms of interacting breathers (Slunyaev and Shrira, 2013). Specifically the Peregrine breather (Peregrine, 1983), which is characterised by only one oscillation in time and an amplitude of three times the initial wave train, has been subject to analysis (Shrira and Geogjaev, 2009). Recently, the growth of crest heights due to nonlinearities that was observed in deep water, has been extended to intermediate water depths (Karmpadakis et al., 2019). However, the relevance of the modulational instability of the NLS equation to the formation of real rogue waves remains unclear because most of these works only consider the specific scenario of perturbed plane wave envelopes (Slunyaev and Shrira, 2013).

The role of nonlinearity with respect to rogue wave generation in shallow water has received considerably less attention than for deep water. Shallow-water wind waves substantially differ from deep-water wind waves and it is not appropriate to simply scale the deep-water nonlinear interaction to shallow-water waves (Janssen and Onorato, 2007). As the water depth becomes more and more shallow, a wave-induced current develops and less wave energy is available for nonlinear focusing (Benjamin and Feir, 1967; Janssen and Onorato, 2007). Although waves in shallow water can also destabilise due to oblique perturbations (Toffoli et al., 2013), the modulational instability in shallow water does not enhance the formation of extreme waves (Fernandez et al., 2014). Fedele et al. (2019) stated that waves in shallow water break before they can start to “breathe” and become rogue waves. Therefore, some authors expect the rogue wave probability to decrease in shallow water (e.g., Slunyaev et al., 2016). Other authors refer to the large ratio between nonlinearity and dispersion in shallow water (Kharif and Pelinovsky, 2003) and concluded that Gaussian statistics are not sufficient for the description of shallow-water waves and that rogue waves are likely to occur more frequently as the water depth decreases (Garett and Gemmrich, 2009; Sergeeva et al., 2011). While in deep water only the free-surface nonlinearity must be taken into account, the nonlinearity in shallow water is mainly a result of the interaction of waves with the sea floor (Prevosto, 1998). Refraction, shoaling and higher-order nonlinear effects change the shapes of waves and their energy spectrum (Bitner, 1980; Tayfun, 2008). However, so far only few studies have addressed the impact of bathymetry on rogue wave generation. For example, Soomere (2010) found that in shallow water, compared to deep water, due to wave-bathymetry interaction, additional processes associated with the generation of extreme waves, like wave amplification along certain coastal profiles, redirection of waves or the formation of crossing seas, are relevant, and therefore more rogue waves should be expected in nearshore regions.

The shallow-water equivalent to the NLS equation is the Korteweg–de Vries (KdV) equation (Korteweg and de Vries, 1895). It describes weakly nonlinear and dispersive progressive unidirectional free-surface waves in shallow water with constant depth (Peregrine, 1983). The solutions of the KdV are stable, in that the wave amplitude does not alter significantly when the initial wave train is perturbed. This is the mathematical explanation of why rogue waves in shallow water cannot be a result of the modulational instability. The inverse scattering transform (IST) was introduced as a tool to solve the KdV equation (Gardner et al., 1967), and later-on also a broader range of evolution equations (Ablowitz et al., 1974). The name scattering transform

https://doi.org/10.5194/nhess-2022-28
Preprint. Discussion started: 4 March 2022



has its roots in physics, where the tools applied in the derivation of the IST are used to analyse how particles behave in the interaction with a scatterer (Wahls and Poor, 2015). When a time series is close to linear, its scattering data essentially reduces to the linear Fourier Transform (FT). Therefore, the IST has been called a "natural extension of Fourier analysis to nonlinear problems" (Ablowitz et al., 1974). Henceforth in this paper, the method is referred to as the nonlinear Fourier transform for the KdV equation (KdV-NLFT). Zabusky and Kruskal (1965) discussed, by numerically solving the KdV equation, the decomposition of an initial signal into a train of solitons. Brühl and Oumeraci (2016) confirmed in laboratory experiments and numerical simulations that long cosine waves in shallow water decompose into trains of solitons that are solutions to the KdV equation and that show larger amplitudes than the initial wave height. The KdV-NLFT yields a discrete set of eigenvalues and a continuous spectrum. Each of the eigenvalues corresponds to a soliton (Peregrine, 1983), and the continuous spectrum to oscillatory waves. The asymptotic development of the solution with time leads to a decay of the oscillatory part and the solitons asymptotically dominate the solution (Zabusky and Kruskal, 1965).

The nonlinear interaction of solitons in shallow water has been discussed with regard to its role in rogue wave generation. Based on the KdV-NLFT, Pelinovsky et al. (2000) showed that dispersive focusing is possible in the nonlinear case, given the nonlinear wave train includes at least one soliton. Equivalently to the linear case, in which rogue waves evolve from the superposition of wave components, nonlinear focusing is then the interaction between one or multiple solitons with oscillatory waves, due to their velocity difference. For the unidirectional case, several authors (Kharif and Pelinovsky, 2003; Soomere and Engelbrecht, 2005) found that the interaction of KdV solitons does not lead to a significant increase in surface elevation. Soomere (2010) considered that since soliton interaction in the unidirectional case does not lead to an enhancement in surface elevation, a higher nonlinearity should even lead to a decrease in rogue wave occurrence probability. Since this is not consistent with observations, he concluded that directionality must play a role for the rogue wave generation in shallow water. Indeed, crossing solitons are known to be able to produce large amplitudes (Peterson et al., 2003). Zakharov and Shabat (1975) found the analytical two-soliton solution of the Kadomtsev-Petviashvili (KP) equation describing this case. Hammack et al. (1989) investigated two long-crested solitary waves propagating in different directions and interacting. In contrast to linear superposition, the interaction of two crossing solitons may produce a crest up to four times higher than the incoming waves (Peterson et al., 2003). Peterson et al. (2003) discussed the interaction of shallow-water solitons against the background of heavy fast ferry traffic. They made this restriction because shallow-water areas with heavy ship traffic are more likely to produce regular, long-crested 2D wave trains, necessary for their model of rogue waves, than wind sea on the open ocean. They emphasised that the interaction area is restricted and it is unlikely to detect an interaction soliton in one-point in-situ measurements. Osborne et al. (1991) analysed nearly unidirectional shallow-water measurement data from the Adriatic Sea in the framework of the KdV equation for an IST with quasi-periodic boundary conditions. They found several solitons in the discrete spectrum of the IST and pointed out their physical relevance for the structure of the time series. Since rogue wave occurrence in shallow water that goes beyond second order has not been sufficiently explained, and almost all investigations in previous work are based on theoretical considerations, numerical simulations or laboratory experiments, we consider real measurement time series in the framework of the KdV equation. We expand the investigation of data measured by a surface-following buoy off the coast of Norderney in the southern North Sea, for which second-order distributions have been shown to underestimate rogue wave

https://doi.org/10.5194/nhess-2022-28
Preprint. Discussion started: 4 March 2022




occurrence (Teutsch et al., 2020). We obtain a discrete soliton spectrum from the nonlinear Fourier transform for the KdV equation with vanishing boundary conditions (vKdV-NLFT) and explore to what extent the presence of solitons might contribute to this enhanced statistical rogue wave occurrence. For this purpose, we compare the soliton spectra of samples with and samples without rogue waves. The paper is structured as follows. Section 2.1 describes the measurement site and the dataset and gives a definition for rogue waves. In Sect. 2.2, the application of vKdV-NLFT to the measurement data is explained. Sect. 3 consists of two parts. In Sect. 3.1, we explore the direct association of solitons calculated from NLFT with rogue waves, while Sect. 3.2 discusses statistical differences in the soliton spectra of time series with and without rogue waves. In Sect. 4, we discuss the time windows and location for which our results are valid, and suggest further investigations. In Sect. 5 our conclusions are presented.

## 2 Methods

### 2.1 Measurement site and dataset

We analysed wave elevation data measured by a surface-following buoy off the coast of the island Norderney in the German Bight in the time period between 2011 and 2016. The measurement buoy was deployed at a nominal water depth of $h = 10$ m, which was assumed to be constant for the following analyses. Actually, the water depth off the coast of Norderney is not constant, as the bathymetry at the location is spatially highly variable with strong gradients (Fig. 2). The buoy is located right above a steep slope, running perpendicular to the mean incoming wave direction (Fig. 3). Since the buoy is restricted only by its mooring, it has the possibility to move horizontally. The actual water depth $h$ below the horizontally moving buoy may then be subject to rapid changes. In addition, the tidal range at the site is about 2.5 m (NLWKN, 2021), which further causes the water depth to vary.

https://doi.org/10.5194/nhess-2022-28
Preprint. Discussion started: 4 March 2022




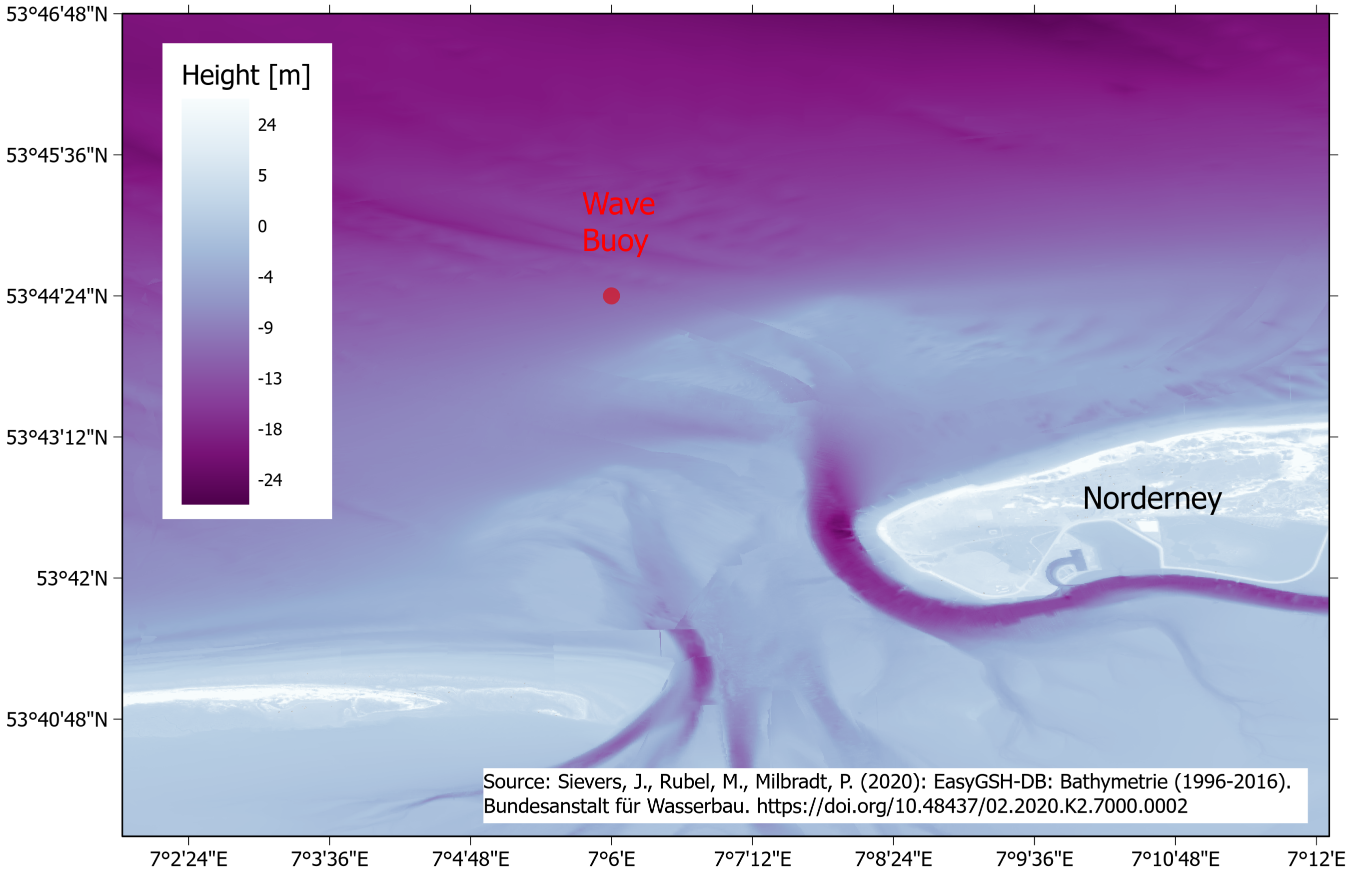


**Figure 2.** Bathymetry conditions [NN+m] at Norderney and the position of the measurement buoy.

https://doi.org/10.5194/nhess-2022-28
Preprint. Discussion started: 4 March 2022


Natural Hazards and Earth System Sciences
Open Access
Discussions

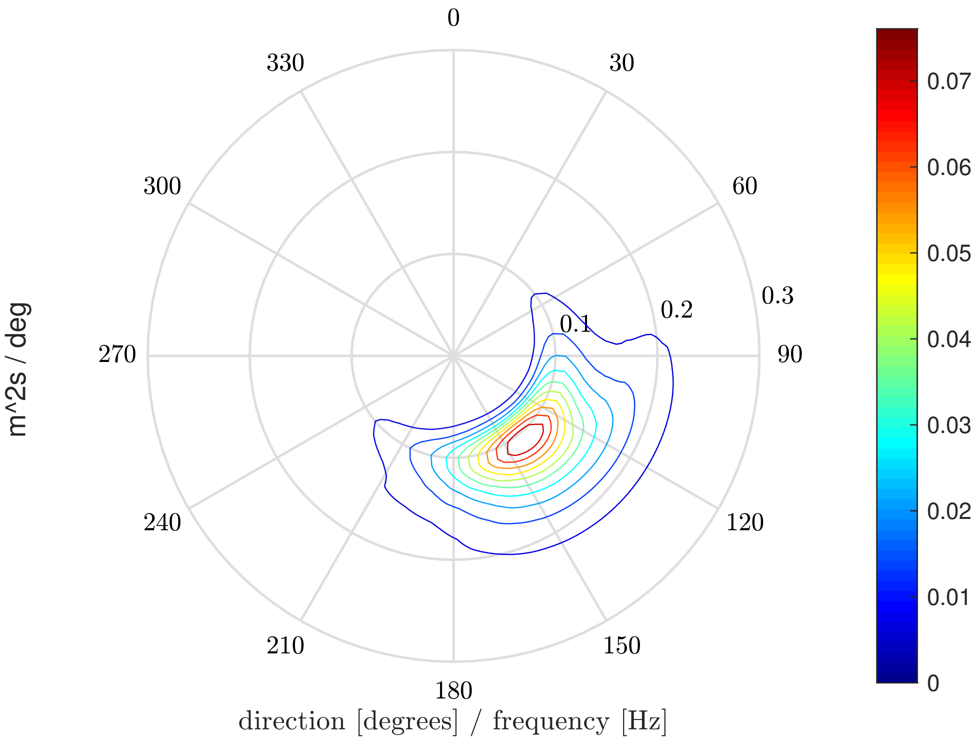


**Figure 3.** Mean directional wave spectrum from the time period 2011-2016, obtained by use of DIWASP (Johnson, 2002).

The wave data were measured at a frequency of 1.28 Hz and are available as a set of time series (samples) of 30 minute length. To exclude low-energy sea states in the following, only samples with a significant wave height $H_s$ above the long-term 70th percentile of the significant wave height, $H_{s,70} = 1.29$ m, were included in the analysis. The significant wave height $H_s$ is here defined as the mean of the highest 30 $\%$ of the wave heights in a 30 minute sample. $H_{s,70}$ was calculated from the significant wave heights $H_s$ of all 30 minute samples during the six years of available measurement data. On the one hand, this excludes possible measurement uncertainties caused by small waves that are only described by a few points, and on the other hand, it includes only rogue waves of heights relevant for offshore activities. Since the KdV equation for shallow water was to be applied to the data, only samples satisfying shallow-water conditions were included in the study. The shallow-water condition used was

$$\frac{h}{L} < 0.22 \qquad (1)$$

with water depth $h$ and wavelength $L$. The wavelength was calculated as

$$L = T_p * c \qquad (2)$$

from the peak period $T_p = 1 f_p^{-1}$ of each sample, with $f_p$ the peak frequency in the linear fast Fourier transform (FFT) spectrum of the sample, and the shallow-water wave celerity $c = \sqrt{gh}$ with gravity $g$. Following Eq. (1) and Eq. (2), the condition for the peak period may be written as

$$T_p > \frac{h}{0.22 \cdot c}. \tag{3}$$

For a water depth of $h = 10$ m, the peak period thus had to satisfy the condition $T_p > 4.6$ s, in order for a sample to classify for shallow-water conditions. We based the shallow-water condition on the peak period $T_p$ of the entire sample to assume that shallow-water wave properties as described by the KdV equation strongly contribute to the wave processes in the sample. Nevertheless, it was additionally ensured that each of the individual rogue waves (or the highest wave in each sample that did not contain a rogue wave) satisfied shallow-water conditions, based on its period $T_{\max}$. Of all the selected samples above $H_{s,70}$, shallow-water conditions applied in more than 98 % of the cases and were thus the dominant condition in these samples. The 2 % of the samples not satisfying shallow-water conditions were discarded and not considered in the analysis.
Rogue waves are commonly defined as waves with an individual height $H$ from crest to trough of (Haver and Andersen, 2000)

$$H \geq 2.0\ H_s \tag{4}$$

and/or waves with a crest height $C$ above still water level of (Haver and Andersen, 2000)

$$C \geq 1.25\ H_s. \tag{5}$$

In a previous study based on measurement data from the southern North Sea (Teutsch et al., 2020), we found that the rogue wave frequency significantly deviated from the Forristall distribution for wave heights larger than $2.3\ H_s$. Therefore, in the present study we further define "extreme rogue waves" by a more strict height criterion of

$$H \geq 2.3\ H_s. \tag{6}$$

For the definition of a wave, the zero-upcrossing method was used.
The measured time series were subdivided into five categories:

**"normal samples"**- measurement samples that did not include any rogue wave.

**"height rogue samples"**- measurement samples that include a rogue wave only according to the height criterion defined in Eq. (4), while excluding the extreme rogue waves according to Eq. (6) and excluding the double rogue samples (see below).

**"crest rogue samples"**- measurement samples that included a rogue wave only according to the crest criterion defined in Eq. (5), while excluding the double rogue samples.

**"double rogue samples"**- measurement samples that included a rogue wave according to both the criteria defined in Eq. (4) and Eq. (5), while excluding the extreme rogue waves according to Eq. (6).

https://doi.org/10.5194/nhess-2022-28
Preprint. Discussion started: 4 March 2022



**"extreme rogue samples"**- measurement samples that included a rogue wave according to the height criterion defined in Eq. (6), while excluding the double rogue samples.

Examples of each time series category are shown in Fig. 4. Table 1 shows the number of samples and its percentage in each category.

https://doi.org/10.5194/nhess-2022-28
Preprint. Discussion started: 4 March 2022




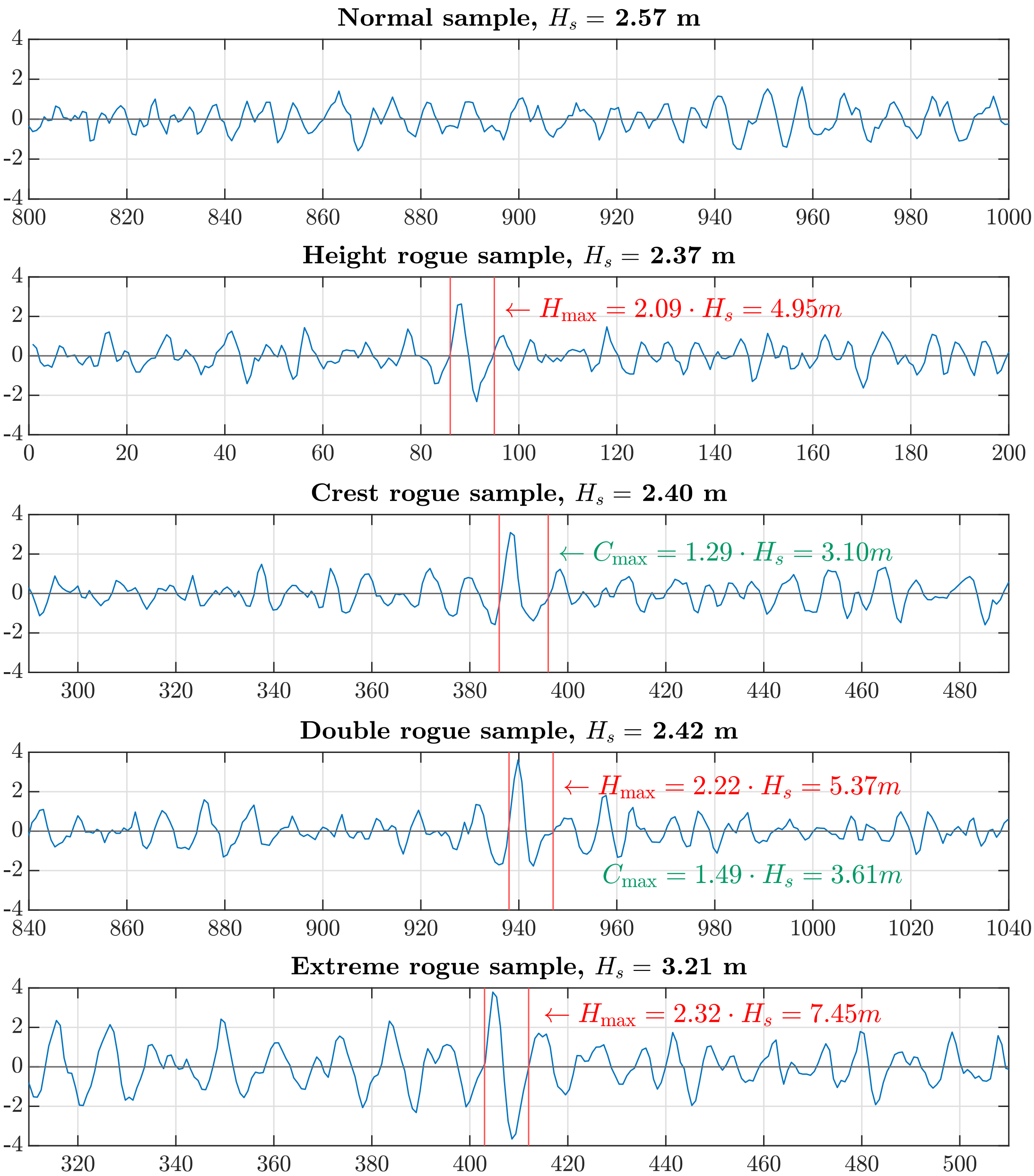


**Figure 4.** 200 s sections taken from example time series illustrating rogue waves for each of the four rogue wave categories, and a normal sample with a similar value of $H_s$ for comparison. Vertical red lines mark the two zero-crossings of the rogue wave. Rogue wave/crest heights are indicated in red/green.

https://doi.org/10.5194/nhess-2022-28
Preprint. Discussion started: 4 March 2022




**Table 1.** Positions and water depths of the measurement sites.

| Sample category | Normal | Height rogue | Crest rogue | Double rogue | Extreme rogue | Total |
|---|---|---|---|---|---|---|
| No. of samples | 13.984 | 833 | 95 | 151 | 93 | 15.156 |
| Percentage | 92.3 % | 5.5 % | 0.6 % | 1.0 % | 0.6 % | 100 % |

### 2.2 Application of the Korteweg–de Vries equation with vanishing boundary conditions to the measurement data

A vKdV-NLFT was applied to the data, to obtain the discrete soliton spectrum of each time series. The KdV equation was introduced by Korteweg and de Vries (1895). It describes the evolution of weakly nonlinear and dispersive progressive unidirectional free-surface waves in shallow water ($h\,L^{-1} < 0.22$) with constant depth. For the analysis of space series (fixed at one point in time), the space-like KdV equation (sKdV) is given e.g. in Osborne (2010), with reference to Korteweg and de Vries (1895) as

$$u_t + c\,u_x + \alpha\,u\,u_x + \beta\,u_{xxx} = 0, \tag{7}$$

in which $u = u(x,t)$ is a free-surface space series, developing in space $x$ and time $t$. The subscripts $x$ and $t$ denote partial derivatives, $c$ is the phase speed in shallow water, $\alpha = (3c)(2h)^{-1}$ and $\beta = (ch^2)/6$ are constants, depending on the phase speed $c$ and the water depth $h$. Equation (7) can be adapted to the analysis of time series (fixed at one point in space, like e.g. buoy measurements. For the case of a free-surface elevation time series $u(x_0,t)$ (see f.ex. Fig. 5) at base point $x_0$, it is then described by the time-like KdV equation (tKdV) (Osborne, 1993)

$$u_x + c' \cdot u_t + \alpha' + u \cdot u_t + \beta' \cdot u_{ttt} = 0, \tag{8}$$

in which $c' = c^{-1} = (\sqrt{gh})^{-1}$, $\alpha' = -\alpha\ (c^2)^{-1}$ and $\beta' = -\beta\ (c^4)^{-1}$. For our application of the KdV-NLFT, we assumed initial conditions with vanishing boundaries

$$\lim_{t\to\pm\infty} u(x_0,t) = 0 \tag{9}$$

sufficiently fast. Since we were mainly interested in the soliton part of the nonlinear spectrum and solitons are not periodic, we preferred vanishing (vKdV-NLFT) to periodic (pKdV-NLFT) boundary conditions. In the KdV-NLFT, solitons are easily identified as the discrete part of the nonlinear spectrum. We applied the vKdV-NLFT by using the MATLAB (2019) interface to the software library FNFT (Wahls et al., 2018), development version (commit 681191c). Its solution consists of a discrete soliton spectrum and a continuous spectrum representing oscillatory waves. Figure 5 shows an example of a measurement time series and its corresponding soliton spectrum. To distinguish them from oscillatory waves, solitons are displayed on a negative frequency axis. Technically, the frequency axis has no physical meaning, because a soliton, for which the surface elevation does not cross the still water level, has no frequency (Brühl and Oumeraci, 2016). However, from the soliton solution of the tKdV, an angular frequency is obtained as

$$\Omega = 2\pi \cdot F = \sqrt{\frac{3Ag}{4h^2}}. \tag{10}$$

https://doi.org/10.5194/nhess-2022-28
Preprint. Discussion started: 4 March 2022

Natural Hazards and Earth System Sciences
Discussions

Since this equation relates the frequency $F$ to the amplitude $A$ of the soliton, the frequency sorts the solitons in the spectrum by their amplitude. The vKdV-NLFT was applied to all 15.156 samples listed in Table 1.

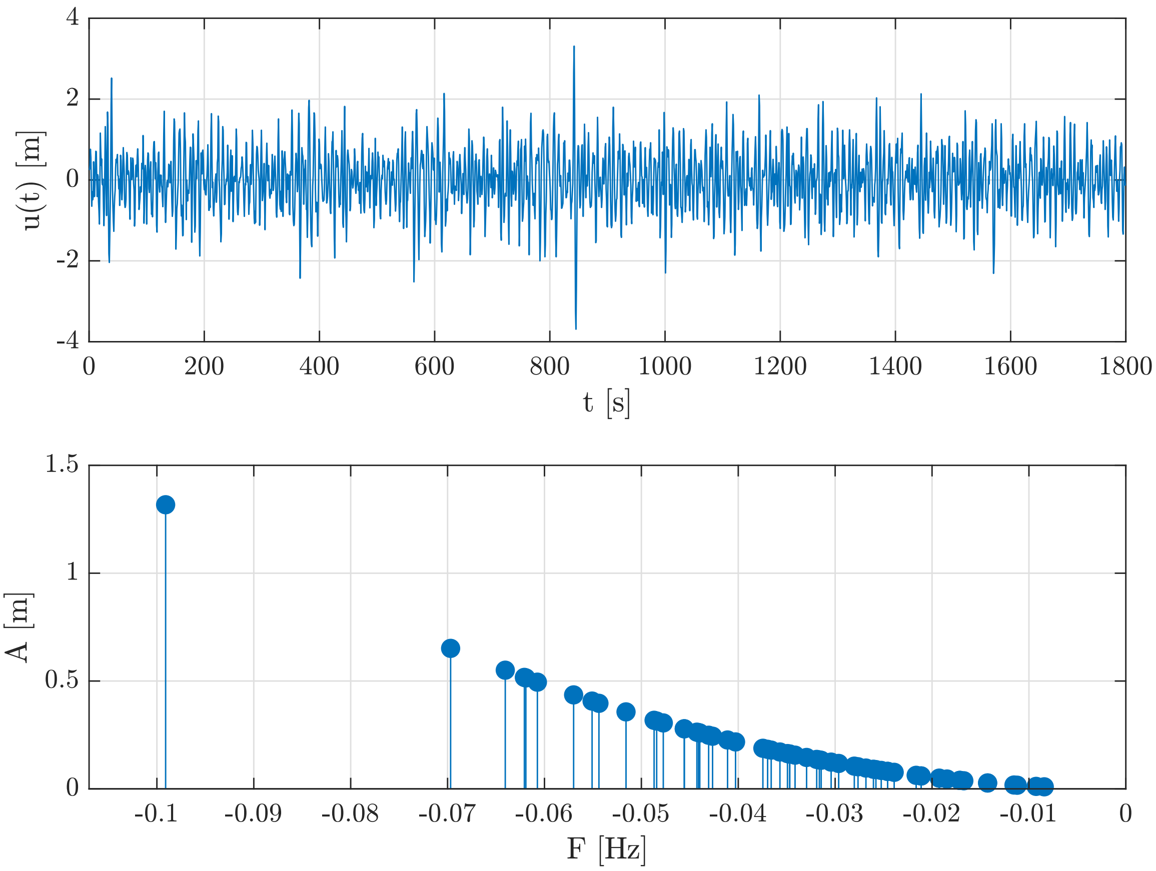


**Figure 5.** Example of a time series including a rogue wave at approx. 820 s, and its corresponding soliton spectrum, calculated from vKdV-NLFT. The time series with $H_{\max}\, H_s^{-1} = 2.58$, $H_{\max} = 7.00$ m and $H_s = 2.71$ m, was measured on 17 October 2013, starting at 11:30.

Solitons were found in all samples, with and without rogue waves. The aim of the study was to explore the role of the determined solitons for the generation of rogue waves. In the first part of the study, it was investigated whether specific solitons in the NLFT spectrum could be associated with the recorded rogue waves. For this purpose, all free-surface elevations between the two zero-crossings of a rogue wave (or largest wave, for normal samples) were scaled down to 80 $\%$ (Fig. 6). The KdV-NLFT was then repeated for the modified time series, which resulted in a new soliton spectrum. It was monitored which of the solitons had changed in amplitude A (and, therefore, in frequency F), due to the change in wave height. These solitons were assumed to have the same position as the rogue/ maximum wave. In the second part of the study, we explored whether

https://doi.org/10.5194/nhess-2022-28
Preprint. Discussion started: 4 March 2022

Natural Hazards and Earth System Sciences
Open Access
EGU
Discussions

the spectra calculated from rogue wave time series showed differences when compared to those calculated from normal time series.

## 3 Results

### 3.1 Attribution of solitons to rogue waves

Solitons were attributed to specific rogue waves, following the procedure described in Sect. 2.2. We found in each case that the amplitude of one large soliton significantly decreased for a reduced rogue wave (or maximum wave) height. Also in the group of smaller solitons, slight changes in amplitudes were observed. Since for solitons, amplitude A and frequency F are related according to Eq. (10), the reduction in amplitude corresponded to a simultaneous shift in frequency, which can be seen in the soliton spectrum (Fig. 6). The reduced solitons can be regarded to be associated with the rogue wave in the time series, while the other solitons in the spectrum maintained their amplitudes. The solitons with constant amplitudes can be regarded not to be associated with the rogue wave. We refer to the amplitudes of the $n = 1 \ldots i$ solitons associated with the rogue wave as $A_S^i$, with $A_S^1$ denoting the largest attributed soliton. Although often the case, the largest soliton attributed to the rogue wave was not necessarily the largest soliton in the spectrum (Fig. 7).

https://doi.org/10.5194/nhess-2022-28
Preprint. Discussion started: 4 March 2022

Natural Hazards and Earth System Sciences
Open Access
Discussions

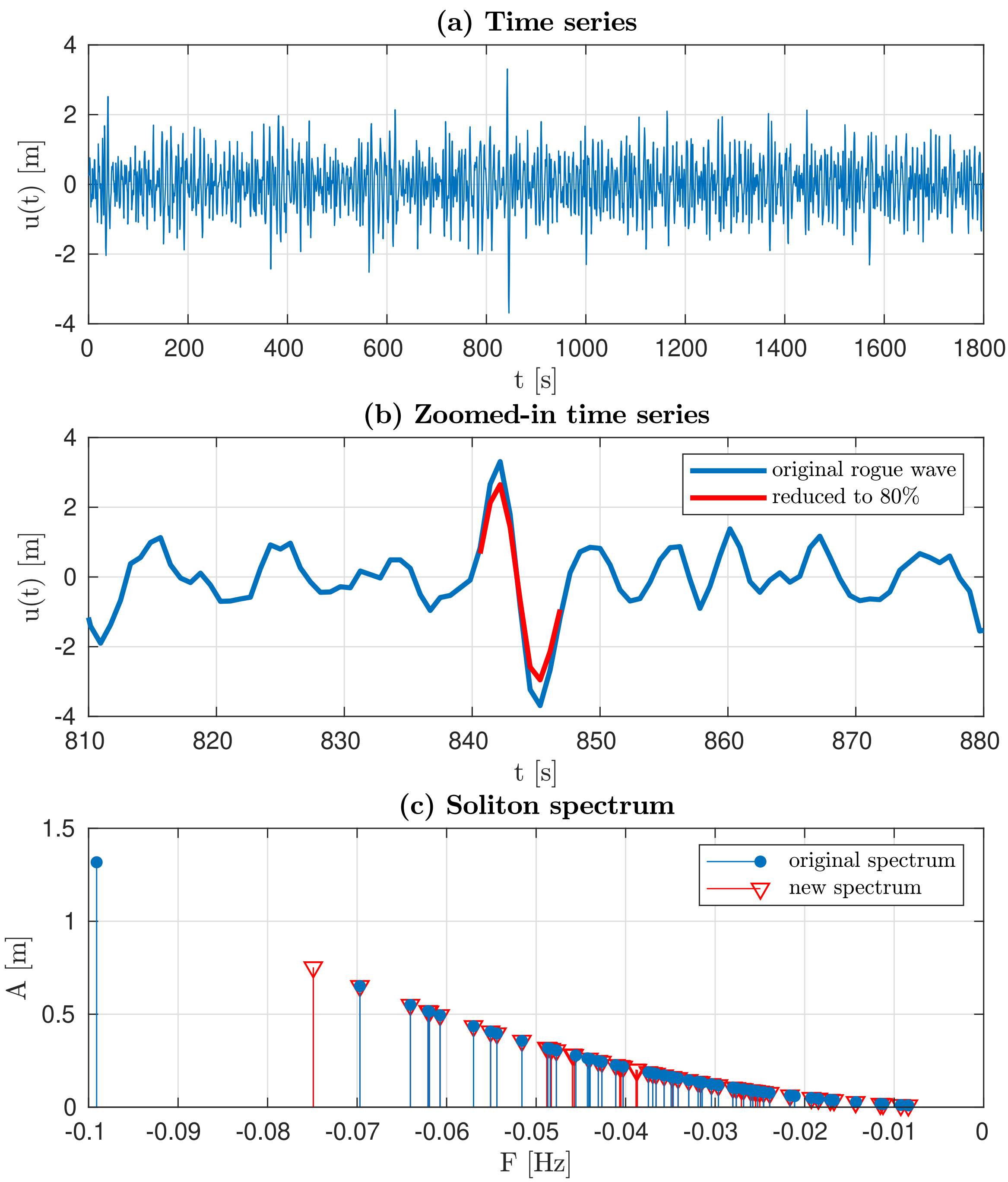


**Figure 6.** From top to bottom: (a) extreme rogue wave time series from 17 October 2013, starting at 11:30; (b) magnified view of the rogue wave (blue curve) and reduction of its elevation to 80 % (red curve); (c) soliton spectra of the original (blue circles) and the modified time series (red triangles), resulting from vKdV-NLFT.

https://doi.org/10.5194/nhess-2022-28
Preprint. Discussion started: 4 March 2022




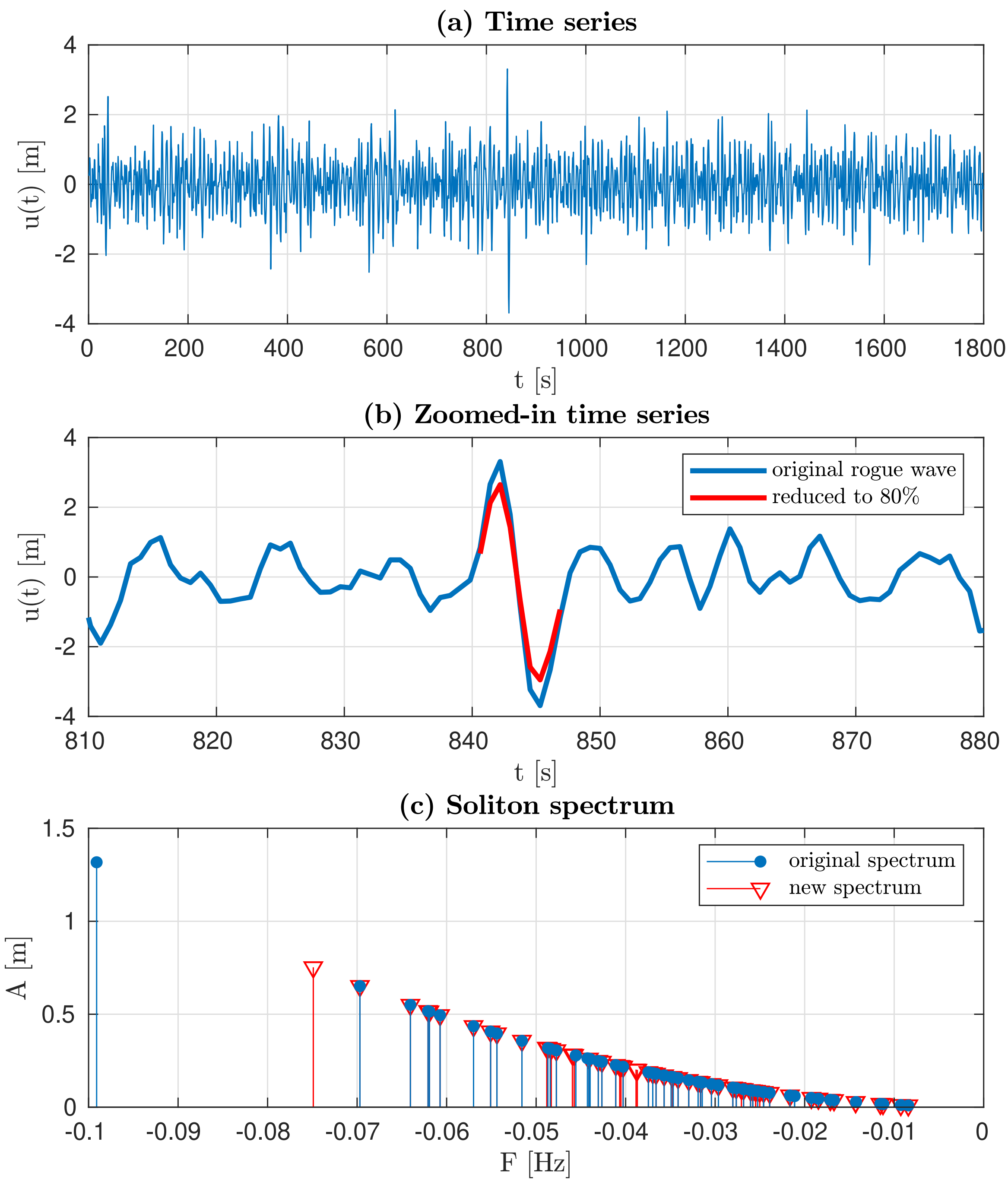


**Figure 7.** From top to bottom: (a) double rogue wave time series from 27 April 2016, starting at 20:30; (b) magnified view of the rogue wave (blue curve) and reduction of its elevation to 80 % (red curve); (c) soliton spectra of the original (blue circles) and the modified time series (red triangles), resulting from vKdV-NLFT.

https://doi.org/10.5194/nhess-2022-28
Preprint. Discussion started: 4 March 2022




We extracted the amplitude of the largest attributed soliton $A_S^1$ for each time series and compared it to the rogue wave height $H$ (for rogue waves according to any of the two height criteria, including double rogue waves, Fig. 8(a)) or the crest height $C$ of the rogue wave (for rogue waves according to the crest criterion, including double rogue waves, Fig. 8(b)). A comparison of the soliton amplitude $A_S^1$ to the largest wave height $H_{\max}$ and the largest crest height $C_{\max}$ in normal samples has been added for reference (Fig. 8(c) and (d)). The gradients of the linear regression curves express increasing $A_S^1$ with increasing $H\ H_{\max}^{-1}$ and $C\ H_{\max}^{-1}$. The scatter of the data suggests an upper limit of $A_S^1$ between 2 m and 3 m. The goodness of fit of each curve to the data is given in terms of the coefficient of determination

$$R^2 = \frac{SS_{\mathrm{res}}}{SS_{\mathrm{total}}}, \tag{11}$$

in which $SS_{\mathrm{res}}$ is the sum of squares of residuals with respect to the regression curve, and $SS_{\mathrm{total}}$ is the sum of squared residuals with respect to the average value of the data and thus a measure of the variance. $R^2$ indicates that the linear curves fit the results from height and extreme rogue wave samples better than the results from normal, double and crest rogue samples. $R^2$ is higher in Fig. 8(a) than in Fig. 8(b)-(d).

Moreover, it is seen that the amplitude of the largest soliton is always smaller than the rogue wave crest/ height itself. This is in agreement with results by Osborne et al. (1991), who identified solitons in measurement data from the Adriatic sea by applying the NLFT with quasi-periodic boundary conditions to the KdV equation. Thus, the mere existence of a soliton is not sufficient to explain the presence of a rogue wave in our data. Our investigation revealed that in all cases some smaller solitons were additionally associated with a rogue wave. Typical values of the amplitude of the second-largest soliton $A_S^2$ are 20-30 $\%$ of $A_S^1$. The amplitude of the third-largest attributed soliton $A_S^3$ is typically 10-20 $\%$ of $A_S^1$. The interaction of unidirectional solitons, however, as described by KdV, is known not to result in exceptional increases in wave elevation(Kharif and Pelinovsky, 2003). Hence, the soliton spectrum alone does not yield a satisfactory explanation of the generation mechanism of extreme waves/ crests. One may speculate that the formation of the rogue wave in these cases is a result of the interaction of one or several solitons with the underlying oscillating wave field, a hypothesis which will need further analyses to be validated.

https://doi.org/10.5194/nhess-2022-28
Preprint. Discussion started: 4 March 2022




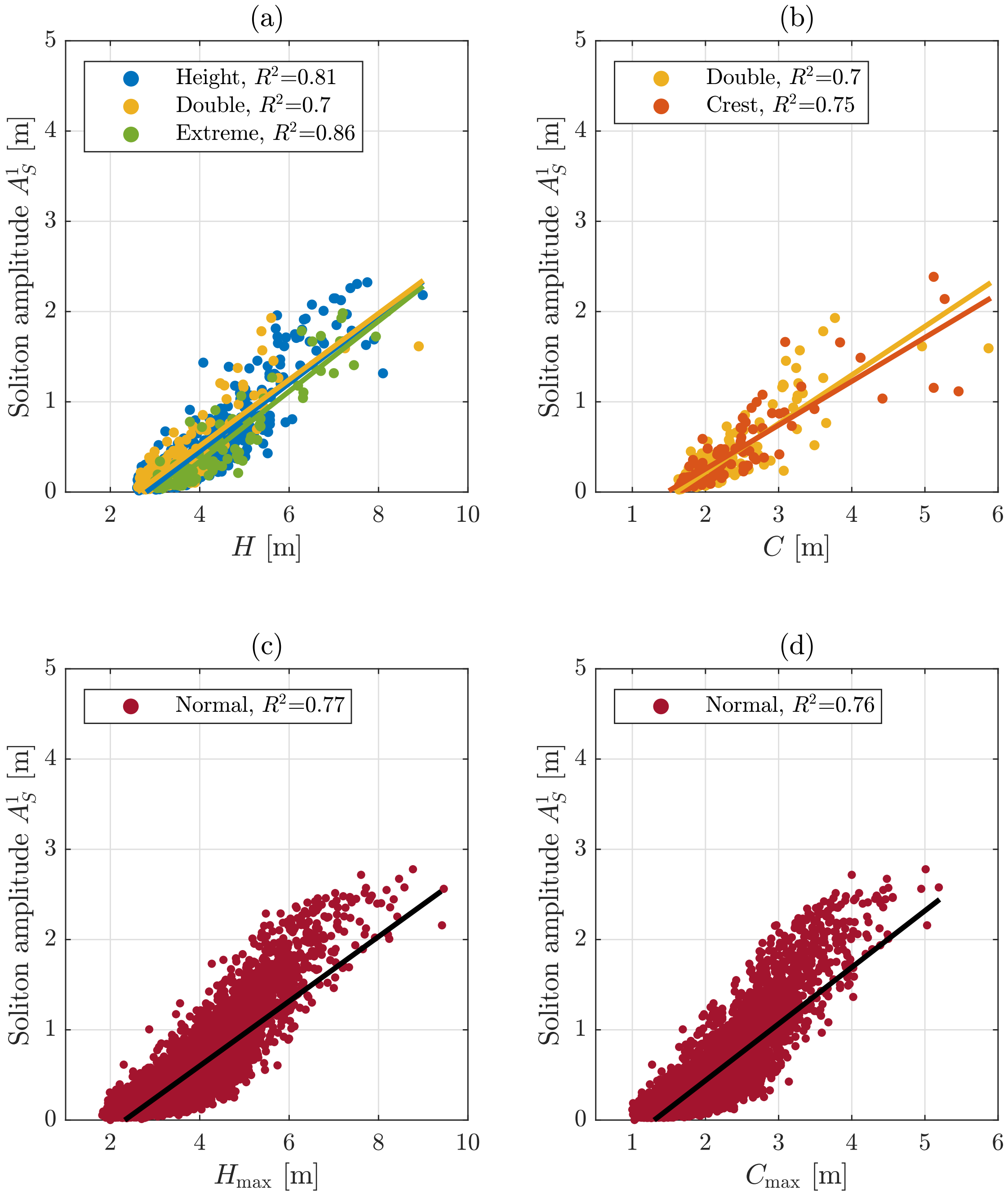


**Figure 8.** Amplitude of the largest soliton attributed to the highest wave, $A_S^1$, in the time series for normal samples (upper row) or the rogue wave (lower row) as a function of maximum wave height (left column) or maximum crest height (right column). The goodness of fit of the linear regression curves is given in terms of $R^2$.

https://doi.org/10.5194/nhess-2022-28
Preprint. Discussion started: 4 March 2022


So far, the results show that high soliton amplitudes in the spectrum are associated with high absolute values of wave heights or crests. However, this does not necessarily imply that high solitons play a role in forming individual waves that are exceptional with respect to the surrounding wave field. To remove the influence of the underlying sea state, the soliton amplitudes $A_S^1$ were normalised by the significant wave height $H_s$ of the corresponding sample. By relating the normalised soliton amplitudes to the different time series categories, the importance of solitons for the relative height of rogue or maximum waves was investigated (Fig. 9). If solitons are to play a major role for the presence of rogue waves, their normalised amplitudes are expected to increase from normal samples with $H\ (H_s)^{-1} < 2.0$ through height and double rogue waves ($2.0 \leq H\ (H_s)^{-1} < 2.3$) to extreme rogue waves ($H\ (H_s)^{-1} \geq 2.3$). In fact, the median values of $A_S^1\ (H_s)^{-1}$ are higher for rogue wave samples than for normal samples, meaning the distributions calculated from the rogue wave samples are shifted to the right with respect to the distribution calculated from normal samples (Fig. 9). Additionally, the rogue wave sample distributions, and especially those calculated from crest and extreme rogue samples, show heavier right tails. The differences in the distributions suggest that solitons play a role in rogue wave generation. It is striking that not only extreme rogue waves, but also crest rogue waves had a tendency to be associated with higher solitons. This makes sense when recalling that a soliton is not an oscillating wave and because of its shape contributes more to wave crests than to wave heights. However, although differences in normalised soliton amplitudes $A_S^1\ (H_s)^{-1}$ are present for the different categories, the distributions overlap and the positive trend with increasing relative wave height is not as pronounced as the positive trend of $A_S^1$ with increasing maximum wave height, as presented in Fig. 8. This emphasises the relevance of the considered sea state for the soliton amplitude, in that large solitons are only found in high sea states. Large solitons correspond to high wave heights $H$ and high crest heights $C$, but not necessarily to high relative wave heights $H\ (H_s)^{-1}$ or high relative crest heights $C\ (H_s)^{-1}$. Consequently, the presence of a large soliton is not sufficient to explain the presence of a rogue wave. Again, it is presumed that oscillatory wave components and/ or nonlinear interactions must contribute to the formation of rogue waves.

Natural Hazards and Earth System Sciences
Open Access
Discussions

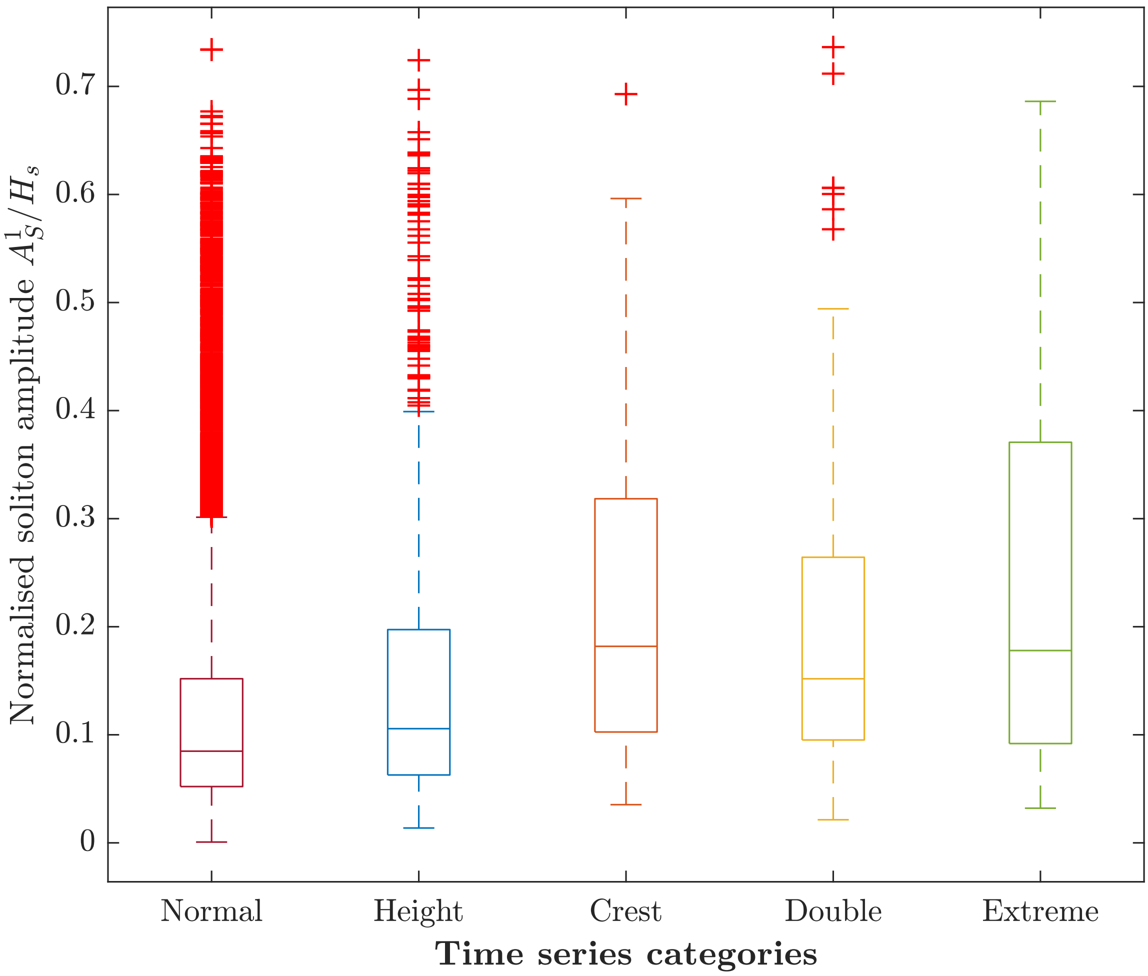


**Figure 9.** Amplitude of the highest soliton attributed to the rogue wave or maximum wave in the time series, normalised by the significant wave height, for the different categories of time series. Distributions are shown as box-and-whisker plots (box: interquartile range; whiskers: 1.5 times the interquartile range; horizontal line inside the box: median; red crosses: data outside the whiskers).

Since we were interested in the importance of nonlinearity in the rogue wave generation at the buoy location, we intended to quantify the nonlinearity of the rogue waves. In shallow water, the nonlinearity of waves can be described by the Ursell number (Ursell, 1953). The Ursell number in its time-like form is given, according to Osborne (2010), by

$$U = \frac{3ac^2T^2}{16\pi^2h^3} = \frac{3}{16\pi^2}(\frac{a}{h})(\frac{cT}{h})^2, \tag{12}$$

in which we interpreted $a = C$ as the maximum elevation of the rogue wave above the still water level, following LeMéhauté (1976). The Ursell number $U$ is known to be an equivalent to the BFI for deep water waves (Slunyaev et al., 2011; Onorato

https://doi.org/10.5194/nhess-2022-28
Preprint. Discussion started: 4 March 2022



et al., 2001) and has been used to classify wave types. It has been stated that an Ursell number of $U = 0$ corresponds to linear waves, while $U = 1$ points to solitary waves (Miles, 1980). In our case, the amplitudes of the largest attributed solitons show an almost linear positive trend with increasing Ursell number up until approximately $U = 0.5$ (Fig. 10). Brühl (2022) classifies waves with $0.559 \leq U$ as solitary-like wave types and waves with $U < 0.559$ as Airy-like, Stokes-like or cnoidal-like. For our data, in which the bulk of waves are located below $U = 0.559$, this means that most rogue wave crests are not soliton-like. This is in agreement with several previous studies, which have shown that rogue waves in shallow water, despite their large amplitudes, have very small ratios of nonlinearity to dispersion (Ursell numbers), thus are almost linear (Pelinovsky et al., 2000; Kharif and Pelinovsky, 2003; Pelinovsky and Sergeeva, 2006). This again reinforces a point made earlier, that the rogue waves in our case cannot be explained by solitons alone. This may lead to the conclusion that solitons need to interact with other wave components for the formation of these rogue waves, which we have not verified. Another observation made from Fig. 10 is a threshold in soliton amplitude between $A_S^1 = 2.0$ m and $A_S^1 = 2.8$ m, depending on the time series category, for Ursell numbers larger than approximately $U = 0.5$. Referring to the classification by Brühl (2022), this implies that for the most nonlinear waves, which are those satisfying solitary wave theory, soliton amplitudes are limited. A limit in soliton height as a result of breaking is expected at amplitudes of approximately $A = 8$ m for a water depth of $h = 10$ m, as the breaking criterion for solitary waves is $A\,h^{-1} = 0.78$ (McCowan, 1891) or $A\,h^{-1} = 0.83$ (Lenau, 1966). Therefore, shallow-water wave breaking at the location of the buoy can be excluded. The reason for the limit in soliton amplitude already at $A_S^1 = 2.5$ m to $A_S^1 = 3$ m could be limited energy input by wind (see Middleton and Mellen (1985) for soliton generation by wind), or a shoal in front of the measurement buoy causing the larger waves to break before they reach the buoy.

Natural Hazards and Earth System Sciences
Discussions

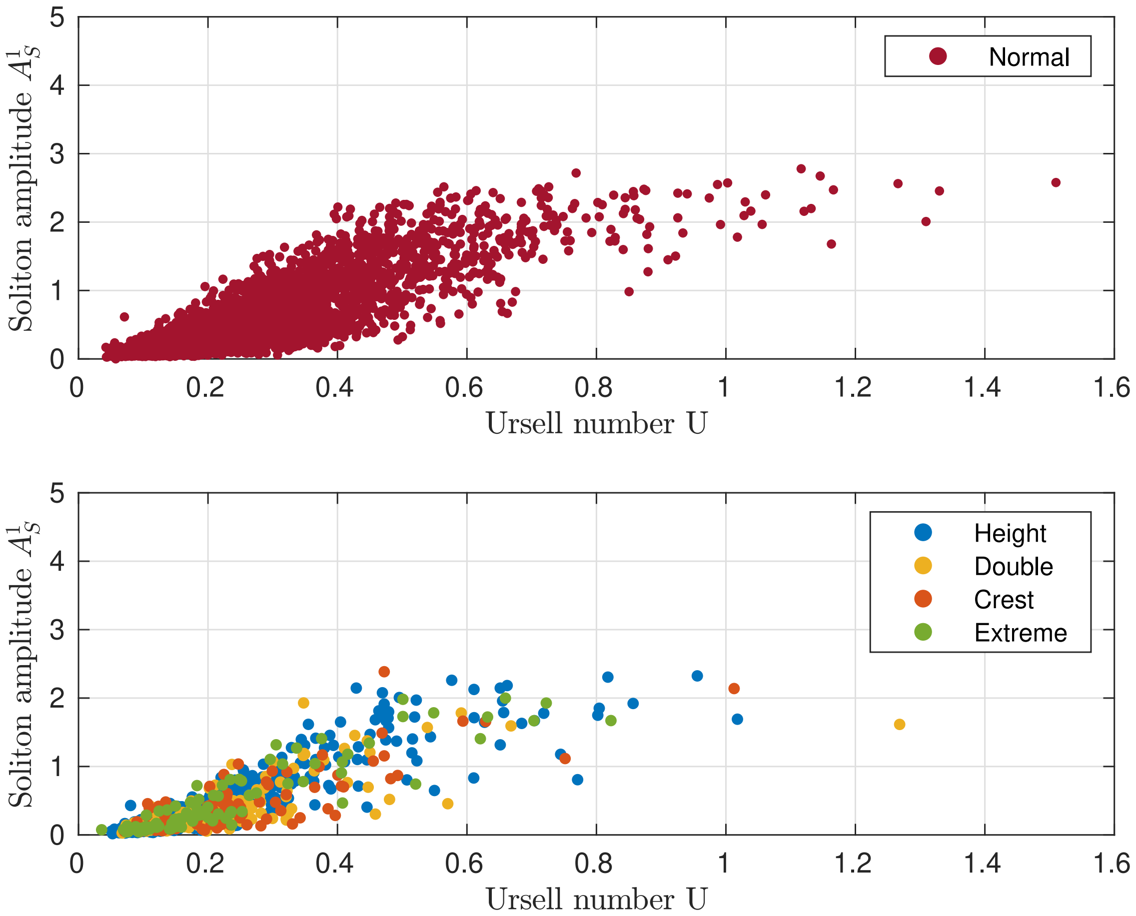


**Figure 10.** Upper panel: amplitude of the highest soliton attributed to the maximum wave in the time series as a function of the Ursell number of the maximum wave in the time series. Lower panel: amplitude of the highest soliton attributed to the rogue wave as a function of the Ursell number of this rogue wave.

### 3.2 Soliton spectra for time series with and without rogue waves

When investigating the attribution of solitons to rogue waves in Sect. 3.1, we found in the majority of cases that the largest soliton in the nonlinear spectrum could be attributed to the rogue wave. In addition, this soliton was often outstanding from the other solitons in the spectrum, with a much larger amplitude than the remaining solitons in the spectrum (see the example in Fig. 6). We were therefore interested in whether the existence of an outstanding soliton in the nonlinear spectrum was typical for rogue wave samples off Norderney. We investigated this question statistically by comparing soliton spectra, calculated from vKdV-NLFT, for normal samples and the four different categories of rogue wave samples. In fact, while all 15.156 considered time series yielded discrete spectra with a large number of solitons, we identified two characteristic classes of soliton spectra.

https://doi.org/10.5194/nhess-2022-28
Preprint. Discussion started: 4 March 2022



The typical appearance of a soliton spectrum calculated from a time series without rogue waves, was a cluster of solitons (Fig. 11). On the contrary, soliton spectra calculated from time series including a rogue wave in the majority of cases showed one outstanding soliton with an amplitude much larger than that of the remaining cluster of solitons in the spectrum (Fig. 5).

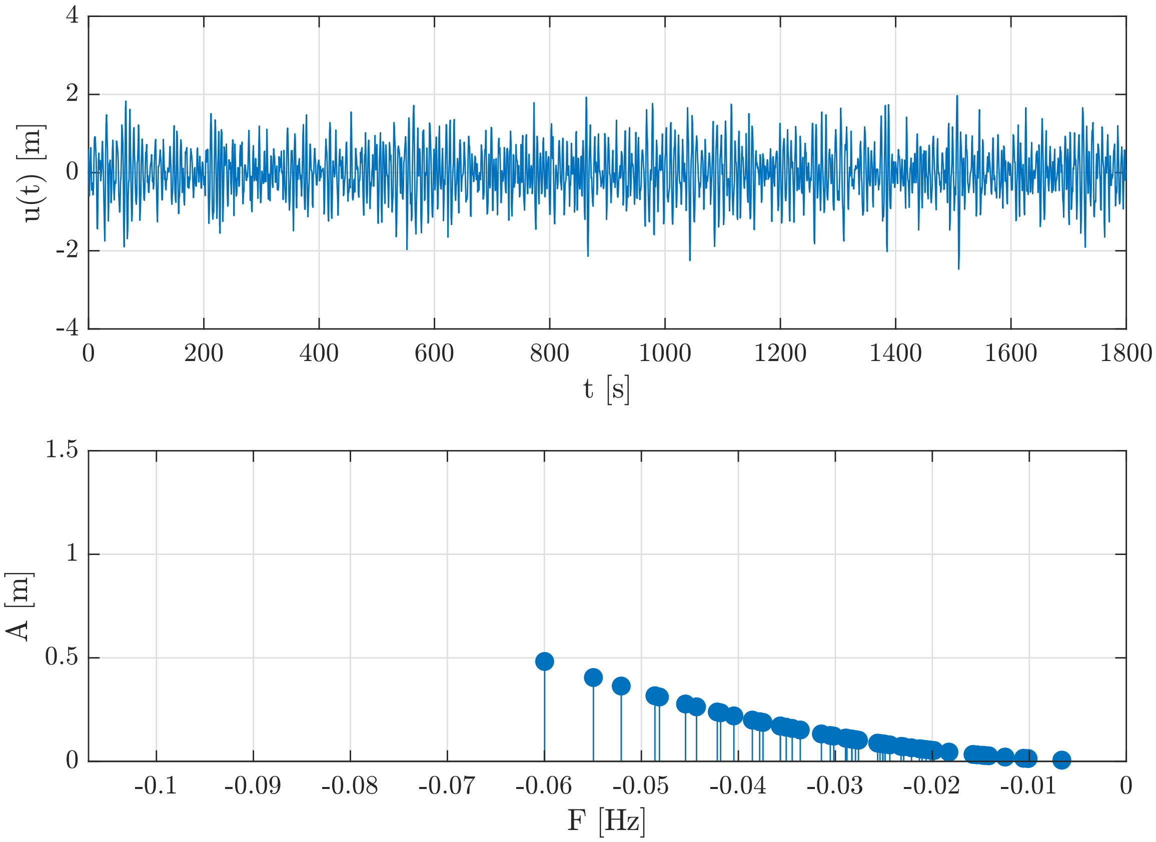


**Figure 11.** Example of a normal time series without rogue waves, and its corresponding soliton spectrum, calculated from vKdV-NLFT. The soliton spectrum displays a cluster of solitons, found to be typical for the majority of spectra calculated from normal time series. The time series was measured on 26 December 2016, starting at 11:30, with the parameters $H_{\max} = 4.44$ m, $H_s = 2.46$ m and $H_{\max}\,(H_s)^{-1} = 1.80$.

To distinguish between clustered soliton spectra and those featuring an outstanding soliton, we compared the amplitudes of the largest soliton, $A_1$, and the second-largest soliton, $A_2$, in the discrete spectrum. From the visual inspection of the spectra, we identified a threshold of the ratio $A_2\,(A_1)^{-1}$, below which the largest soliton could be called outstanding:

$$\frac{A_2}{A_1} \leq 0.8. \tag{13}$$

Thus, a soliton spectrum had an outstanding soliton if the second-largest soliton was at least 20 % smaller than the largest soliton in the spectrum. The choice of this threshold was further supported by the fact that the threshold $A2\,(A1)^{-1} = 0.8$

https://doi.org/10.5194/nhess-2022-28
Preprint. Discussion started: 4 March 2022




coincides with the median value of $A2\,(A1)^{-1}$ for maximum wave heights just below the rogue wave criterion $H\,(H_s)^{-1} \geq 2.0$ (Fig. 12). This reveals that our threshold chosen for the distinction between clustered spectra and those featuring an outstanding soliton, at the same time indicates a difference between the spectra calculated from normal and those calculated from rogue wave time series.

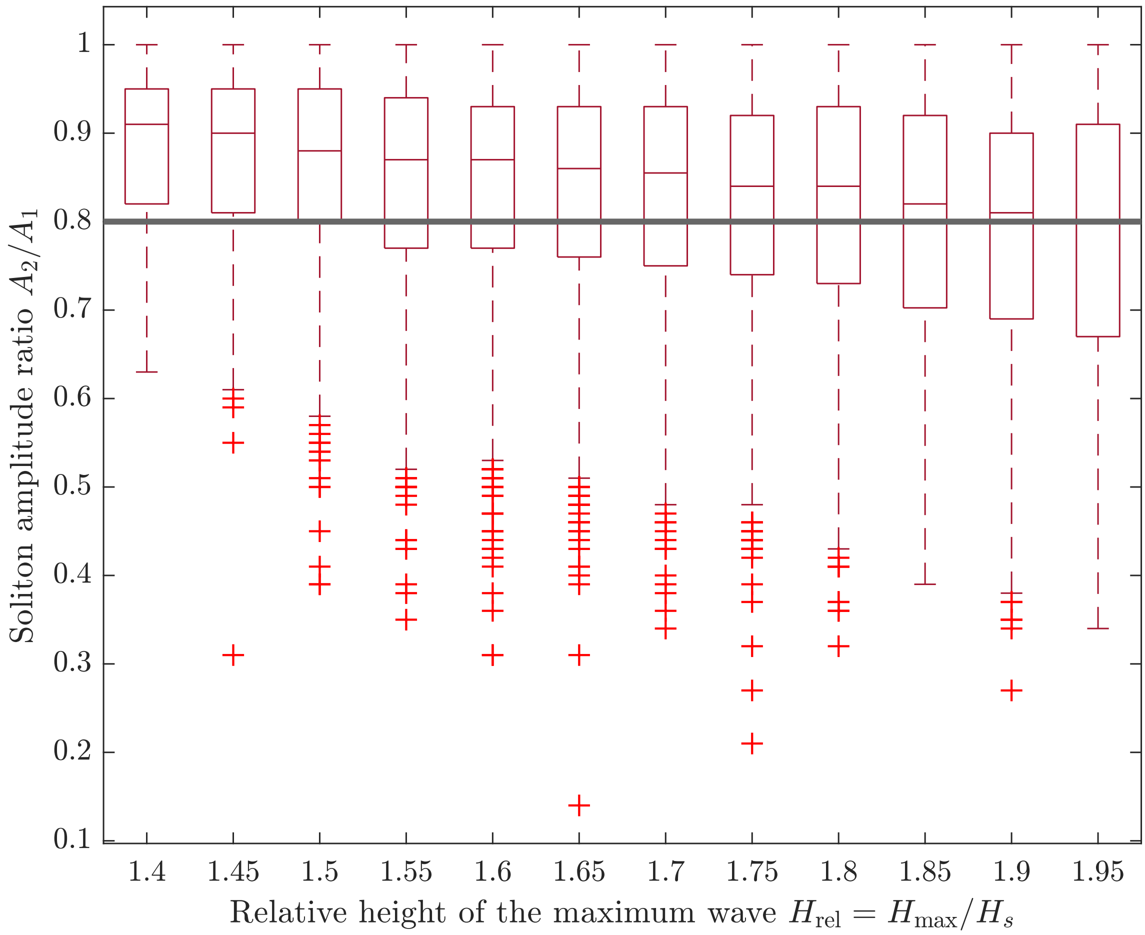


**Figure 12.** Distribution of the ratio between the second-largest and the largest soliton in the discrete spectrum calculated from normal time series. $H\,(H_s)^{-1}$ bins of width 0.05 are shown up until $H\,(H_s)^{-1} < 2.0$, which corresponds to the definition of height rogue waves (Eq. (4)). Distributions are shown as box-and-whisker plots (box: interquartile range; whiskers: 1.5 times the interquartile range; horizontal line inside the box: median; red crosses: data outside the whiskers).

325 Equation (13) is valid for 30 minute samples, which is the standard window size of measurement samples delivered by Datawell Waverider buoys. Since the ratio between soliton amplitudes might be dependent on the window size, it is not clear if

https://doi.org/10.5194/nhess-2022-28
Preprint. Discussion started: 4 March 2022



Eq. (13) would apply to other than 30 minute time windows. The effect of a larger time window size will be discussed in Sect. 4. Table 2 shows the share of outstanding solitons and clustered soliton spectra in each of the categories defined in Sect. 2.1. It is seen that the typical appearance of the soliton spectrum for 30 minute wave measurement samples off Norderney without rogue waves is a cluster of solitons (64 % of the samples), while at the same time it is not unlikely to obtain a soliton spectrum with one outstanding soliton from vKdV-NLFT (36 % of the samples). For 30 minute rogue wave samples in contrast, it is more likely to obtain a soliton spectrum with one outstanding soliton than a clustered soliton spectrum. This is true for height rogue samples (57 %), and even more pronounced for crest rogue samples (64 %), double rogue samples (72 %) and, finally, extreme rogue samples (87 %). The conclusion can be drawn that the absence of an outstanding soliton is a strong predictor for the absence of an extreme rogue wave. The differences between the four rogue wave categories, indicating that the presence of an outstanding soliton is not equally expressive for all types of rogue waves, may lead to the presumption that not all rogue waves found off Norderney can necessarily be explained by the same theory.

**Table 2.** Share of samples in each category showing an outstanding soliton or a clustered soliton spectrum, respectively.

| | Normal | Height rogue | Crest rogue | Double rogue | Extreme rogue |
|---|---|---|---|---|---|
| Outstanding soliton | 36 % | 57 % | 64 % | 72 % | 87 % |
| Clustered solitons | 64 % | 43 % | 36 % | 28 % | 13 % |

The question whether inferences can be made from the time to the spectral domain and vice versa, is answered by a contingency table (Fig. 13). Here, all previously defined rogue wave categories are combined into one joint group of rogue wave samples. Two statements can be made based on the table. On the one hand, the probability that an NLFT spectrum calculated from a normal sample shows an outstanding soliton, is 4986/13.984 = 36 %, while the probability that a spectrum calculated from a rogue wave sample shows an outstanding soliton, is 726/1172 = 62 %. This indicates that, although not all rogue waves can necessarily be explained by the same theory, outstanding solitons occurred in connection with the majority of observed rogue waves off Norderney. While in the combined group of rogue waves, outstanding solitons play a role in 62 % of the cases, the share differs between the rogue wave categories (Table 2). On the other hand, although rogue waves are more likely to be observed when an outstanding soliton is present in the NLFT spectrum, the presence of an outstanding soliton alone is not sufficient as an indicator for the detection of rogue waves. The main difficulty is the imbalance in sample size between normal samples and rogue wave samples.

https://doi.org/10.5194/nhess-2022-28
Preprint. Discussion started: 4 March 2022

Natural Hazards and Earth System Sciences
Open Access
Discussions

**Rogue wave sample (all categories combined)**

| **Outstanding soliton** | **yes** | **no** | **total** |
|---|---|---|---|
| **yes** | a= 726 | b= 4986 | a+b = 5712 |
| **no** | c= 446 | d= 8998 | c+d = 9444 |
| **total** | a+c = 1172 | b+d = 13.984 | n = a+b+c+d = 15.156 |

**Figure 13.** Contingency table of forecast/event pairs. a- hits. b- false alarms. c- misses. d- correct negatives.

In Fig. 14, the ratio between the amplitudes of the second-largest and the largest soliton in the nonlinear spectrum, $A_2\ (A_1)^{-1}$, is visualised in a boxplot for each of the time series categories. A ratio above $A_2\ (A_1)^{-1} = 80\ \%$, meaning that the second-largest soliton has a rather similar amplitude to the largest soliton, implies that the soliton spectrum is clustered (Eq. (13)). For normal samples, this is the case for the bulk of time series. The median of the ratio $A_2\ (A_1)^{-1}$ decreases from the most-left to the most-right category on the right axes in Fig. 14. For height rogue waves, the median of $A_2\ (A_1)^{-1}$ is below the 80 %-line, with the distribution extending above and below. For double and extreme rogue waves, the gap between the soliton amplitudes may become much larger than for height rogue waves. In some cases, the amplitude $A_2$ amounts to less than 30 % of the amplitude $A_1$. In all categories except extreme rogue samples, there are samples for which the first and second solitons are almost similar in amplitude ($A_2\ (A_1)^{-1} \approx 1$). On the contrary, for all extreme rogue wave samples, $A_2$ is below 93 % of $A_1$. The large part of soliton spectra from extreme rogue samples shows an outstanding soliton.

https://doi.org/10.5194/nhess-2022-28
Preprint. Discussion started: 4 March 2022


Natural Hazards and Earth System Sciences
Discussions

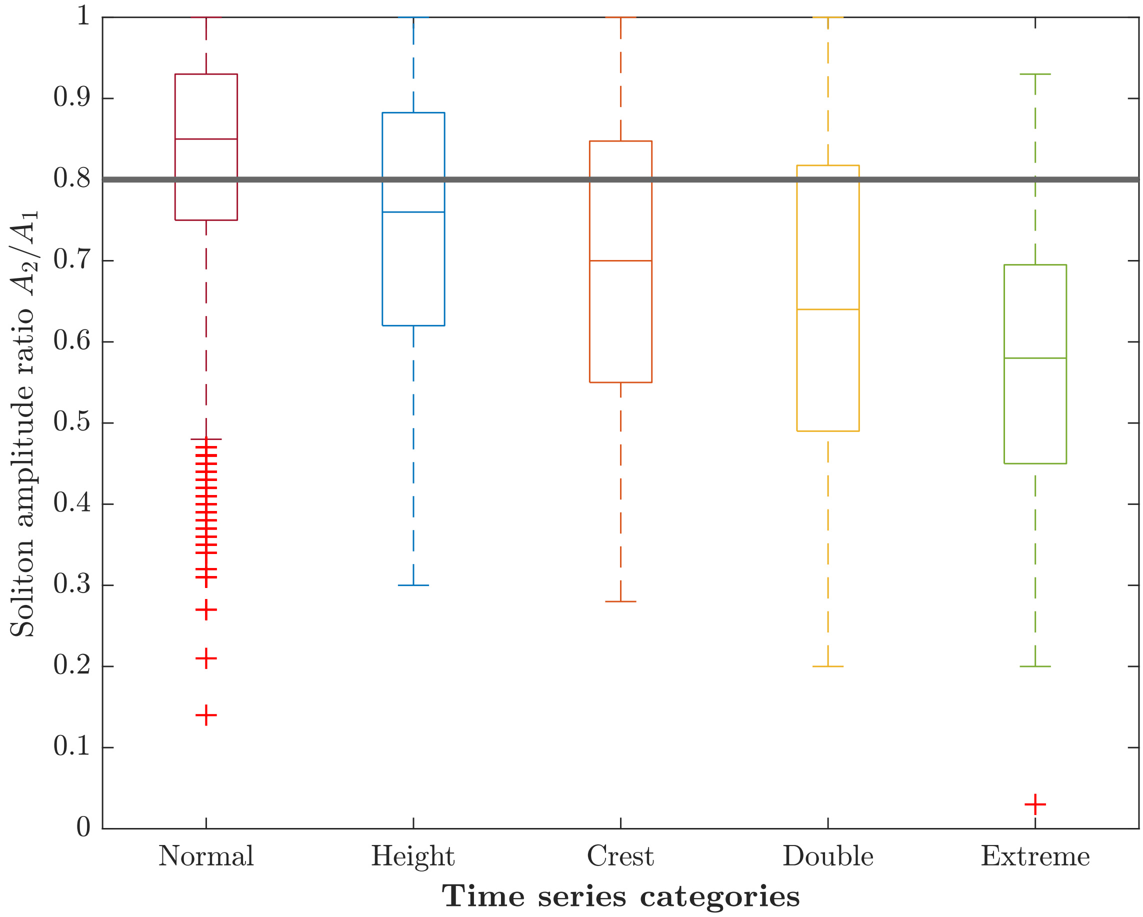


**Figure 14.** Boxplots of the ratio between the second-largest soliton ($A_2$) and the largest soliton ($A_1$) in the spectrum for the different categories of time series. Distributions are shown as box-and-whisker plots (box: interquartile range; whiskers: 1.5 times the interquartile range; horizontal line inside the box: median; red crosses: data outside the whiskers). Below the horizontal line of 80 %, the highest soliton in the spectrum is classified as outstanding.

Figure 15 presents the ratio $A_2\ (A_1)^{-1}$ in a scatter plot with one data point for each individual time series. According to this representation, although the presence of an outstanding soliton with $A_2\ (A_1)^{-1} \leq 0.8$ is not a useful indicator of whether a rogue wave is present in the time series or not, the presence of a rogue wave becomes much more likely when one soliton in the nonlinear spectrum is strongly outstanding with $A_2\ (A_1)^{-1} \leq 0.3$: of all 23 samples satisfying $A_2\ (A_1)^{-1} \leq 0.3$, only $4/23 = 17$ % are normal samples, while $19/23 = 83$ % of the samples are rogue wave samples (1 height, 1 crest, 8 double, 9 extreme rogue wave samples).

https://doi.org/10.5194/nhess-2022-28
Preprint. Discussion started: 4 March 2022



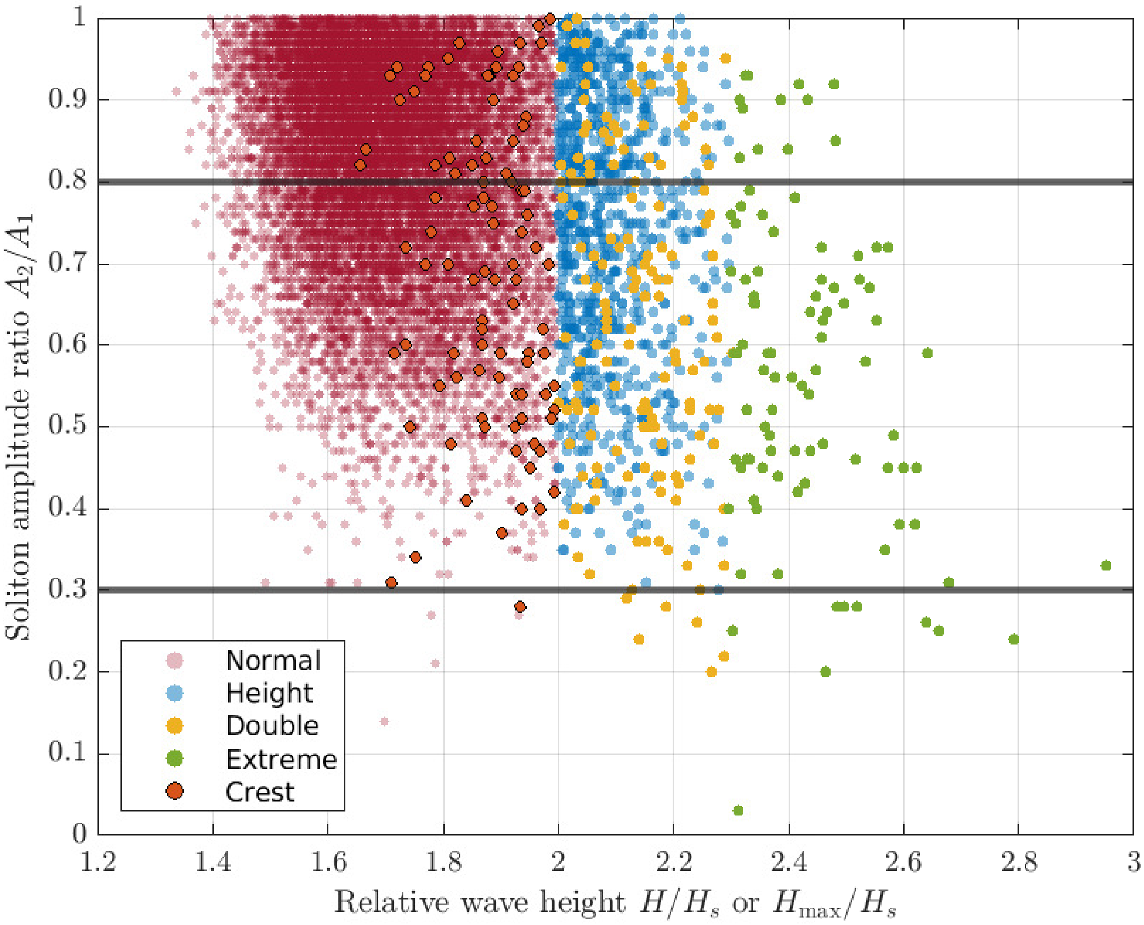


**Figure 15.** Ratio between the second-largest soliton ($A_2$) and the largest soliton ($A_1$) in the spectrum as a function of relative wave height $H\ (H_s)^{-1}$ or $H_{\max}\ (H_s)^{-1}$ for the different categories of time series. Below the horizontal line of 80 %, the highest soliton in the spectrum is classified as outstanding. Below the horizontal line of 30 %, the highest soliton in the spectrum is referred to as strongly outstanding.

## 4 Discussion

We investigated discrete nonlinear soliton spectra obtained by the application of the vKdV-NLFT to time series measured by a surface-following buoy off the coast of the island Norderney in the southern North Sea. The impulse for investigating the data at this specific site by using nonlinear methods was given by a previous study (Teutsch et al., 2020). There, it was found that while second-order distributions were sufficient to describe rogue wave occurrences at nearby stations in somewhat deeper water, the Norderney buoy recorded a larger number of rogue waves than expected according to second-order theory. The results described in this paper suggest that nonlinear processes may explain the enhanced rogue wave occurrence at this

https://doi.org/10.5194/nhess-2022-28
Preprint. Discussion started: 4 March 2022




specific site. The results were derived by the application of vKdV-NLFT and are therefore strictly valid for shallow-water conditions. In a future study, it may be interesting to extend the investigation to additional shallow-water sites.

The bathymetry below the measurement buoy at Norderney is characterized by a strong decrease in water depth. Non-Gaussian wave characteristics as a result of decreasing water depth have already been described e.g. by Huntley et al. (1977)] and gained increased attention in the context of rogue wave occurrence. Increased rogue wave frequencies behind slopes or steps were confirmed by numerous numerical (Sergeeva et al., 2011; Majda et al., 2019; Zhang and Benoit, 2021) and experimental studies (Trulsen et al., 2012; Zeng and Trulsen, 2012; Kashima et al., 2014; Ma et al., 2014; Zhang et al., 2019; Trulsen et al., 2020). Li et al. (2021) have explained the higher occurrence of rogue waves due to an abrupt depth transition from deeper to shallower water by additional second-order free waves generated at the transition. The main subject that the mentioned studies are concerned with, is that waves propagating over a slope, step or bar, are forced into new equilibrium conditions (Zeng and Trulsen, 2012). This mechanism is associated with strong non-Gaussian statistics and an increased rogue wave probability (Zhang and Benoit, 2021). Zeng and Trulsen (2012) anticipate that it may explain the spatially varying occurrence frequency of rogue waves on the continental shelf, where waves enter from the deep sea. Therefore, the described processes associated with a strong decrease in depth might be an explanation for the observed increased rogue wave occurrence off the coast of Norderney (Teutsch et al., 2020). A connection between rogue waves and solitons in this context was established by Sergeeva et al. (2011). The authors showed by applying a KdV equation, that the number of solitons increases in the shallow water behind a slope. They linked this increased soliton occurrence to an increased rogue wave probability. The solutions of the KdV equation for a given free-surface elevation time series strongly depend on the water depth (see Eq. (7)). While for our calculations, we assumed a constant water depth of $h = 10$ m, there are in fact major uncertainties regarding the water depth at the actual location of the buoy, due to tidal changes and bathymetry gradients, together with the movement of the buoy, as mentioned in Sect. 2.1 (Fig. 2). The mean tidal range at Norderney is approximately $\pm 1.25$ m, while due to an additional movement of the buoy of 2 m to each side of the slope a total deviation from the nominal water depth of $\pm 2$ m is reasonable. We performed a sensitivity analysis to test the robustness of the results with respect to these uncertainties. To do so, we repeated the computation of the soliton spectrum for water depths of $h = 8$ m and 12 m, respectively, while using the same free-surface data as in the previous analysis. A changed water depth leads to different shallow-water conditions (Eq. (3)). For the calculation with a depth of $h = 12$ m, we repeated the identification of the samples that fulfill shallow-water conditions, as samples and maximum waves due to the larger water depth now had to satisfy the condition $T_p$ or $T > 5$ s, in order to classify as shallow-water samples/ waves. Therefore, only 14.206 samples, that is, approximately 94 $\%$ of the original sample size, were available for the calculation at $h = 12$ m. For the calculation with a depth of $h = 8$ m, we used the same samples as for the calculation with $h = 10$ m, because these automatically fulfilled shallow-water conditions at $h = 8$ m. Irrespective of the water depth adopted in the calculation, the result remained that samples with rogue waves, and especially extreme rogue waves, were more likely to contain an outstanding soliton in the nonlinear spectrum than samples without rogue waves (Table 3). Thus, the results are robust with respect to potential uncertainties in water depth.

https://doi.org/10.5194/nhess-2022-28
Preprint. Discussion started: 4 March 2022




**Table 3.** Share of samples in each category showing an outstanding soliton in the soliton spectrum, for the respective water depth adopted in the NLFT calculation. Note that for a water depth of $h = 12$ m, the shallow-water criterion in Eq. (3) changes to $T_p > 5$ s, which left approximately 94 % of the samples for the calculation at a water depth of 12 m.

| Water depth | Normal | Height rogue | Crest rogue | Double rogue | Extreme rogue |
|---|---|---|---|---|---|
| 8 m | 32 % | 57 % | 61 % | 73 % | 75 % |
| 10 m | 36 % | 57 % | 64 % | 72 % | 87 % |
| 12 m | 36 % | 53 % | 62 % | 70 % | 76 % |

The KdV equation is only valid for unidirectional waves. Although Osborne (1993) recommends the application of the NLFT for KdV to measurement data only for samples in which the largest part of the energy is in the dominant propagation direction, we applied the KdV-NLFT outside the limits that are given in the literature. At our measurement site, the sea state was always multidirectional, with a directional spreading of the wave energy approximately between 28° and 55°, while in the dataset of Osborne (1993), only 5 % of the energy were perpendicular to the dominant direction of propagation. We repeated the first part of the analysis, for which the results are described in Sect. 3.1, for the approximately 10 % of samples in each category with the lowest directional spread. This corresponded to a threshold in directional spread of 35° for most categories, except crest rogue waves, which tended to occur in broader sea states (threshold at 36.5°) and extreme rogue waves, which statistically occur in more narrow sea states (Christou and Ewans, 2014) (threshold at 34°). We found our result- that an outstanding soliton is more typical for a rogue wave time series than for a normal time series- confirmed and partly emphasised (Table 4). Therefore, we rate vKdV-NLFT, although assuming unidirectionality in multidirectional measurement samples, an appropriate tool to evaluate the connection between solitons and rogue waves off Norderney.

**Table 4.** Share of samples in each category showing an outstanding soliton, for the approximately 10 % most narrow samples.

| | Normal | Height rogue | Crest rogue | Double rogue | Extreme rogue |
|---|---|---|---|---|---|
| No. of samples | 1614 | 91 | 12 | 17 | 10 |
| Outstanding soliton | 31 % | 57 % | 67 % | 88 % | 90 % |

We would like to put an emphasis on the limitation of our suggested definition of an outstanding soliton (Eq. (13)) to the size of the measurement window. Our criterion was chosen based on the inspection of soliton spectra from 30 minute time series. However, the gap size might change depending on the chosen window size. An increase in window size, meaning more waves in the time series, will introduce additional solitons to the spectrum. If these are larger than $A_1$ or emerge in between $A_1$ and $A_2$, the gap size between the two largest solitons will be influenced. If these are smaller than $A_2$, their emergence will not alter the gap between $A_1$ and $A_2$. Similarly, a reduction in window size would exclude waves in the time series and remove solitons corresponding to these waves. If this modification leads to the removal of the largest or second-largest soliton, the gap between the new $A_1$ and $A_2$ will become larger or smaller than for a 30 minute time window. If this modification only affects solitons smaller than $A_2$, the size of the gap between $A_1$ and $A_2$ will not be influenced. We applied the ratio between $A_2$ and $A_1$ merely

https://doi.org/10.5194/nhess-2022-28
Preprint. Discussion started: 4 March 2022


Natural Hazards and Earth System Sciences
Discussions

as a measure to statistically evaluate differences in the soliton spectra calculated from 30 minute normal and rogue wave time series. For different window sizes, it might be necessary to define new criteria.

Our result that rogue wave samples have a higher probability of showing an outstanding soliton in the nonlinear spectrum compared to normal samples becomes most obvious in the categories of double and extreme rogue samples. In these categories, differences from normal samples are visible not only in the percentage of outstanding solitons, but also in the magnitude of the amplitude gap between the first and second solitons in the spectrum. Height rogue waves, on the contrary, do not seem to differ very much from high waves in normal samples, both in terms of the gap between first and second soliton in the spectrum, and the height of the solitons associated with the maximum wave. The fact that differences between time series with and without rogue waves become apparent only in some of the chosen categories, raises the question whether the choice of rogue wave definitions has been reasonable for the considered location. The rogue wave definitions serving as a basis to this study have been introduced by Haver and Andersen (2000) for deep water waves. The relative height and crest values in their definitions represent outliers, being exceeded in 1 of 100 cases when applying a second-order model to the deep-water sea-surface elevation (Haver, 2000). The definitions have been taken up numerous times in the literature. Authors have been investigating whether rogue waves according to Haver and Andersen's definition (2000) are outliers with respect to typical wave distributions in the real ocean as well (e.g., Forristall, 2005; Gemmrich and Garrett, 2008). The question has been raised whether the rogue wave definition by a certain height or crest threshold is useful in practice (Häfner et al., 2021). Several authors have, based on large measurement datasets, come to the conclusion that these rogue waves are rare, but nevertheless realisations of commonly used wave distributions (e.g., Waseda et al., 2011; Christou and Ewans, 2014). In a previous study (Teutsch et al., 2020), we were able to confirm this conclusion at buoy measurement stations in intermediate water. However, at the shallow water buoy station off Norderney, which showed a larger number of rogue waves than expected according to the common wave distributions, the interaction of solitons with oscillating waves might be a mechanism explaining the increased occurrence of rogue waves.

## 5 Conclusions

Rogue wave occurrence recorded off the coast of the island Norderney is not sufficiently explained by second-order theory. We investigated the role of solitons in the enhanced rogue wave occurrence by calculating discrete soliton spectra of time series from vKdV-NLFT. Our main results for this specific measurement site are the following.

- Each measured rogue wave could be associated with at least one soliton in the NLFT spectrum.
- The soliton heights were always smaller than those of the rogue waves. Samples with rogue waves were more likely to contain an outstanding soliton in the NLFT spectrum than samples without rogue waves.
- The presence of a strongly outstanding soliton, with a ratio between the second-largest and the largest soliton in the nonlinear spectrum of $A_2\,(A_1)^{-1} \leq 0.3$, was found to be a strong indicator for the presence of a rogue wave.

https://doi.org/10.5194/nhess-2022-28
Preprint. Discussion started: 4 March 2022


Natural Hazards and Earth System Sciences
Open Access
Discussions

- Conversely, the absence of an outstanding soliton in the spectrum is a strong indicator for the absence of an extreme rogue wave of $H\ (H_s)^{-1} \geq 2.3$.

We conclude that nonlinear processes are important in the generation of rogue waves at this specific site and may explain the enhanced occurrence of such waves beyond second-order theory. Rogue waves at Norderney are likely to be a result of the interaction of solitons with the underlying field of oscillatory waves.

*Author contributions.* All authors contributed to the idea and scope of the paper. IT performed the analyses and wrote the manuscript. MB, RW and SW provided help with data analysis, discussed the results, and contributed to the writing of the paper. RW supervised the work.

*Competing interests.* The authors declare that they have no conflict of interest.

*Acknowledgements.* This project has received funding from the European Research Council (ERC) under the European Union's Horizon 2020 research and innovation programme (grant agreement No 716669). Ina Teutsch received funding for this work from the Federal Maritime and Hydrographic Agency (BSH). The buoy data were kindly provided by the Lower Saxony Water Management, Coastal Defence and Nature Conservation Agency (NLWKN).

https://doi.org/10.5194/nhess-2022-28
Preprint. Discussion started: 4 March 2022




## References

Ablowitz, M. J., Kaup, D. J., Newell, A. C., and Segur, H.: The Inverse Scattering Transform-Fourier Analysis for Nonlinear Problems, Studies in Applied Mathematics, 53, 249–315, https://doi.org/10.1002/sapm1974534249, 1974.

Alber, I. E.: The effects of randomness on the stability of two-dimensional surface wavetrains, Proceedings of the Royal Society of London. A. Mathematical and Physical Sciences, 363, 525–546, https://doi.org/10.1098/rspa.1978.0181, 1978.

Baschek, B. and Imai, J.: Rogue Wave Observations Off the US West Coast, Oceanography, 24, 158–165, https://doi.org/10.5670/oceanog.2011.35, 2011.

Benjamin, T. B. and Feir, J. E.: The disintegration of wave trains on deep water, Journal of Fluid Mechanics, 27, 417–430, https://doi.org/10.1017/s002211206700045x, 1967.

Bitner, E. M.: Non-linear effects of the statistical model of shallow-water wind waves, Applied Ocean Research, 2, 63–73, https://doi.org/10.1016/0141-1187(80)90031-0, 1980.

Brühl, M. and Oumeraci, H.: Analysis of long-period cosine-wave dispersion in very shallow water using nonlinear Fourier transform based on KdV equation, Applied Ocean Research, 61, 81–91, https://doi.org/10.1016/j.apor.2016.09.009, 2016.

Brühl, M.: Spectral analysis of nonlinear waves in the coastal area, 2022.

Cattrell, A. D., Srokosz, M., Moat, B. I., and Marsh, R.: Can Rogue Waves Be Predicted Using Characteristic Wave Parameters?, Journal of Geophysical Research: Oceans, 123, 5624–5636, https://doi.org/10.1029/2018jc013958, 2018.

Christou, M. and Ewans, K.: Field Measurements of Rogue Water Waves, Journal of Physical Oceanography, 44, 2317–2335, https://doi.org/10.1175/jpo-d-13-0199.1, 2014.

Clamond, D., Francius, M., Grue, J., and Kharif, C.: Long time interaction of envelope solitons and freak wave formations, European Journal of Mechanics - B/Fluids, 25, 536–553, https://doi.org/10.1016/j.euromechflu.2006.02.007, 2006.

de León, S. P. and Soares, C. G.: Hindcast of extreme sea states in North Atlantic extratropical storms, Ocean Dynamics, 65, 241–254, https://doi.org/10.1007/s10236-014-0794-6, 2014.

Dysthe, K., Krogstad, H. E., and Müller, P.: Oceanic Rogue Waves, Annual Review of Fluid Mechanics, 40, 287–310, https://doi.org/10.1146/annurev.fluid.40.111406.102203, 2008.

Dysthe, K. B. and Trulsen, K.: Note on Breather Type Solutions of the NLS as Models for Freak-Waves, Physica Scripta, T82, 48, https://doi.org/10.1238/physica.topical.082a00048, 1999.

Fedele, F., Herterich, J., Tayfun, A., and Dias, F.: Large nearshore storm waves off the Irish coast, Scientific Reports, 9, https://doi.org/10.1038/s41598-019-51706-8, 2019.

Fernandez, L., Onorato, M., Monbaliu, J., and Toffoli, A.: Modulational instability and wave amplification in finite water depth, Natural Hazards and Earth System Sciences, 14, 705–711, https://doi.org/10.5194/nhess-14-705-2014, 2014.

Forristall, G. Z.: On the statistical distribution of wave heights in a storm, Journal of Geophysical Research, 83, 2353, https://doi.org/10.1029/jc083ic05p02353, 1978.

Forristall, G. Z.: Understanding rogue waves: Are new physics really necessary?, 2005.

Gardner, C. S., Greene, J. M., Kruskal, M. D., and Miura, R. M.: Method for solving the Korteweg–deVries equation., Phys. Rev. Lett., 19: 1095-7(Nov. 6, 1967)., https://doi.org/10.1103/PhysRevLett.19.1095, 1967.

Garett, C. and Gemmrich, J.: Rogue waves, Physics Today, 62, 62–63, https://doi.org/10.1063/1.3156339, 2009.

Gemmrich, J. and Garrett, C.: Unexpected Waves, Journal of Physical Oceanography, 38, 2330–2336, https://doi.org/10.1175/2008jpo3960.1, 2008.

Gramstad, O. and Trulsen, K.: Influence of crest and group length on the occurrence of freak waves, Journal of Fluid Mechanics, 582, 463–472, https://doi.org/10.1017/s0022112007006507, 2007.

Häfner, D., Gemmrich, J., and Jochum, M.: Real-world rogue wave probabilities, Scientific Reports, 11, https://doi.org/10.1038/s41598-021-89359-1, 2021.

Hammack, J., Scheffner, N., and Segur, H.: Two-dimensional periodic waves in shallow water, Journal of Fluid Mechanics, 209, 567–589, https://doi.org/10.1017/s0022112089003228, 1989.

Haver, S.: Evidences of the existence of freak waves, in: Proc. Rogue Waves, Brest, 2000.

Haver, S. and Andersen, O. J.: Freak waves: rare realizations of a typical population or typical realizations of a rare population?, in: The Tenth International Offshore and Polar Engineering Conference, International Society of Offshore and Polar Engineers, 2000.

Huntley, D. A., Guza, R. T., and Bowen, A. J.: A universal form for shoreline run-up spectra?, Journal of Geophysical Research, 82, 2577–2581, https://doi.org/10.1029/jc082i018p02577, 1977.

Janssen, P. A. E. M.: Nonlinear Four-Wave Interactions and Freak Waves, Journal of Physical Oceanography, 33, 863–884, 2003.

Janssen, P. A. E. M. and Onorato, M.: The Intermediate Water Depth Limit of the Zakharov Equation and Consequences for Wave Prediction, Journal of Physical Oceanography, 37, 2389–2400, https://doi.org/10.1175/jpo3128.1, 2007.

Johnson, D.: DIWASP, a directional wave spectra toolbox for MATLAB®: User Manual, Centre for Water Research, University of Western Australia., 2002.

Karmpadakis, I., Swan, C., and Christou, M.: Laboratory investigation of crest height statistics in intermediate water depths, Proceedings of the Royal Society A: Mathematical, Physical and Engineering Sciences, 475, 20190 183, https://doi.org/10.1098/rspa.2019.0183, 2019.

Karmpadakis, I., Swan, C., and Christou, M.: Assessment of wave height distributions using an extensive field database, Coastal Engineering, 157, 103 630, https://doi.org/10.1016/j.coastaleng.2019.103630, 2020.

Kashima, H., Hirayama, K., and Mori, N.: ESTIMATION OF FREAK WAVE OCCURRENCE FROM DEEP TO SHALLOW WATER REGIONS, Coastal Engineering Proceedings, 1, 36, https://doi.org/10.9753/icce.v34.waves.36, 2014.

Kharif, C. and Pelinovsky, E.: Physical mechanisms of the rogue wave phenomenon, European Journal of Mechanics - B/Fluids, 22, 603–634, https://doi.org/10.1016/j.euromechflu.2003.09.002, 2003.

Korteweg, D. J. and de Vries, G.: XLI. On the change of form of long waves advancing in a rectangular canal, and on a new type of long stationary waves, The London, Edinburgh, and Dublin Philosophical Magazine and Journal of Science, 39, 422–443, https://doi.org/10.1080/14786449508620739, 1895.

LeMéhauté, B.: An introduction to hydrodynamics and water waves, Springer-Verlag, New York, 1976.

Lenau, C. W.: The solitary wave of maximum amplitude, Journal of Fluid Mechanics, 26, 309–320, https://doi.org/10.1017/s0022112066001253, 1966.

Li, Y., Draycott, S., Zheng, Y., Lin, Z., Adcock, T. A., and van den Bremer, T. S.: Why rogue waves occur atop abrupt depth transitions, Journal of Fluid Mechanics, 919, R5, https://doi.org/10.1017/jfm.2021.409, 2021.

Longuet-Higgins, M. S.: On the Statistical Distribution of the Height of Sea Waves, Journal of Marine Research, 11, 1952.

Ma, Y., Dong, G., and Ma, X.: EXPERIMENTAL STUDY OF STATISTICS OF RANDOM WAVES PROPAGATING OVER A BAR, Coastal Engineering Proceedings, 1, 30, https://doi.org/10.9753/icce.v34.waves.30, 2014.

https://doi.org/10.5194/nhess-2022-28
Preprint. Discussion started: 4 March 2022

Natural Hazards and Earth System Sciences
Open Access
Discussions

Majda, A. J., Moore, M. N. J., and Qi, D.: Statistical dynamical model to predict extreme events and anomalous features in shallow water waves with abrupt depth change, Proceedings of the National Academy of Sciences, 116, 3982–3987, https://doi.org/10.1073/pnas.1820467116, 2019.

MATLAB: version 9.6.0.1072779 (R2019a), The MathWorks Inc., Natick, Massachusetts, 2019.

McCowan, J.: VII. On the solitary wave, The London, Edinburgh, and Dublin Philosophical Magazine and Journal of Science, 32, 45–58, https://doi.org/10.1080/14786449108621390, 1891.

Middleton, D. and Mellen, R.: Wind-generated solitons: A potentially significant mechanism in ocean surface wave generation and surface scattering, IEEE Journal of Oceanic Engineering, 10, 471–476, https://doi.org/10.1109/JOE.1985.1145130, 1985.

Miles, J. W.: Solitary Waves, Annual Review of Fluid Mechanics, 12, 11–43, https://doi.org/10.1146/annurev.fl.12.010180.000303, 1980.

NLWKN: Tideaußenpegel, https://www.pegelonline.nlwkn.niedersachsen.de/Pegel/Tideau\T1\ssenpegel/ID/452, accessed: 2021-12-23, 2021.

Olagnon, M. and v. Iseghem, S.: Some observed characteristics of sea states with extreme waves, in: Proc. 10th Int. Offshore Polar Engineering Conf., Seattle, pp. 84–90, International Society of Offshore and Polar Engineers, 2000.

Onorato, M., Osborne, A. R., Serio, M., and Bertone, S.: Freak Waves in Random Oceanic Sea States, Physical Review Letters, 86, 5831–5834, https://doi.org/10.1103/physrevlett.86.5831, 2001.

Orzech, M. D. and Wang, D.: Measured Rogue Waves and Their Environment, Journal of Marine Science and Engineering, 8, 890, https://doi.org/10.3390/jmse8110890, 2020.

Osborne, A. R.: Behavior of solitons in random-function solutions of the periodic Korteweg–de Vries equation, Physical Review Letters, 71, 3115–3118, https://doi.org/10.1103/physrevlett.71.3115, 1993.

Osborne, A. R.: Nonlinear ocean waves and the inverse scattering transform, Elsevier, Amsterdam, 2010.

Osborne, A. R., Segre, E., Boffetta, G., and Cavaleri, L.: Soliton basis states in shallow-water ocean surface waves, Physical Review Letters, 67, 592–595, https://doi.org/10.1103/physrevlett.67.592, 1991.

Pelinovsky, E. and Sergeeva, A.: Numerical modeling of the KdV random wave field, European Journal of Mechanics - B/Fluids, 25, 425–434, https://doi.org/10.1016/j.euromechflu.2005.11.001, 2006.

Pelinovsky, E., Talipova, T., and Kharif, C.: Nonlinear-dispersive mechanism of the freak wave formation in shallow water, Physica D: Nonlinear Phenomena, 147, 83–94, https://doi.org/10.1016/s0167-2789(00)00149-4, 2000.

Peregrine, D. H.: Water waves, nonlinear Schrödinger equations and their solutions, The Journal of the Australian Mathematical Society. Series B. Applied Mathematics, 25, 16–43, https://doi.org/10.1017/S0334270000003891, 1983.

Peterson, P., Soomere, T., Engelbrecht, J., and van Groesen, E.: Soliton interaction as a possible model for extreme waves in shallow water, Nonlinear Processes in Geophysics, 10, 503–510, https://doi.org/10.5194/npg-10-503-2003, 2003.

Pinho, U., Liu, P., Eduardo, C., and Ribeiro, C.: Freak Waves at Campos Basin, Brazil, Geofizika, 21, 2004.

Prevosto, M.: Effect of Directional Spreading and Spectral Bandwidth on the Nonlinearity of the Irregular Waves, 1998.

Sergeeva, A., Pelinovsky, E., and Talipova, T.: Nonlinear random wave field in shallow water: variable Korteweg-de Vries framework, Natural Hazards and Earth System Sciences, 11, 323–330, https://doi.org/10.5194/nhess-11-323-2011, 2011.

Serio, M., Onorato, M., Osborne, A., and Janssen, P.: On the computation of the Benjamin-Feir Index, Il Nuovo Cimento C, 28, 893–903, https://doi.org/10.1393/ncc/i2005-10134-1, 2006.

Shrira, V. I. and Geogjaev, V. V.: What makes the Peregrine soliton so special as a prototype of freak waves?, Journal of Engineering Mathematics, 67, 11–22, https://doi.org/10.1007/s10665-009-9347-2, 2009.

https://doi.org/10.5194/nhess-2022-28
Preprint. Discussion started: 4 March 2022



Slunyaev, A., Didenkulova, I., and Pelinovsky, E.: Rogue waters, Contemporary Physics, 52, 571–590, https://doi.org/10.1080/00107514.2011.613256, 2011.

Slunyaev, A., Sergeeva, A., and Didenkulova, I.: Rogue events in spatiotemporal numerical simulations of unidirectional waves in basins of different depth, Natural Hazards, 84, 549–565, https://doi.org/10.1007/s11069-016-2430-x, 2016.

Slunyaev, A. V.: A high-order nonlinear envelope equation for gravity waves in finite-depth water, Journal of Experimental and Theoretical Physics, 101, 926–941, https://doi.org/10.1134/1.2149072, 2005.

Slunyaev, A. V. and Shrira, V. I.: On the highest non-breaking wave in a group: fully nonlinear water wave breathers versus weakly nonlinear theory, Journal of Fluid Mechanics, 735, 203–248, https://doi.org/10.1017/jfm.2013.498, 2013.

Soares, C. G., Cherneva, Z., and Antão, E.: Characteristics of abnormal waves in North Sea storm sea states, Applied Ocean Research, 25, 337–344, https://doi.org/10.1016/j.apor.2004.02.005, 2003.

Soomere, T.: Rogue waves in shallow water, The European Physical Journal Special Topics, 185, 81–96, https://doi.org/10.1140/epjst/e2010-01240-1, 2010.

Soomere, T. and Engelbrecht, J.: Interaction of shallow-water solitons as a possible model for freak waves, 2005.

Stansell, P.: Distributions of freak wave heights measured in the North Sea, Applied Ocean Research, 26, 35–48, https://doi.org/10.1016/j.apor.2004.01.004, 2004.

Tayfun, M. A.: Distributions of Envelope and Phase in Wind Waves, Journal of Physical Oceanography, 38, 2784–2800, https://doi.org/10.1175/2008jpo4008.1, 2008.

Teutsch, I., Weisse, R., Moeller, J., and Krueger, O.: A statistical analysis of rogue waves in the southern North Sea, Natural Hazards and Earth System Sciences, 20, 2665–2680, https://doi.org/10.5194/nhess-20-2665-2020, 2020.

Toffoli, A., Fernandez, L., Monbaliu, J., Benoit, M., Gagnaire-Renou, E., Lefèvre, J. M., Cavaleri, L., Proment, D., Pakozdi, C., Stansberg, C. T., Waseda, T., and Onorato, M.: Experimental evidence of the modulation of a plane wave to oblique perturbations and generation of rogue waves in finite water depth, Physics of Fluids, 25, 091 701, https://doi.org/10.1063/1.4821810, 2013.

Trulsen, K., Zeng, H., and Gramstad, O.: Laboratory evidence of freak waves provoked by non-uniform bathymetry, Physics of Fluids, 24, 097 101, https://doi.org/10.1063/1.4748346, 2012.

Trulsen, K., Raustøl, A., Jorde, S., and Rye, L. B.: Extreme wave statistics of long-crested irregular waves over a shoal, Journal of Fluid Mechanics, 882, R2, https://doi.org/10.1017/jfm.2019.861, 2020.

Ursell, F.: The long-wave paradox in the theory of gravity waves, Mathematical Proceedings of the Cambridge Philosophical Society, 49, 685–694, https://doi.org/10.1017/s0305004100028887, 1953.

Wahls, S. and Poor, H. V.: Fast Numerical Nonlinear Fourier Transforms, IEEE Transactions on Information Theory, 61, 6957–6974, https://doi.org/10.1109/tit.2015.2485944, 2015.

Wahls, S., Chimmalgi, S., and Prins, P. J.: FNFT: A Software Library for Computing Nonlinear Fourier Transforms, Journal of Open Source Software, 3, 597, https://doi.org/10.21105/joss.00597, 2018.

Waseda, T., Hallerstig, M., Ozaki, K., and Tomita, H.: Enhanced freak wave occurrence with narrow directional spectrum in the North Sea, Geophysical Research Letters, 38, n/a–n/a, https://doi.org/10.1029/2011gl047779, 2011.

Zabusky, N. J. and Kruskal, M. D.: Interaction of "Solitons" in a Collisionless Plasma and the Recurrence of Initial States, Physical Review Letters, 15, 240–243, https://doi.org/10.1103/physrevlett.15.240, 1965.

Zakharov, V. E. and Shabat, A. B.: A scheme for integrating the nonlinear equations of mathematical physics by the method of the inverse scattering problem. I, Functional Analysis and Its Applications, 8, 226–235, https://doi.org/10.1007/bf01075696, 1975.

https://doi.org/10.5194/nhess-2022-28
Preprint. Discussion started: 4 March 2022




Zeng, H. and Trulsen, K.: Evolution of skewness and kurtosis of weakly nonlinear unidirectional waves over a sloping bottom, Natural Hazards and Earth System Sciences, 12, 631–638, https://doi.org/10.5194/nhess-12-631-2012, 2012.

Zhang, J. and Benoit, M.: Wave–bottom interaction and extreme wave statistics due to shoaling and de-shoaling of irregular long-crested wave trains over steep seabed changes, Journal of Fluid Mechanics, 912, https://doi.org/10.1017/jfm.2020.1125, 2021.

Zhang, J., Benoit, M., Kimmoun, O., Chabchoub, A., and Hsu, H.-C.: Statistics of Extreme Waves in Coastal Waters: Large Scale Experiments and Advanced Numerical Simulations, Fluids, 4, 99, https://doi.org/10.3390/fluids4020099, 2019.

# References

Ablowitz, M. J., Kaup, D. J., Newell, A. C., and Segur, H., 1974: The Inverse Scattering Transform-Fourier Analysis for Nonlinear Problems. *Studies in Applied Mathematics*, **53 (4)**, 249–315, URL https://doi.org/10.1002/sapm1974534249.

Adcock, T. A. A., Taylor, P. H., Yan, S., Ma, Q. W., and Janssen, P. A. E. M., 2011: Did the Draupner wave occur in a crossing sea? *Proceedings of the Royal Society A: Mathematical, Physical and Engineering Sciences*, **467 (2134)**, 3004–3021, URL https://doi.org/10.1098/rspa.2011.0049.

Alber, I. E., 1978: The effects of randomness on the stability of two-dimensional surface wavetrains. *Proceedings of the Royal Society of London. A. Mathematical and Physical Sciences*, **363 (1715)**, 525–546, URL https://doi.org/10.1098/rspa.1978.0181.

Allender, J., and Coauthors, 1989: The wadic project: A comprehensive field evaluation of directional wave instrumentation. *Ocean Engineering*, **16 (5-6)**, 505–536, URL https://doi.org/10.1016/0029-8018(89)90050-4.

Baschek, B., and Imai, J., 2011: Rogue wave observations off the US West Coast. *Oceanography*, **24 (2)**, 158–165, URL https://doi.org/10.5670/oceanog.2011.35.

Benjamin, T. B., 1967: Instability of periodic wavetrains in nonlinear dispersive systems. *Proceedings of the Royal Society of London. Series A. Mathematical and Physical Sciences*, **299 (1456)**, 59–76, URL https://doi.org/10.1098/rspa.1967.0123.

Benjamin, T. B., and Feir, J. E., 1967: The disintegration of wave trains on deep water. *Journal of Fluid Mechanics*, **27 (3)**, 417–430, URL https://doi.org/10.1017/s002211206700045x.

Bitner-Gregersen, E. M., and Gramstad, O., 2016: Rogue waves. Impact on ships and offshore structures. *R+I Position Paper*.

Casas-Prat, M., Holthuijsen, L., and van Gelder, P. H. A. J. M., 2009: Short-term statistics of 10,000,000 waves observed by buoys. *Proceedings of the Coastal Engineering Conference*, 560–572, URL https://doi.org/10.1142/9789814277426_0047.

Cattrell, A. D., Srokosz, M., Moat, B. I., and Marsh, R., 2018: Can Rogue Waves Be Predicted Using Characteristic Wave Parameters? *Journal of Geophysical Research: Oceans*, **123 (8)**, 5624–5636, URL https://doi.org/10.1029/2018jc013958.

Christou, M., and Ewans, K., 2014: Field Measurements of Rogue Water Waves. *Journal of Physical Oceanography*, **44 (9)**, 2317–2335, URL https://doi.org/10.1175/jpo-d-13-0199.1.

de Pinho, U. F., Liu, P. C., and Ribeiro, C. E. P., 2004: Freak Waves at Campos Basin, Brazil. *Geofizika*, **21**, 53–67.

Didenkulova, E., 2020: Catalogue of rogue waves occurred in the World Ocean from 2011 to 2018 reported by mass media sources. *Ocean & Coastal Management*, **188**, 105 076, URL https://doi.org/10.1016/j.ocecoaman.2019.105076.

Donelan, M. A., and Magnusson, A. K., 2005: The role of meteorological focusing in generating rogue wave conditions, Honolulu, Hawaii. In: Proc. 14th Aha Huliko'a Winter Workshop.

Draper, L., 1964: 'Freak' Ocean Waves. *Oceanus*, **10**, 13–15.

Dysthe, K., Krogstad, H. E., and Müller, P., 2008: Oceanic Rogue Waves. *Annual Review of Fluid Mechanics*, **40 (1)**, 287–310, URL https://doi.org/10.1146/annurev.fluid.40.111406.102203.

Dysthe, K. B., and Trulsen, K., 1999: Note on Breather Type Solutions of the NLS as Models for Freak-Waves. *Physica Scripta*, **T82 (1)**, 48–52, URL https://doi.org/10.1238/physica.topical.082a00048.

Fedele, F., Brennan, J., de León, S. P., Dudley, J., and Dias, F., 2016: Real world ocean rogue waves explained without the modulational instability. *Scientific Reports*, **6 (1)**, URL https://doi.org/10.1038/srep27715.

Fedele, F., Herterich, J., Tayfun, A., and Dias, F., 2019: Large nearshore storm waves off the Irish coast. *Scientific Reports*, **9 (1)**, URL https://doi.org/10.1038/s41598-019-51706-8.

Fernandez, L., Onorato, M., Monbaliu, J., and Toffoli, A., 2014: Modulational instability and wave amplification in finite water depth. *Natural Hazards and Earth System Sciences*, **14 (3)**, 705–711, URL https://doi.org/10.5194/nhess-14-705-2014.

FINO1, 2022: Hydrography. Accessed: 2022-04-06, https://www.fino1.de/en/research/project/hydrography.html.

Forristall, G. Z., 1978: On the Statistical Distribution of Wave Heights in a Storm. *Journal of Geophysical Research*, **83 (C5)**, 2353–2358, URL https://doi.org/10.1029/jc083ic05p02353.

Forristall, G. Z., 2000: Wave Crest Distributions: Observations and Second-Order Theory. *Journal of Physical Oceanography*, **30 (8)**, 1931–1943, URL https://doi.org/10.1175/1520-0485(2000)030<1931:wcdoas>2.0.co;2.

Forristall, G. Z., 2005: Understanding rogue waves: Are new physics really necessary?

Freeman, K., Frost, C., Hundleby, G., Roberts, A., Valpy, B., Holttinen, H., Ramírez, L., and Pineda, I., 2019: Our energy, our future: How offshore wind will help Europe go carbon-neutral. *WindEurope*.

Gardner, C. S., Greene, J. M., Kruskal, M. D., and Miura, R. M., 1967: Method for solving the Korteweg–deVries equation. *Physical Review Letters*, **19**, 1095–1097, URL https://www.osti.gov/biblio/4516457.

Gemmrich, J., and Cicon, L., 2022: Generation mechanism and prediction of an observed extreme rogue wave. *Scientific Reports*, **12 (1)**, URL https://doi.org/10.1038/s41598-022-05671-4.

Goda, Y., 2000: *Random Seas and Design of Maritime Structures*. ISBN 978-981-4282-39-0, World Scientific, 732 pp., URL https://doi.org/10.1142/7425.

Gramstad, O., and Trulsen, K., 2007: Influence of crest and group length on the occurrence of freak waves. *Journal of Fluid Mechanics*, **582**, 463–472, URL https://doi.org/10.1017/s0022112007006507.

Grønlie, Ø., 2006: Wave radars: Techniques and technologies.

Häfner, D., Gemmrich, J., and Jochum, M., 2021: Real-world rogue wave probabilities. *Scientific Reports*, **11 (1)**, URL https://doi.org/10.1038/s41598-021-89359-1.

Haver, S., 2000: Evidences of the Existence of Freak Waves. *Proc. Rogue Waves, Brest*.

Haver, S., and Andersen, O. J., 2000: Freak Waves: Rare Realizations of a Typical Population or Typical Realizations of a Rare Population? *The Tenth International Offshore and Polar Engineering Conference*, International Society of Offshore and Polar Engineers.

Holthuijsen, L. H., 2007: *Waves in Oceanic and Coastal Waters*. ISBN 978-0-52-112995-4, Cambridge University Press, 404 pp., URL https://doi.org/10.1017/cbo9780511618536.

IACS, 2001: IACS Rec. No. 34. Standard Wave Data. Revision November 2001. URL http://www.iacs.org.uk/publications/default.aspx.

Jahns, H. O., and Wheeler, J. D., 1973: Long-Term Wave Probabilities Based on Hindcasting of Severe Storms. *Journal of Petroleum Technology*, **25**, 473–486, URL https://doi.org/10.2118/3934-PA.

Janssen, P. A. E. M., and Bidlot, J.-R., 2009: On the extension of the freak wave warning system and its verification. *Technical Memorandum*, **588**, URL https://www.ecmwf.int/node/10243.

Janssen, P. A. E. M., and Onorato, M., 2007: The Intermediate Water Depth Limit of the Zakharov Equation and Consequences for Wave Prediction. *Journal of Physical Oceanography*, **37 (10)**, 2389–2400, URL https://doi.org/10.1175/jpo3128.1.

Janssen, T. T., and Herbers, T. H. C., 2009: Nonlinear Wave Statistics in a Focal Zone. *Journal of Physical Oceanography*, **39 (8)**, 1948–1964, URL https://doi.org/10.1175/2009jpo4124.1.

Jones, I., and Jones, J., 2008: *Oceanography in the Days of Sail*. ISBN 978-0-9807445-1-4, Hale & Iremonger, 289 pp.

Karmpadakis, I., Swan, C., and Christou, M., 2019: Laboratory investigation of crest height statistics in intermediate water depths. *Proceedings of the Royal Society A: Mathematical, Physical and Engineering Sciences*, **475 (2229)**, 20190 183, URL https://doi.org/10.1098/rspa.2019.0183.

Karmpadakis, I., Swan, C., and Christou, M., 2020: Assessment of wave height distributions using an extensive field database. *Coastal Engineering*, **157**, 103 630, URL https://doi.org/10.1016/j.coastaleng.2019.103630.

Kharif, C., and Pelinovsky, E., 2003: Physical mechanisms of the rogue wave phenomenon. *European Journal of Mechanics - B/Fluids*, **22 (6)**, 603–634, URL https://doi.org/10.1016/j.euromechflu.2003.09.002.

Kinsman, B., 1965: *Wind Waves : Their Generation and Propagation On the Ocean Surface*. ISBN 978-0-13-960344-0, Englewood Cliffs (N.J.): Prentice-Hall, 676 pp.

Korteweg, D. J., and de Vries, G., 1895: XLI. on the change of form of long waves advancing in a rectangular canal, and on a new type of long stationary waves. *Philosophical Magazine Series*, **39 (240)**, 422–443, URL https://doi.org/10.1080/14786449508620739.

Lake, B. M., Yuen, H. C., Rungaldier, H., and Ferguson, W. E., 1977: Nonlinear deep-water waves: theory and experiment. Part 2. Evolution of a continuous wave train. *Journal of Fluid Mechanics*, **83 (1)**, 49–74, URL https://doi.org/10.1017/s0022112077001037.

Lavrenov, I. V., 1998: The Wave Energy Concentration at the Agulhas Current off South Africa. *Natural Hazards*, **17 (2)**, 117–127, URL https://doi.org/10.1023/a:1007978326982.

Lawton, G., 2001: Monsters of the deep. *New Scientist*, **170 (2297)**, 28–32.

Longuet-Higgins, M. S., 1952: On the statistical distribution of the heights of sea waves. *Journal of Marine Research*, **11 (3)**, 245–266.

Magnusson, A. K., Jenkins, A., Niedermayer, A., and Nieto-Borge, J. C., 2003: Extreme wave statistics from time-series data. *Proceedings of MAXWAVE Final Meeting, Geneva*, 17: 231–245.

Mallory, J. K., 1974: Abnormal Waves on the South East Coast of South Africa. *The International Hydrographic Review*, **51 (2)**.

McAllister, M. L., Draycott, S., Adcock, T. A. A., Taylor, P. H., and van den Bremer, T. S., 2018: Laboratory recreation of the Draupner wave and the role of breaking in crossing seas. *Journal of Fluid Mechanics*, **860**, 767–786, URL https://doi.org/10.1017/jfm.2018.886.

Mendes, S., Scotti, A., and Stansell, P., 2021: On the physical constraints for the exceeding probability of deep water rogue waves. *Applied Ocean Research*, **108**, 102 402, URL https://doi.org/10.1016/j.apor.2020.102402.

Miles, J. W., 1980: Solitary Waves. *Annual Review of Fluid Mechanics*, **12 (1)**, 11–43, URL https://doi.org/10.1146/annurev.fl.12.010180.000303.

Mori, N., Liu, P. C., and Yasuda, T., 2002: Analysis of freak wave measurements in the Sea of Japan. *Ocean Engineering*, **29 (11)**, 1399–1414, URL https://doi.org/10.1016/s0029-8018(01)00073-7.

Onorato, M., Osborne, A. R., Serio, M., and Bertone, S., 2001: Freak Waves in Random Oceanic Sea States. *Physical Review Letters*, **86 (25)**, 5831–5834, URL https://doi.org/10.1103/physrevlett.86.5831.

Onorato, M., Osborne, A. R., Serio, M., Cavaleri, L., Brandini, C., and Stansberg, C. T., 2004: Observation of strongly non-Gaussian statistics for random sea surface gravity waves in wave flume experiments. *Physical Review E*, **70 (6)**, URL https://doi.org/10.1103/physreve.70.067302.

Onorato, M., and Coauthors, 2009: Statistical properties of mechanically generated surface gravity waves: a laboratory experiment in a three-dimensional wave basin. *Journal of Fluid Mechanics*, **627**, 235–257, URL https://doi.org/10.1017/s002211200900603x.

Orzech, M. D., and Wang, D., 2020: Measured Rogue Waves and Their Environment. *Journal of Marine Science and Engineering*, **8 (11)**, 890, URL https://doi.org/10.3390/jmse8110890.

Osborne, A. R., 2010: *Nonlinear Ocean Waves and the Inverse Scattering Transform.* ISBN 978-0-12-528629-9, Elsevier, 977 pp.

Osborne, A. R., Segre, E., Boffetta, G., and Cavaleri, L., 1991: Soliton basis states in shallow-water ocean surface waves. *Physical Review Letters*, **67 (5)**, 592–595, URL https://doi.org/10.1103/physrevlett.67.592.

Pelinovsky, E., Talipova, T., and Kharif, C., 2000: Nonlinear-dispersive mechanism of the freak wave formation in shallow water. *Physica D: Nonlinear Phenomena*, **147 (1-2)**, 83–94, URL https://doi.org/10.1016/s0167-2789(00)00149-4.

Peregrine, D., 1976: Interaction of Water Waves and Currents. **16**, 9–117, URL https://doi.org/10.1016/s0065-2156(08)70087-5.

Peregrine, D. H., 1983: Water waves, nonlinear Schrödinger equations and their solutions. *The Journal of the Australian Mathematical Society. Series B. Applied Mathematics*, **25 (1)**, 16–43, URL https://doi.org/10.1017/S0334270000003891.

Peters, K., and Pohl, M., 2020: Die Küste, Heft 88, EAK 2002, Empfehlungen für Küstenschutzwerke, 3. korrigierte Ausgabe 2020. URL https://doi.org/10.18171/1.088100.

Peterson, P., Soomere, T., Engelbrecht, J., and van Groesen, E., 2003: Soliton interaction as a possible model for extreme waves in shallow water. *Nonlinear Processes in Geophysics*, **10 (6)**, 503–510, URL https://doi.org/10.5194/npg-10-503-2003.

Pleskachevsky, A. L., Lehner, S., and Rosenthal, W., 2012: Storm observations by remote sensing and influences of gustiness on ocean waves and on generation of rogue waves. *Ocean Dynamics*, **62 (9)**, 1335–1351, URL https://doi.org/10.1007/s10236-012-0567-z.

Prevosto, M., 1998: Effect of Directional Spreading and Spectral Bandwidth on the Nonlinearity of the Irregular Waves. *Proceedings of the Eighth International Offshore and Polar Engineering Conference*, The International Society of Offshore and Polar Engineers, 119–123.

Rosenthal, W., 2005: Results of the MAXWAVE project.

Sand, S. E., Hansen, N. E. O., Klinting, P., Gudmestad, O. T., and Sterndorff, M. J., 1990: Freak Wave Kinematics. *Water Wave Kinematics. NATO ASI Series (E: Applied Sciences)*, Vol. 178, Springer, Dordrecht, 535–549, URL https://doi.org/10.1007/978-94-009-0531-3_34.

Savvopoulos, G., and Cerquenich, D., 2021: Shipping analysis of the North Sea. *ABL Report No. : 025057.00-RPT-ABL-001.*

Sergeeva, A., Pelinovsky, E., and Talipova, T., 2011: Nonlinear random wave field in shallow water: variable Korteweg–de Vries framework. *Natural Hazards and Earth System Sciences*, **11 (2)**, 323–330, URL https://doi.org/10.5194/nhess-11-323-2011.

Sergeeva, A., and Slunyaev, A., 2013: Rogue waves, rogue events and extreme wave kinematics in spatio-temporal fields of simulated sea states. *Natural Hazards and Earth System Sciences*, **13 (7)**, 1759–1771, URL https://doi.org/10.5194/nhess-13-1759-2013.

Seymour, R. J., and Castel, D., 1998: Systematic underestimation of maximum crest heights in deep water using surface-following buoys. *Proc. of the 17th*

*International Conference on Offshore Mechanics and Arctic Engineering*, 1–8.

Shrira, V. I., and Geogjaev, V. V., 2009: What makes the Peregrine soliton so special as a prototype of freak waves? *Journal of Engineering Mathematics*, **67**, 11–22, URL https://doi.org/10.1007/s10665-009-9347-2.

Slunyaev, A., Didenkulova, I., and Pelinovsky, E., 2011: Rogue waters. *Contemporary Physics*, **52 (6)**, 571–590, URL https://doi.org/10.1080/00107514.2011.613256.

Slunyaev, A., Sergeeva, A., and Didenkulova, I., 2016: Rogue events in spatiotemporal numerical simulations of unidirectional waves in basins of different depth. *Natural Hazards*, **84 (S2)**, 549–565, URL https://doi.org/10.1007/s11069-016-2430-x.

Slunyaev, A. V., 2005: A high-order nonlinear envelope equation for gravity waves in finite-depth water. *Journal of Experimental and Theoretical Physics*, **101 (5)**, 926–941, URL https://doi.org/10.1134/1.2149072.

Slunyaev, A. V., and Shrira, V. I., 2013: On the highest non-breaking wave in a group: fully nonlinear water wave breathers versus weakly nonlinear theory. *Journal of Fluid Mechanics*, **735**, 203–248, URL https://doi.org/10.1017/jfm.2013.498.

Soares, C. G., Cherneva, Z., and Antão, E., 2003: Characteristics of abnormal waves in North Sea storm sea states. *Applied Ocean Research*, **25 (6)**, 337–344, URL https://doi.org/10.1016/j.apor.2004.02.005.

Soomere, T., 2010: Rogue waves in shallow water. *The European Physical Journal Special Topics*, **185**, 81–96, URL https://doi.org/10.1140/epjst/e2010-01240-1.

Stansell, P., 2004: Distributions of freak wave heights measured in the North Sea. *Applied Ocean Research*, **26 (1-2)**, 35–48, URL https://doi.org/10.1016/j.apor.2004.01.004.

Stansell, P., Wolfram, J., and Linfoot, B., 2002: Effect of sampling rate on wave height statistics. *Ocean Engineering*, **29 (9)**, 1023–1047, URL https://doi.org/10.1016/s0029-8018(01)00066-x.

Tayfun, M. A., 2008: Distributions of Envelope and Phase in Wind Waves. *Journal of Physical Oceanography*, **38 (12)**, 2784–2800, URL https://doi.org/10.1175/2008jpo4008.1.

Teutsch, I., Brühl, M., Weisse, R., and Wahls, S., 2022: Contribution of solitons to enhanced rogue wave occurrence in shallow water: a case study in the southern North Sea. *Natural Hazards and Earth System Sciences Discussions*, **2022**, 1–37, URL https://doi.org/10.5194/nhess-2022-28.

Teutsch, I., and Weisse, R., 2022: Intermediate-Water Rogue Waves in the Southern North Sea- Generated by a Modulational Instability? *submitted to Journal of Physical Oceanography.*

Teutsch, I., Weisse, R., Moeller, J., and Krueger, O., 2020: A statistical analysis of rogue waves in the southern North Sea. *Natural Hazards and Earth System Sciences*, **20 (10)**, 2665–2680, URL https://doi.org/10.5194/nhess-20-2665-2020.

Toffoli, A., Waseda, T., Houtani, H., Cavaleri, L., Greaves, D., and Onorato, M., 2015: Rogue waves in opposing currents: an experimental study on deterministic and stochastic wave trains. *Journal of Fluid Mechanics*, **769**, 277–297, URL https://doi.org/10.1017/jfm.2015.132.

Trulsen, K., 2018: Rogue Waves in the Ocean, the Role of Modulational Instability, and Abrupt Changes of Environmental Conditions that Can Provoke Non Equilibrium Wave Dynamics. *The Ocean in Motion*, ISBN 978-3-319-71933-7, Springer Oceanography. Springer, Cham., 239–247, URL https://doi.org/10.1007/978-3-319-71934-4_17.

Trulsen, K., Raustøl, A., Jorde, S., and Rye, L. B., 2020: Extreme wave statistics of long-crested irregular waves over a shoal. *Journal of Fluid Mechanics*, **882**, R2, URL https://doi.org/10.1017/jfm.2019.861.

Vandever, J. P., Siegel, E. M., Brubaker, J. M., and Friedrichs, C. T., 2008: Influence of Spectral Width on Wave Height Parameter Estimates in Coastal Environments. *Journal of Waterway, Port, Coastal, and Ocean Engineering*, **134 (3)**, 187–194, URL https://doi.org/10.1061/(ASCE)0733-950X(2008)134:3(187).

Waseda, T., 2006: Impact of directionality on the extreme wave occurrence in a discrete random wave system. *9th International Workshop on Wave Hindcasting and Forecasting, September 24-29*, American Society of Civil Engineers.

Waseda, T., Hallerstig, M., Ozaki, K., and Tomita, H., 2011: Enhanced freak wave occurrence with narrow directional spectrum in the North Sea. *Geophysical Research Letters*, **38 (13)**, URL https://doi.org/10.1029/2011gl047779.

Zabusky, N. J., and Kruskal, M. D., 1965: Interaction of "Solitons" in a Collisionless Plasma and the Recurrence of Initial States. *Physical Review Letters*, **15 (6)**, 240–243, URL https://doi.org/10.1103/physrevlett.15.240.

Zakharov, V. E., and Shabat, A. B., 1974: A scheme for integrating the nonlinear equations of mathematical physics by the method of the inverse scattering problem. I. *Functional Analysis and Its Applications*, **8**, 226–235, URL https://doi.org/10.1007/bf01075696.

## Acknowledgements

I am grateful to have met so many wave-enthusiastic scientists.
Ralf Weisse. Jens Möller. Christian Senet and Mayumi Wilms. Nikolaus Groll. Cordula Berkenbrink. Markus Brühl. Michael Stresser. Anne Wiese. Tobias Teich. Saulo da Silva Mendes. Thilo Grotebrune and Lukas Fröhling. Discussing with you has been an honour and a great motivation.

Thanks to those who have given me an understanding of the amazing mathematics behind waves.
Oliver Krüger. Sander Wahls. Yu-Chen Lee. Frauke Albrecht, Tobias Weigel and Felix Stiehler. Karsten Trulsen and Susanne Støle-Hentschel.

I would like to thank Brian Boland for the language check.

I am grateful to those who have given me the possibility to conduct this work and to those who have created a continuously positive working atmosphere. Corinna Schrum. The incomparable team of KSA. Sabine Billerbeck and the "Forschung vor Anker" team. The coffee break in Harmut Kapitza's office and Linda Baldewein, the helper in need. My fellow PhD students at Hereon, especially Lucas Porz and Elena Mikheeva. Berit Hachfeld, Ingo Harms and my fellow PhD students at the SICSS graduate school.

Investigating rogue waves has been a pleasure.

# Eidesstattliche Versicherung

Hiermit erkläre ich an Eides statt, dass ich die vorliegende Dissertationsschrift selbst verfasst und keine anderen als die angegebenen Quellen und Hilfsmittel benutzt habe.

I hereby declare upon oath that I have written the present dissertation independently and have not used further resources and aids than those stated.

Hamburg, 08.04.2022